FINE STRUCTURE AND MOLECULAR ORGANIZATION OF THE PERIOSTRACUM IN A GASTROPOD MOLLUSC *BUCCINUM UNDATUM* L. AND ITS RELATION TO SIMILAR STRUCTURAL PROTEIN SYSTEMS IN OTHER INVERTEBRATES

By S. HUNT and K. OATES
Department of Biological Sciences, University of Lancaster, Bailrigg, Lancaster LA1 4YQ, U.K.

(*Communicated by I. Manton, F.R.S.* – *Received* 22 *April* 1977 – *Revised* 15 *September* 1977)

[Plates 1–14]

CONTENTS

The horny layer of periostracum which covers the shell of *Buccinum undatum* L. has been studied by a combination of the fine structural techniques including high resolution transmission electron microscopy and scanning electron microscopy as well as by chemical analysis and X-ray diffraction. It has been found that the main structural component is a tectin type protein with globular and probably coiled-coil α-helical regions accompanied by a small amount of polysaccharide. Much of the periostracum is built up of protein sheets superposed in a regular manner and stabilized by some type of covalent cross-linking involving aromatic molecules. The protein is one of the class of structural macromolecules called scleroproteins.

Each sheet of protein is made up of molecular sub-units which have a characteristic dumb-bell shape and which are about 32 nm long and 6.5 nm wide at their globular ends. End-to-end long-axis aggregation of these units produces filaments which aggregate further by side-to-side association into ribbons and ultimately sheets. The side-to-side association is always in register and hence the sheets have a major transverse striation repeating at 32 nm intervals.

The protein sheets can be ascribed a longitudinal axis in terms of the direction of their component filaments. On this basis it can be shown that successive superposed sheets are rotated in a horizontal plane through an angle of 20–25° relative to one another, in a constant direction either clockwise or anticlockwise. Such helicoidal organization is of the cholesteric liquid crystal type which is often found in a biological context, e.g. chitin fibril disposition in arthropod cuticle. This helicoidal layering of the protein sheets is manifested in oblique sections of periostracum as repeated parabolic lamellae. Irregularities in the form of the parabolic lamellae can be accounted for on the basis of the curvature and extensive folding of the periostracum.

The outer and innermost layers of the periostracum tend not to show helicoidal organization but exhibit a different aggregation mode of the dumb-bell-shaped units into a three-dimensional hexagonally packed network matrix. This matrix is much interrupted by vacuoles and localized smooth transitions into the ribbon mode of aggregation. This ability to exist in both fibrous and network aggregation states is comparable to that known among the collagens and muscle proteins.

The amino acid compositions and conformations of proteins which can form cholesteric helicoidal systems are reviewed and compared with the protein of *Buccinum* periostracum. This property is apparently confined to alpha helical rod-shaped proteins and globular tektins. The beta conformation does not favour cholesteric organization.

The structures and compositions of other molluscan periostraca and periostracum-like structures from other invertebrate phyla are compared with the periostracum of *Buccinum*. While all periostraca and functionally related structures have certain basic features in common there is a considerable degree of variation at the molecular and organizational levels.

Introduction

The shells of molluscs have, as an outermost layer, a coating of uncalcified scleroprotein called the periostracum. Although this layer is frequently referred to as protective it is possible that this is now a secondary rôle, its primary function being an involvement in the deposition of the inorganic phase of the shell, possibly acting as a substratum or more actively as a selectively permeably membrane, generating a potential utilized in the nucleation of calcium carbonate (see for example, Digby 1968). Older molluscs are frequently found in the condition where large areas of the periostracum have been lost, probably through abrasion, without any apparent serious erosion of the shell. This latter observation helps to reinforce the suggestion that the water and corrosion proofing qualities of the periostracum may only be of secondary importance in present day species.

Examination of the fine structure of periostraca from lamellibranch molluscs has in most cases revealed a rather simple organization which, apart from differences in layering, shows only a relatively low degree of order (Kawaguti & Ikemoto 1962; Kawakami & Yasuzami 1964; Bevelander & Nakahara 1967; Tsujii 1968; Taylor & Kennedy 1969; Neff 1972*a*). In gastropods the situation may be more complex. Hunt & Oates (1970) in a preliminary account described the fine structure of the structural protein in the periostracum of the gastropod *Buccinum undatum* L. showing it to be made up of protein ribbons built by periodic aggregation of small sub-units, as in the formation of fibrin from fibrinogen. The preliminary studies suggested that these ribbons were laid down in parallel to form large sheets, the sheets being apparently overlaid in such a manner that the ribbon axis in successive sheets was rotated progressively through a small angle relative to those above and below. The effect, known as helicoidal layering, is observed as a parabolic lamellar structure when obliquely sectioned and has been described in a variety of other biological and non-biological situations (Bouligand 1965*a*, 1972; Locke 1964; Neville 1967; Robinson 1966; Kenchington & Flower 1969).

At the same time that Hunt & Oates (1970) published their observations of *Buccinum* periostracum a similar study of the periostracum of the gastropod *Littorina littorea* was also published by Bevelander & Nakahara (1970). Here the outer layers of the periostracum seemed to contain sheets and ribbons with a regular periodicity very similar in appearance to those in *Buccinum* but with no evidence of a helical type of organization. More recently a study of the mode of formation of periostracum in the gastropod *Lymnea stagnalis* by Kniprath (1972) has shown that in this case the periostracum, although composed of distinguishably different layers, is apparently formed from amorphous scleroprotein without a periodic organization. The structure is similar to that seen in bivalve molluscs.

The present communication is a more detailed account of the structure of the periostracum in *Buccinum undatum* in which we show that the helicoidal model is sufficient to account for many of the features of the organization of the material and in which we demonstrate that the constituent macromolecules are in the alpha helical class of structural proteins. The molluscan periostracum is discussed in the context of other similar biological materials and its mode of assembly compared with other structural protein systems. We also discuss the important point of the basis underlying the great chemical stability of the periostracum.

Materials and methods

Living *Buccinum undatum* were obtained either from the laboratories of the Marine Biological Association, U.K., Plymouth, England or the Scottish Marine Biological Association, Millport, Isle of Cumbrae, Scotland. Animals from the former source were found to be preferable as the shells were cleaner with the periostracum less contaminated with algal and other growths.

The periostracum in this species is quite thick and can be readily peeled from the shells with forceps. Material for sectioning was fixed overnight in pH 7, 0.1 M cacodylate buffer containing 5% glutaraldehyde and 0.25 M sucrose followed by post-fixation in cacodylate buffer containing 2% osmium tetroxide for 30 min. Following dehydration through alcohols the fixed material was embedded in Epon via propylene oxide.

Sections were cut at 50 nm or less with a diamond knife and stained with ethanolic uranyl acetate and Reynold's lead citrate for 30–60 min in each. The response to stain was poor. Considerable difficulty was experienced in sectioning this material since it is both extremely hard and poorly permeable to resin as well as contaminated by sand grains included in the structure during its synthesis. Sections were examined at 80 kV in either a Siemens Elmiskop 1 or an AE1 801 electron microscope.

For examination of dissociated material, periostracum was abraded from the shell by scraping with a scalpel and the fibrous powder suspended in water. The suspension was subjected first to maceration in a Silverson high speed homogenizer followed by prolonged disruption in an M.S.E. ultrasonic disintegrator over a period of about 30 min at 4 °C. Dispersates were deposited on carbon-coated copper grids and negatively stained with phosphotungstic acid (PTA) pH 5.6, or shadowed with gold-palladium, or positively stained with uranyl acetate. Positive staining was achieved only with difficulty and results were poor, probably due to the low reactivity of the material.

For scanning electron microscopy, small fragments of periostracum were mounted in various orientations on aluminium stubs, thinly coated with gold to prevent charging effects and examined in a Cambridge 'Stereoscan' electron microscope. We are indebted to Dr T. Gray of the Department of Botany, Liverpool University for providing the facilities of this instrument.

The preparation of cleaved sheets for surface replication and transmission electron microscope examination was as follows. Sheets of periostracum about 1 cm square, having no obvious tears or holes were selected and cemented with Araldite between the machined ends of two aluminium rods 3 cm diameter. Care was taken to ensure that there was only adhesive contact between periostracum and metal on either side of the periostracum sheet and that there was

---

Description of plate 1

Figure 1. Scanning electron micrograph of a fragment of periostracum showing the surface normally in contact with the shell. (Magn. × 21.)

Figure 2. Detail of part of the specimen shown in figure 1, showing the elaborate convolution of the material. (Magn. × 104.)

Figure 3. Scanning electron micrograph of the outer surface of the periostracum showing its papillate character. (Magn. × 23.)

Figure 4. Detail from figure 3, showing the folding of the material at the base of a papilla. (Magn. × 528.)

Figure 5. This electron micrograph of disrupted periostracum shadowed with Au/Pd shows the ribbon-like character of the constituent fibres and the striation of the ribbons. (Magn. × 20400.)

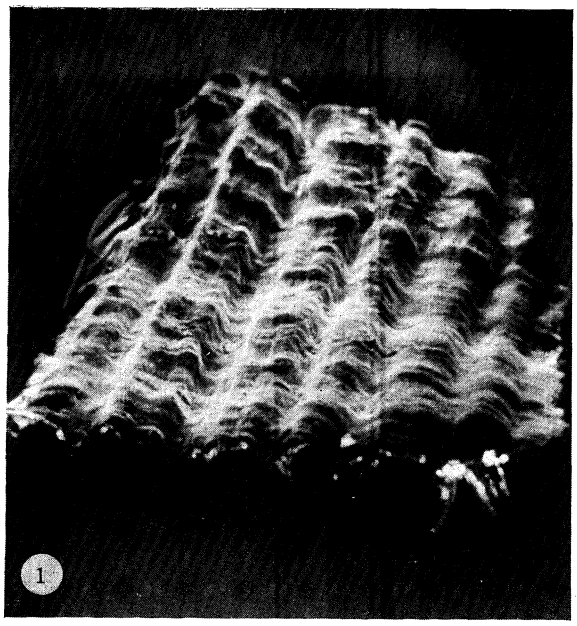

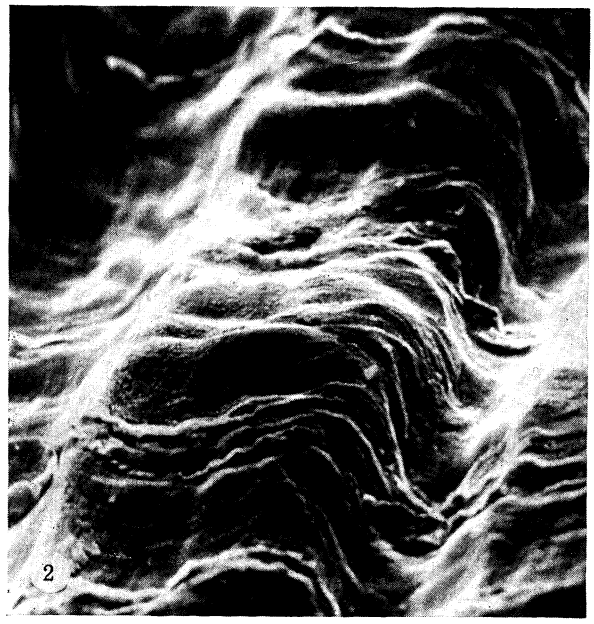

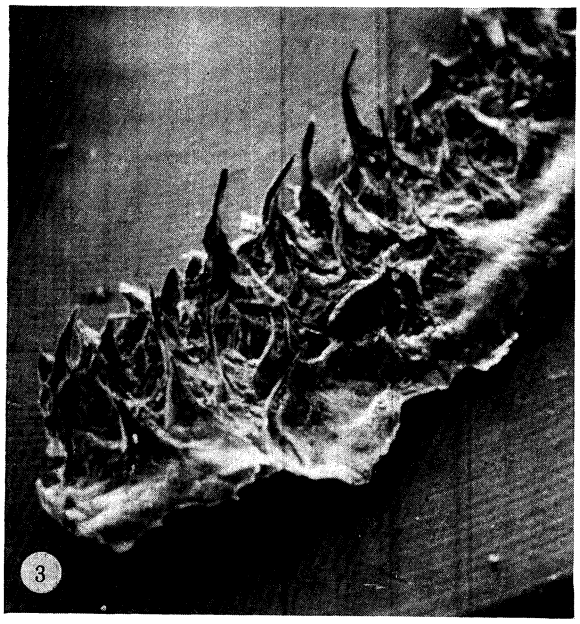

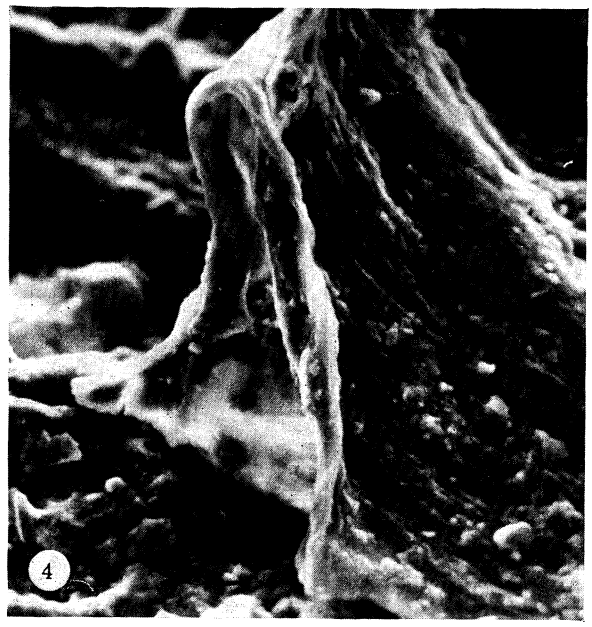

FIGURES 1–5. For description see opposite.

(*Facing p.* 420)

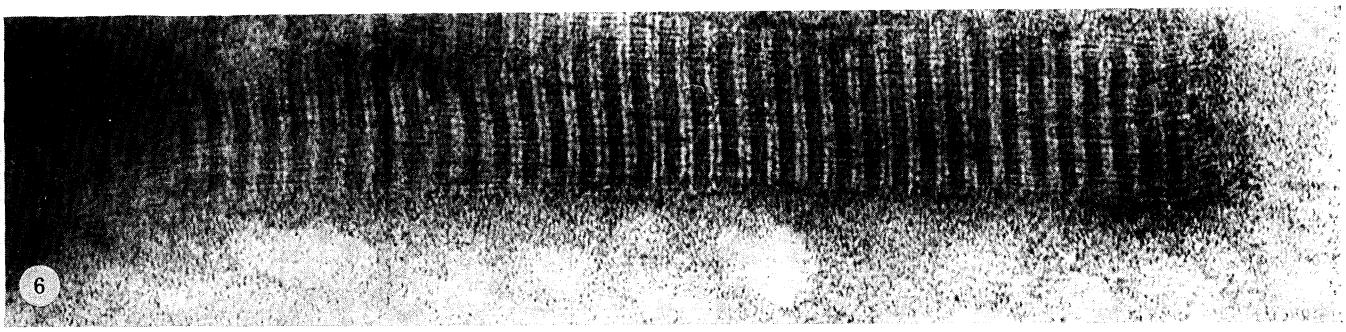

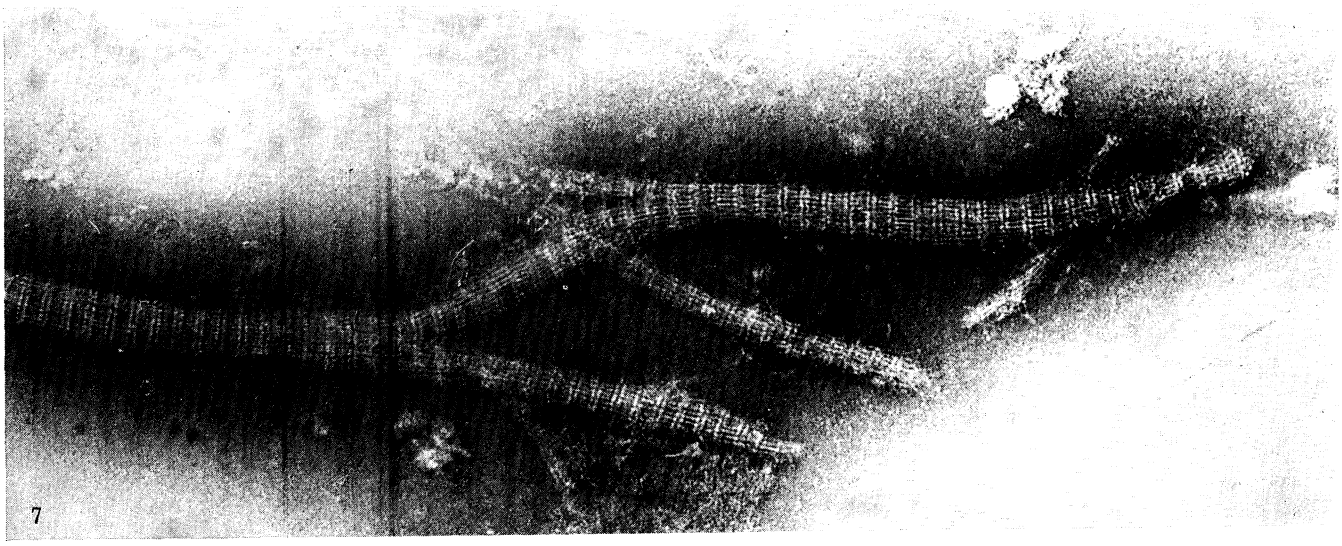

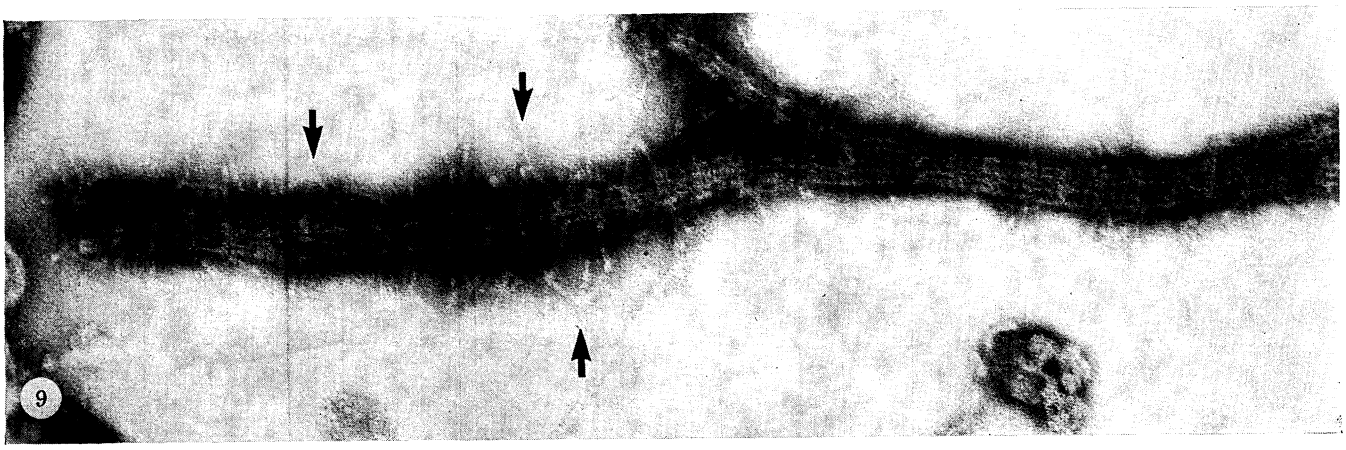

FIGURES 6–9. For description see opposite.

no metal to metal adhesion. After allowing adequate time for setting of the adhesive at room temperature the aluminium bars were flexed relative to one another. This had the effect of cleaving the periostracum along the lamellae of the stacked protein sheets composing it, in such a manner that sheets at several levels in the stack were usually visible in one cleaved surface. Gold–palladium-shadowed carbon replicas of cleaved surfaces were made, with cellulose acetate (Bioden R.F.A.) by a single step method.

Certain periodic structures observed in electron micrographs were linearly integrated in the following manner. An area of micrograph showing a considerable length of uninterrupted linear periodicity was selected and printed as a strip long enough to fix around a tube of about 10 cm diameter so that the periodicities repeated around the tube. The tube was placed in the chuck of a lathe and rotated rapidly while illuminated by a stroboscopic lamp. Flash rate was adjusted to achieve a setting where the periodicity was optically stationary and reinforced optimally. Photographs of the integrated pattern were taken at shutter speeds longer than the rotation period of the lathe.

Sections for light microscopy were cut on a Slee cryostat from unfixed material embedded in agar and were examined unstained through polarization optics in a Reichert Zetopan microscope.

X-ray diffraction studies of periostracum are rendered difficult by contamination of the material with calcium salts derived from the shell, microscopic grains of sand and other extraneous mineral particles and possibly bound iron. However material which has been carefully demineralized with EDTA and agitated in water over long periods to remove solid particles can be dried flat so that strips can be cut and assembled in bundles for X-ray study. Sandwiches of periostracum were examined at high angles in a flat camera system with the beam of Ni-filtered Cu radiation perpendicular to, or in the plane of, the periostracal sheet.

General description of the periostracum

Gastropod periostraca vary considerably from species to species in thickness, colour, flexibility, strength and macroscopic architecture. In *Buccinum* the periostracum is usually brown although this may vary markedly depending upon the habitat from which the animal has been taken. Specimens from Plymouth have a clean light brown periostracum while it is a darker greenish brown in those taken around the Isle of Cumbrae. In the latter case the colour seems to be due to the algae which flourish on the shell surface. After cleaning with alcohol and acetone most samples of periostraca have a similar colour and do not fluoresce or only slightly under

---

Description of plate 2

Figures 6–16 are of disrupted periostracum negatively stained with phosphotungstic acid.

Figure 6. This electron micrograph and figure 7 show the compact form of the protein ribbon. For further details see the text. (Magn. × 120000.)

Figure 7. For details see text. (Magn. × 112500.)

Figure 8. The less compact form of the protein ribbon. The filament organization of the ribbon is more obvious. (Magn. × 124000.)

Figure 9. A similar ribbon to that shown in figure 8 but demonstrating the almost total separation of a single filament (lower centre) and the organization of the sub-units at the edges of the ribbon in a nonlinear aggregation mode (arrows). (Magn. × 189000.)

ultraviolet light. The periostracum is thick in *Buccinum* and can be easily stripped from the surface of the shell although it tends to tear readily along the line of the spirals of the shell. Detached sheets are not smooth but elaborately convoluted conforming to the contours of the underlying shell (figures 1 and 2, plate 1) which in *Buccinum* is intricately sculptured. The surface of the periostracum is covered externally by numerous fine papillae (figures 3 and 4, plate 1) which make it velvety both in appearance and to the touch. These papillae appear to consist of layers drawn out from the major body of the periostracum. All these factors render examination and interpretation of thin sections difficult at the ultrastructural level since one is not dealing with relatively simply orientated planar sheets of secreted material applied to a 'smooth' surface as is more nearly the case with many (although by no means all) of the shells of lamellibranch molluscs. Instead planes of orientation may change rapidly over short distances.

Composition of the periostracum

As has been previously shown (Hunt 1970*a*, 1971) the periostracum in *Buccinum* is composed almost entirely of a scleroprotein with a small amount of covalently bound carbohydrate as pentoses, methyl pentose, hexose and hexosamine. The report of Peters (1972) that the periostracum of *Buccinum* contains chitin has recently been confirmed by us. Periostracum can be solubilized by suspending in anhydrous formic acid at room temperatures for several months. These solutions yield a small precipitate on dialysis against water and this precipitate has the composition and infrared spectrum of a partly formylated chitin–peptide complex. Compositionally the scleroprotein is of a structural protein type relatively low in glycine (Hunt 1971) and resembling in its amino acid make up some of the alpha types of structural protein such as for example the keratins. Evidence at present available from studies being carried out in this laboratory suggest that the scleroprotein is stabilized in part by some form of tanning with aromatic compounds although perhaps not by a process exactly similar to that found in arthropods. The presence of a number of brominated and chlorinated tyrosine residues in the scleroprotein and in particular dibromotyrosine (S. Hunt, unpublished results) points to the presence near the locus of synthesis of the periostracum of an oxidase which could perhaps be a phenol oxidase.

In the absence of precursor protein in the untanned or unstabilized form it is difficult to say with certainty that the protein of the periostracum is a single molecular species. However, it seems likely from the results obtained with the small amounts of material solubilized by autoclaving (Hunt 1971) that there is one dominant protein type present with perhaps very much smaller amounts of others. It would seem reasonable to assume therefore for the present that material observed at the ultrastructural level in disrupted preparations of the periostracum can be discussed in the same context as its overall amino acid composition.

Fine structure of the fibrous protein of the periostracum

Periostracum which has been homogenized and then further disrupted by ultrasonic treatment to a fine suspension is revealed as composed of ribbon-like fibrils when examined in the electron microscope (figures 5–8, plates 1 and 2). These ribbons are usually between about 5 and 100 nm wide having a distinctive longitudinal repeat pattern 32 nm which in shadowed preparations (figure 5, plate 1) gives an alternately thick and thin corrugated appearance to the

ribbon. These striations are further revealed in negatively stained preparations in two slightly different forms. In the first (figures 6 and 7, plate 2) the fibril has a compact form and the major striation appears as a pair of prominent closely separated light bands (the A bands) each 6.0–6.5 nm wide separated from one another on one side by a wider gap of about 16 nm.

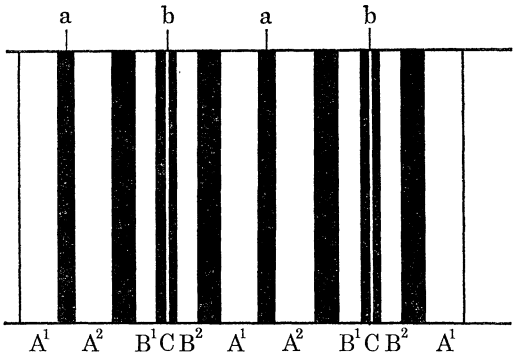

FIGURE 10. Diagrammatic representation of the banding pattern seen in negatively stained ribbons of periostracal protein 'a' and 'b' represent centres of symmetry. Numbered superscripts to capital letters designate members of identical pairs of bands. For details see text.

In this latter gap there can be just discerned at lower magnifications a second pair of light bands (the B bands) each 3.5–4.0 nm wide and separated from one another by a centre to centre distance of 6.5–7.0 nm. The B bands are separated from the A bands by a distance of about 2.5–3.0 nm on either side. The repeat pattern has centres of symmetry at 'a' and 'b' (figure 10) and in this respect resembles longitudinally repeating ribbonlike fibrous proteins such as fibrinogen and differs from native collagen. The light bands appear to originate as globular thickenings of a longitudinal filament system, running along the ribbon, which traverses the larger gap between the A bands, i.e. the gap in which the B bands occur, passing through the B bands but not in many cases continuing through the paired A bands. These filaments, approximately 6.5–7.0 nm apart, appear as longitudinal striations (figures 6–8). Continuity of the filaments across the A bands is not always obvious but is necessarily present since serially arranged globular thickenings can often be traced over considerable distances in phase with those of adjacent filaments. At high resolution (figure 12, plate 3) the space between adjacent B bands can be seen to contain a further layer of globular thickenings, the C band, lying in the symmetry axis b.

In the second type of ribbon (figures 8 and 9, plate 2), which appears in negative stain to be a variant only of the first, the major striation, i.e. that at the thicker part of the ribbon is less clearly separated into pairs of similar bands, overlaps appear to occur, the whole structure is less compact and separation of the longitudinally running filaments composing the ribbons can be discerned in many places. This is particularly apparent in figure 9 where a length of a single longitudinal filament has separated together with several smaller sections of the ribbon. These ribbons also sometimes appear to be composed of two or more overlaid layers (figure 8). The longitudinal filaments with their globular expansions also frequently appear in this second type of ribbon to deviate from the parallel and to cross over each other.

Under high resolution conditions the fine structure giving rise to the repeat along the axis of the ribbon resolves into what appears to be a series of dumb-bell shaped sub-units laid end to end along the fibre and side by side (figures 11 and 12, plate 3). These dumb-bells are some

32 nm long. The spherical expansions at their ends are 6.5 nm diameter and are connected by a bar or rod about 19 nm long. The central 'grip' region of the bar comprises three globular swellings. One swelling 3 nm diameter lies at the exact mid-point of the bar and is closely flanked by the two other swellings which are each 4 nm diameter (figure 12). There is no stagger in the side by side aggregation. It is tempting to assume from the appearance of these high resolution micrographs that these dumb-bells do indeed constitute the basic sub-unit. The larger globular units of the A bands in the negatively stained preparations would thus constitute the ends of the sub-unit while the two smaller globular units which form the B bands lie on either side of the

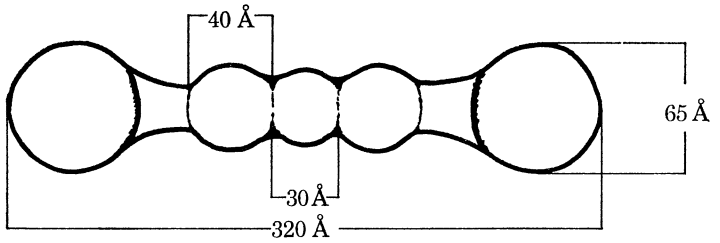

FIGURE 19. Diagrammatic representation of a single protein sub-unit component of the periostracal ribbon. For details see text.

partly globular central 'grip' region of the dumb-bell bar. The tenuity of connection across the two halves of the A band pair leads to the belief that it is here that individual subunits polymerize to form the long filaments. There is however no real reason, in the absence of micrographic evidence to the contrary such as might be forthcoming from observation of protein monomers, not to suggest that the reverse might apply, i.e. that the smaller globular regions lie on either side of the centre of symmetry at the extremities of the molecular long axis. This presupposes that each fundamental sub-unit is composed of two larger and two or three smaller globular areas arranged longitudinally along a rod-shaped molecule and not some multiple of this. Precedent for this type of structure exists in the form of the fibrinogen monomer of fibrin. Of course it would be possible for the sub-unit to be a rod-shaped asymmetric molecule with one end a larger globular region and the other a small globular unit with the mode of assembly producing symmetric units from these by linking at the globular thickening between the two B bands. Other variants including two different monomer basic units one small and one large are also clearly feasible. It would also be possible to account for the periodicity of the ribbons on the basis of an aggregation of rod-shaped sub-units with globular regions not along the axis of the ribbon but at 90° to it as has been suggested for certain forms of fibrin. (Hall & Slayter 1959). The latter postulate would seem to be readily dismissed by examination of (figures 13–16, plate 2). As already mentioned when commenting upon figure 9, a continuous chain of globular sub-units interspersed with rod-shaped regions is readily discerned and can be matched with the ribbon from which it has been detached. Similar areas can be seen in figure 8. At the ends of the ribbons where breaks have occurred (figures 13–16) single units can be seen protruding beyond the points of termination of others. In such places it ought also to be possible to detect the ends of the subunits themselves if, as seems probable the mechanically weakest places are at the junctions between the aligned subunits and not in their peptide backbones. In practice it was found that, in the majority of cases examined (figures 14–16) the ribbon ends sharply in the region of the large globular part of one half of an A band. This strongly supports the hypothesis that the sub-unit is the dumb-bell already described. That lateral cross-linking with

other sub-units does indeed occur between the ends of the dumb-bells seems strongly suggested by figure 9 (arrowed areas) where several units appear joined at this point to one another (but see later). The appearance of these multiple junctions suggests that, as well as the expected end to end covalent cross-linkage of sub-units responsible for the length of the ribbons, side-by-side bondings also exist between the major globular regions. Based on the very highly magnified views shown in figure 12 we tentatively put forward the structure shown in figure 19 which takes into account criteria suggested by Preston (1971) for the assessment of negatively stained fibrous materials.

Organization of the intact periostracum

(*a*) *Light microscopic appearance of periostracal sections*

Sections of the periostracum examined in the light microscope (figures 20 and 22, plate 4) appear much as described by Dakin (1912) in having a layered organization of evenly stained material. Dakin describes the layers as being oblique; this is less obvious in the sections examined here except in the regions of the papillae where the most superficial layers do seem to curve away out from the surface of the general body of the periostracum although this is not wholly confirmed by the fine structural studies which follow. Examined between crossed polaroids (figure 23, plate 4), the periostracum shows a pattern of alternate dark and bright banding suggestive of a layered structure of orientated thin sheets of essentially parallel fibres.

(*b*) *Fine structure of the intact periostracum*

(i) *Fine structure of the structural protein* in situ.

The reason for the dark and light banding observed under polarizing conditions of light microscopy becomes apparent when ultra thin sections of the periostracum are examined in the electron microscope. The banding is now revealed (figure 24, plate 4) as originating in a layered organization of fibres or ribbons exhibiting parabolic disposition of the type which has become familiar from insect cuticle and other sources (Bouligand, 1965*a*, *b*, 1972; Neville 1967; Kenchington & Flower 1969).

A more detailed examination of the lamellae seen in figure 24, as for example in figures 25–27, plates 4 and 5, reveals that they are composed of the same ribbons with a regular repeat observed in the disrupted preparations. However, after staining with uranyl acetate and lead citrate the details of the axial repeat appear differently, the periodicity being nevertheless almost the same (31.3 nm). In some sections more extensive sheet-like arrays have been caught in the plane of the sections as is the case in figures 29 and 35, plates 5 and 6. Here it can be seen that alignment of the molecular sub-units must be possible in a very precise manner over a considerable distance.

Where the section has been cut exactly in the plane of the ribbons or sheets it is possible to look at the structure of the repeat in some detail (figure 17). A major dark band (the *a* band) 6.0–6.4 nm wide is the most prominent feature with a second fainter band (the *b* band) 3.0–3.2 nm wide halfway along the repeat. Slightly asymetrically disposed on either side of the *b* band are two further very faintly discernible dark bands, the *c* bands placed 2.3–3.0 nm from the nearest *a* band. There is some suggestion is certain regions of the sectioned material that the *b* band is further sub-divided. This can be more clearly seen in photographs prepared by linear integration (as described in Materials and methods) of a large number of individual repeats (figure 18). In some micrographs of sectioned material the lateral disposition of filaments

running parallel to the ribbon axis can just be seen. This effect is most prominent in the region of the *a* band (figure 27) where one would feel that the larger globular units, so clearly seen in negatively stained preparations, are pushing the rod-shaped sub-units sufficiently far apart for the filamentous sections of the rods to be visible by contrast against the background.

In some sections the ribbons and sheets show a somewhat different appearance (figures 28–30, plate 5) with a repeat of a major light band 9.0 nm wide separated from a second similar band by a dark area 23 nm wide which contains a centrally placed further fainter lighter band 3.0 nm wide. Here again fine light lines running parallel to the long axis of the ribbons and perpendicular to the cross-striation can just be seen. The effect would seem to be that of negative rather than positive staining and comparison of figures 28–30 with figures 6 and 7 indicates a distinct resemblance. The origin of the phenomenon is not clear but may result from negative staining of areas where embedding medium has failed to penetrate.

Description of plate 3

Figure 11. A more detailed micrograph of an area of figure 7. The linear aggregation of bead and rod structures is apparent here together with the regular, in register, lateral packing. (Magn. × 275 000.)

Figure 12. A highly enlarged detail from figure 11. This photograph was prepared by repeated copying in order to enhance contrast. The apparent mode of organization from dumb-bell-like units linearly aggregated is well seen here. (Magn. × 1 045 000.)

Figure 13. This micrograph shows a region of a ribbon where breakage has taken place. The break is staggered rather than cleanly across at right angles to the long axis of the ribbon. Ends of sub-units can be seen and termination seems to be at an A band (arrows). (Magn. × 198 000.)

Figures 14–16. These micrographs are of areas of ribbons similar to that shown in figure 13. Here the slightly greater magnification shows the termination of the filaments at the break to be probably at the end of a dumb-bell sub-unit (arrowed). In figure 16 a single filament continues beyond the end of the ribbon. (Magn. × 275 000.)

Figure 17. An electron micrograph of a protein ribbon in a sheet fixed, embedded and stained with uranyl acetate. The regularly repeated banded structure is apparent. For details see the text. (Magn. × 220 000.)

Figure 18. A repetitive print of figure 18. The structure of the banding pattern is sharpened and enhanced.

Description of plate 4

Figure 20. Light micrograph of a thin section of periostracum cut perpendicular to the sheet. Note the hair-like papillae. (Magn. × 120.)

Figure 21. The same section as figure 20 viewed between crossed polaroids.

Figure 22. Higher magnification view of a similar section to that seen in figure 20. Apparent layering in the plane of the periostracum is visible. (Magn. × 750.)

Figure 23. The same section as figure 22 between crossed polaroids. The impression of layering is accentuated and the alternation of light and dark bands is suggestive of a change in orientation in successive layers.

Figure 24. This electron micrograph, taken at very low magnification, shows a transverse section through almost the entire width of a sheet of periostracum. It corresponds essentially to the light micrograph shown in figures 22 and 23. The central split is associated with the lifting of layers which accompanies the formation of a papilla. Note the parabolic layered organization of the major part of the structure. (Magn. × 3800.)

Figure 25. A more detailed view of an area similar to that seen in figure 24. The parabolic organization clearly extends over considerable depths in the periostracum although it is equally clearly not of an altogether regular character. The composition from striated ribbons is now apparent. (Magn. × 18 900.)

Figure 26. Details of a parabolic lamellar area. Ribbons are seen edge on running from top to bottom centre and end on at right centre. The parabolicity seems to have broken down in the region left of centre, where a sigmoid effect is seen, but re-establishes at the extreme left. Note the 'ghost' secondary parabolae superimposed on the fans at the left due to the regular arrangement of the cross-striations on the ribbons at right angles to the ribbon sense. (Magn. × 53 200.)

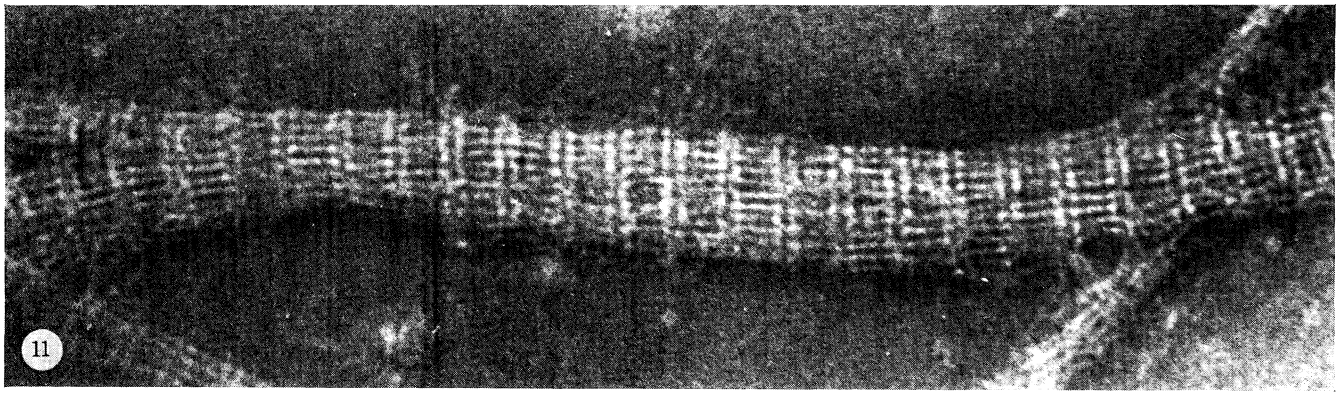

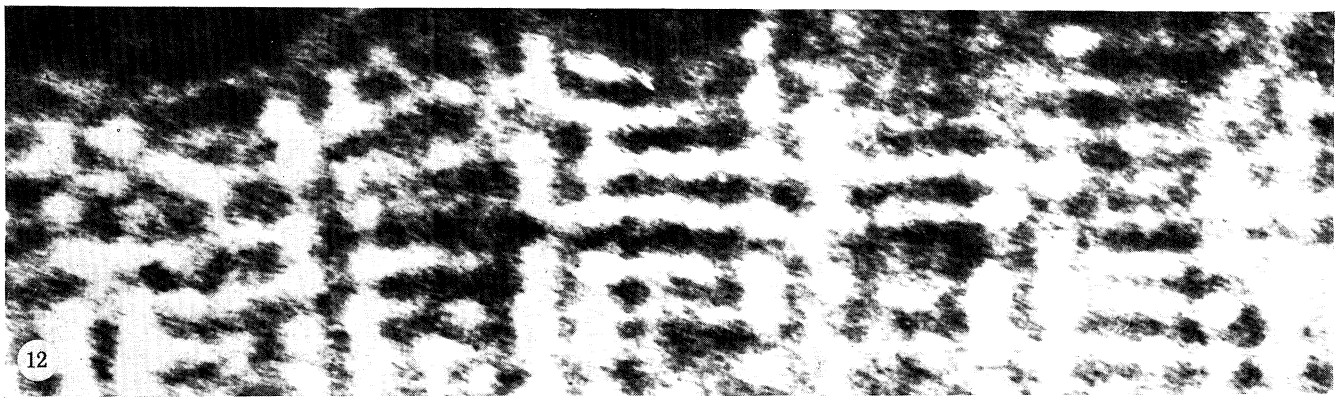

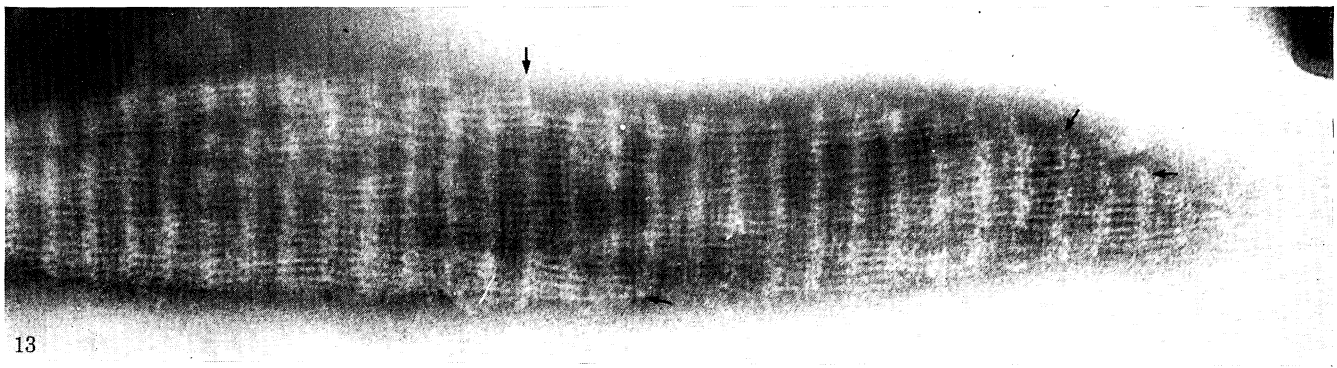

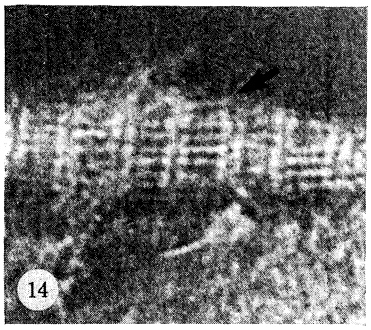

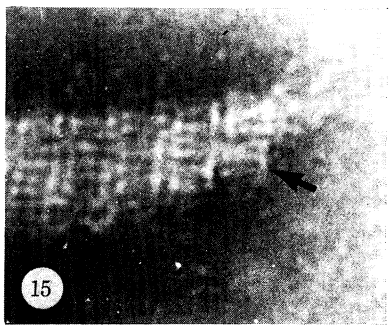

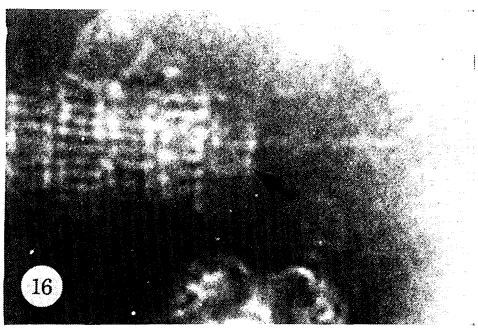

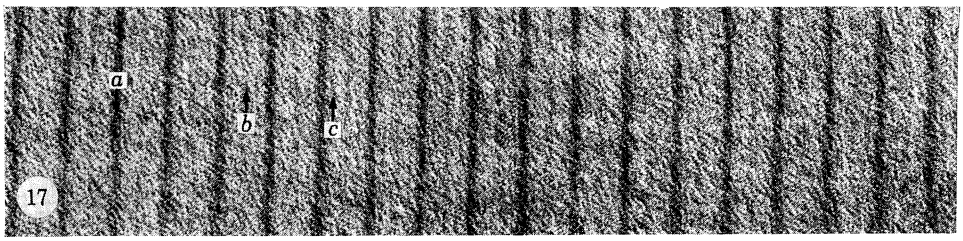

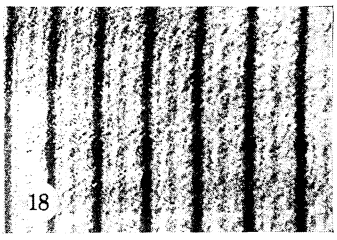

FIGURES 11–18. For description see opposite.

(*Facing p.* 426)

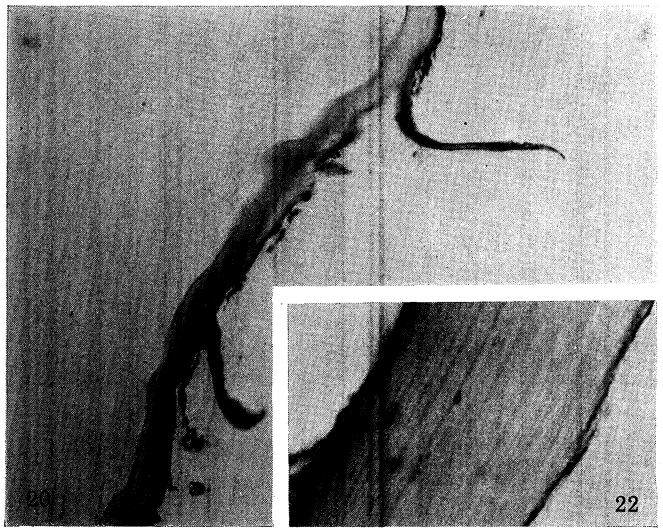

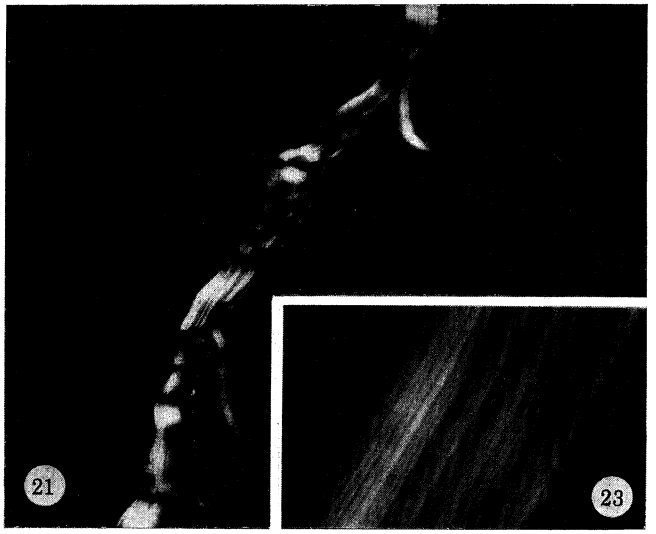

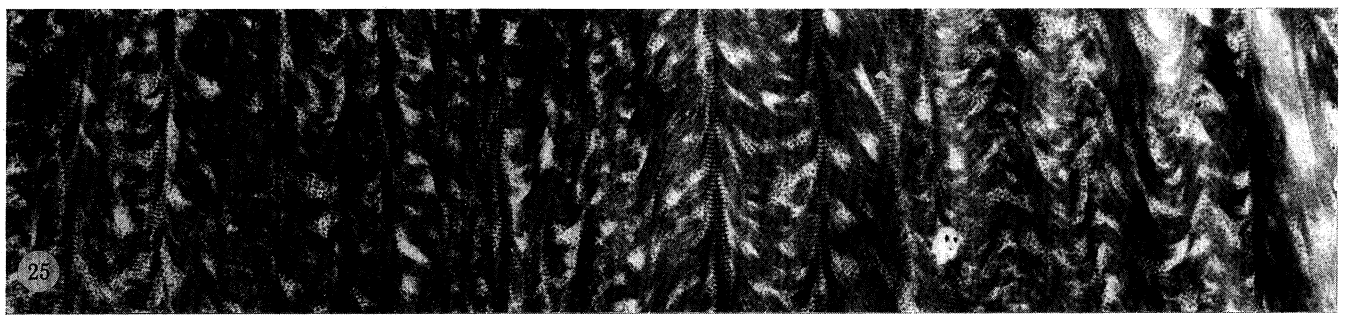

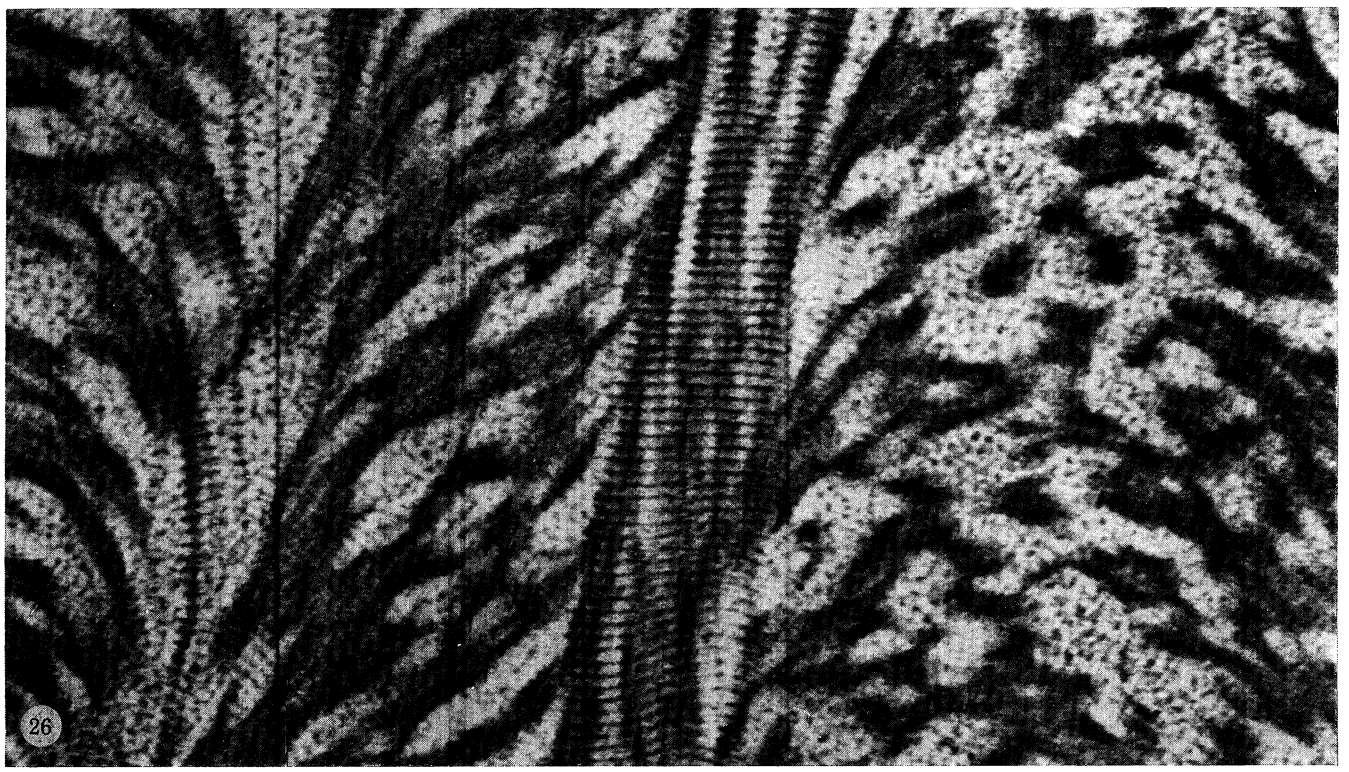

FIGURES 20–26. For description see p. 426.

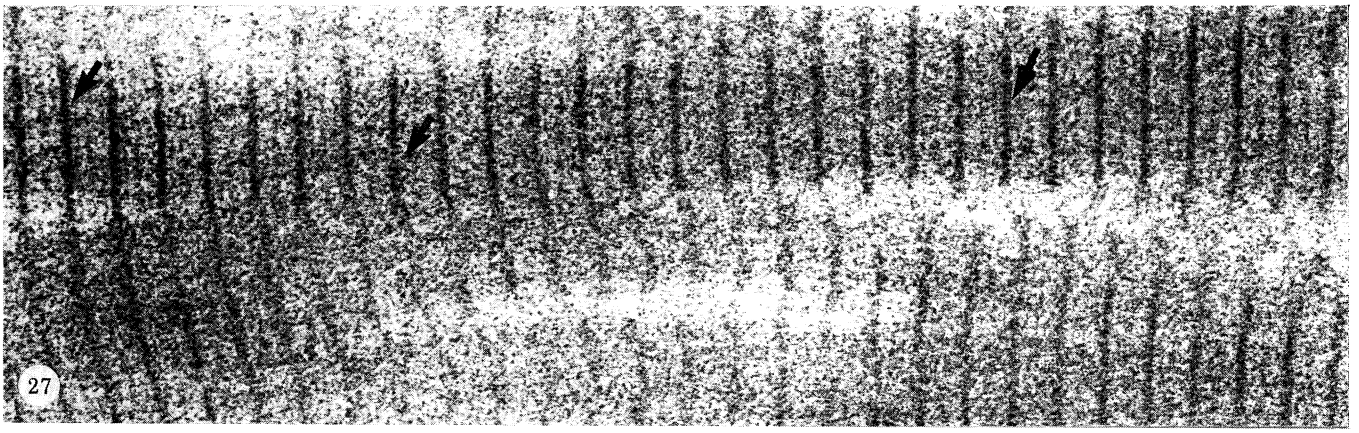

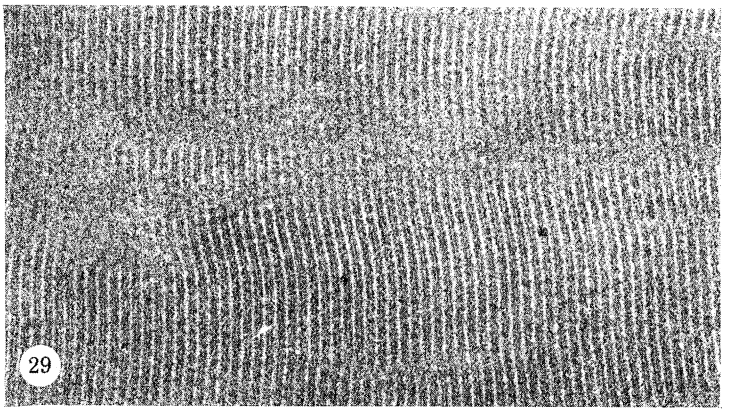

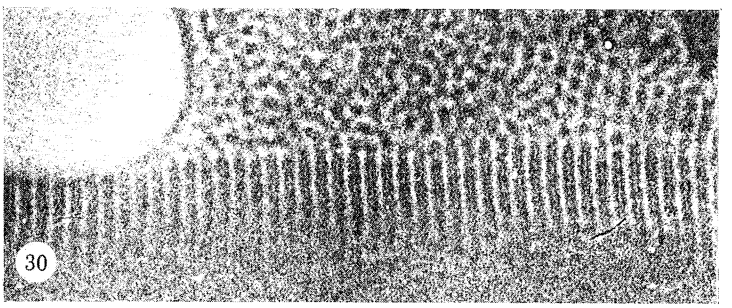

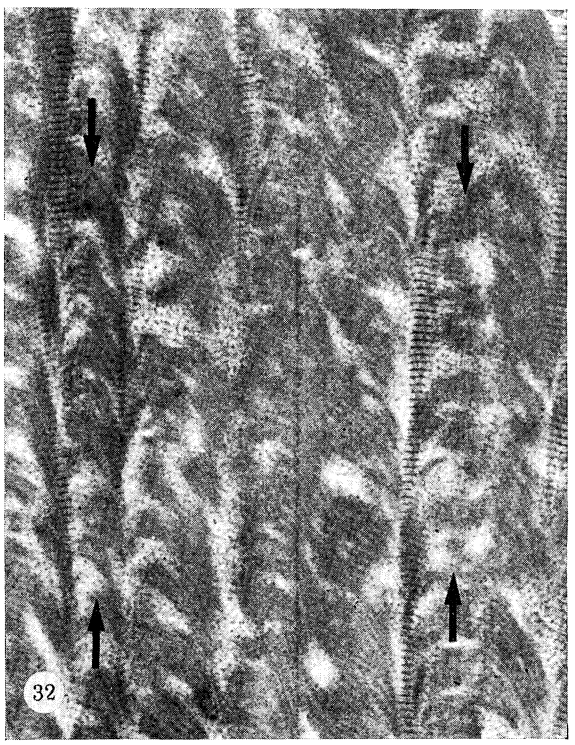

FIGURES 27–33. For description see p. 427.

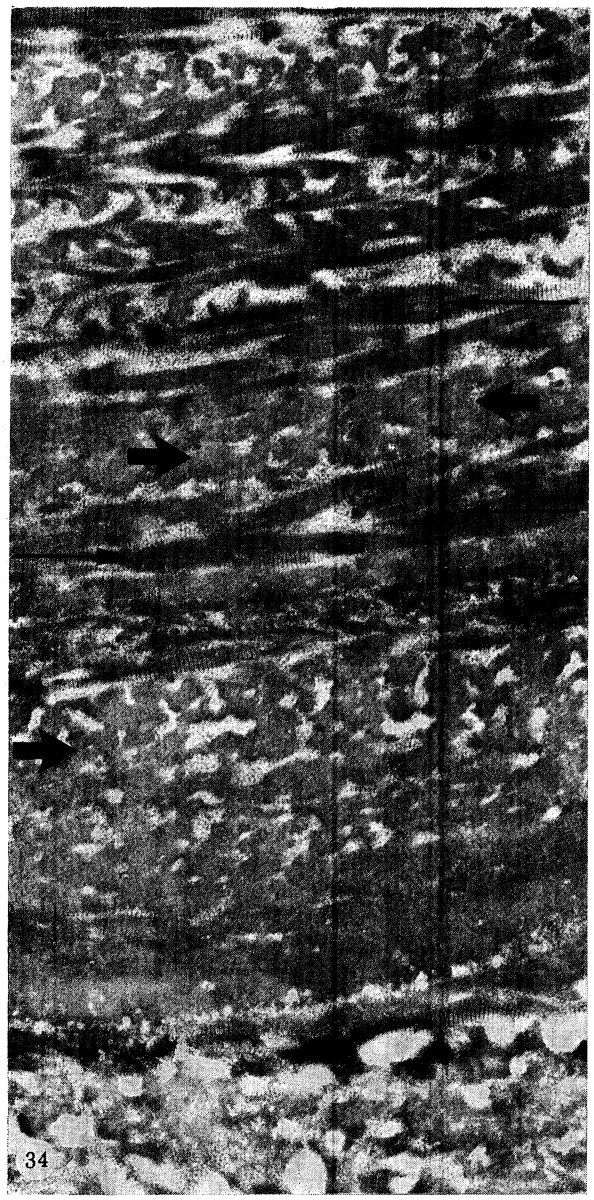

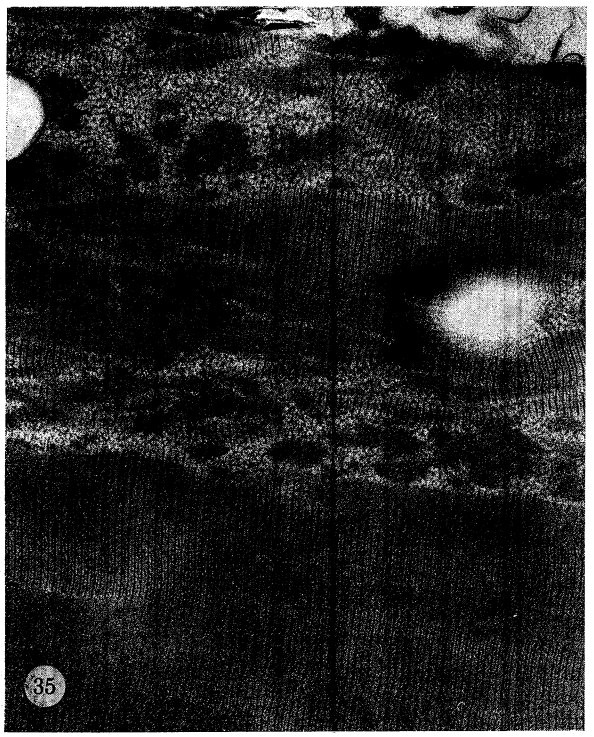

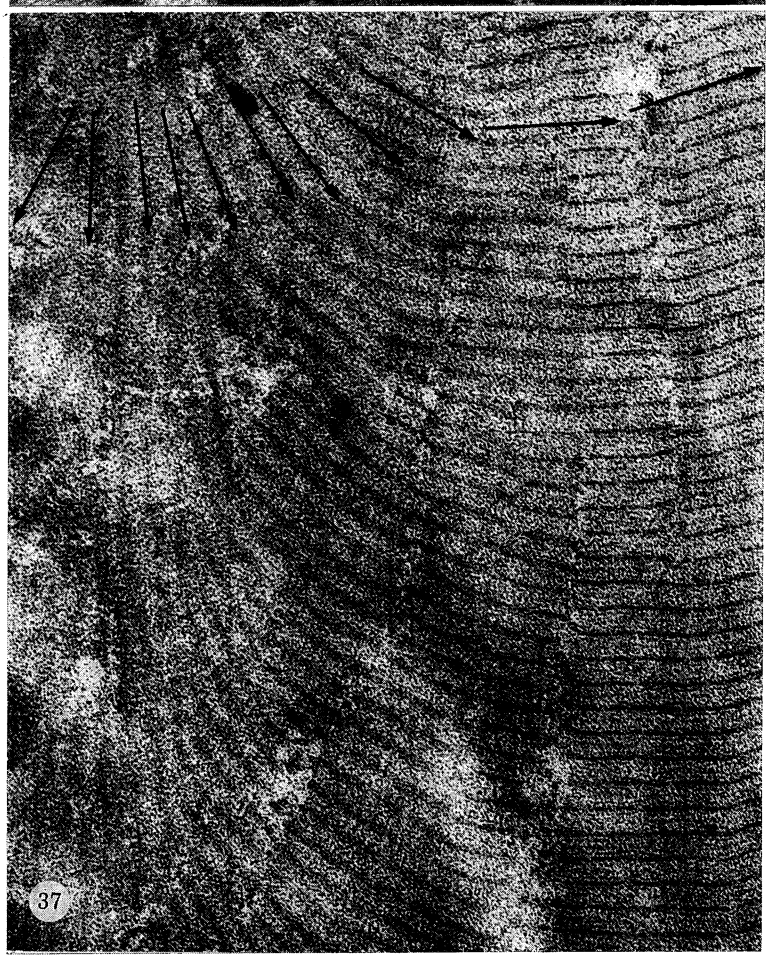

FIGURES 34–37. For description see opposite.

(ii) *Organization of the lamellae*

The most prominent feature of the periostracal sections cut in most planes is the lamellar mode of organization with a layering of protein ribbons roughly parallel to the periostracal surface and demonstrating the parabolic appearance already mentioned as being well known in numerous other situations. The organization is clearly in principal in the class of twisted fibrous arrangements first recognized by Bouligand (1965*a*, *b*) in biological systems and which produce in section parabolic phenomena originating in a regular helicoidal layered distribution of microfibres as shown in figure 31*a*.

The structure of the lamellae are shown in more detail in figures 25 and 26. Here the changing orientation of the protein ribbons from parallel to the plane of sectioning through oblique and perpendicular to that plane and back again to complete one lamella is clear and some of the parabolae are almost truly symmetrical. This indicates that for these particular regions of the periostracum the direction of rotation of the fibres or ribbons in the layers is constant, or nearly so, as is the angle of rotation.

In figure 25 the distribution of the parabolic lamellae is relatively regular over quite a large area perpendicular to the plane of the periostracal sheet, it is however more usual to find a much

---

Description of plate 5

Figure 27. This electron micrograph shows detail of the ribbon organization in an area similar to that of figure 26. Here the ribbon longitudinal axis and the tangents to the parabolae are approaching or identical. Note how the *a* bands tend to show lateral separation into rod-shaped units (arrowed). As the parabolic tangent deviates from the ribbon long axis the transverse striations become less distinct. (Magn. × 192 000.)

Figure 28. A section of periostracum showing the occasionally observed phenomenon of contrast reversal in the staining of the transverse striations on the ribbons or sheets (for details see the text). Note the vacuolation close to the surface of the material and the change from ribbon or sheet-like organization to a lattice of particles. Stained with uranyl acetate and lead citrate exactly as the other sections figured in this paper. (Magn. × 22 800.)

Figure 29. Detail from figure 28. (Magn. × 44 000.)

Figure 30. Detail from figure 28. Note the smooth transition of the ribbon striation into the packing of the dark centres. There is some evidence in the dark striations of lateral separation into rods. (Magn. × 65 600.)

Figure 32. Section of a helicoidal region in which there is a considerable degree of irregularity. Changes in sense of rotation of the layers over short distances appear to give rise to the sigmoid rather than paraboloid figures seen in the arrowed areas. (Magn. × 31 500.)

Figure 33. In this section the parabolae reverse direction (indicated by directional arrows) probably as a result of reversal of mode of sheet rotation. (Magn. × 22 000.)

Description of plate 6

Figure 34. Area of semi-orthogonal organization. In this section the helicoidal organization mode seems to begin to fail progressively from the top of the micrograph. In the region delimited by heavy short arrows the majority of the fibres or ribbons are approximately normal to the plane of the plate while they lie at right angles to this in the immediately adjacent zones marked with long arrows. (Magn. × 18 900.)

Figure 35. Section of periostracum in the vicinity of its outer surface. Helicoidal architecture is not apparent but there is evidence of orientation of the sheets and ribbons in only two directions approximately separated by 90°. (Magn. × 24 000.)

Figure 36. Apparent decussant organization of ribbons (for details see text). (Magn. × 38 400.)

Figure 37. Extreme oblique section in the plane of the periostracum. Each individually rotated layer in the helicoidal system is apparent in this section, which encompasses just over 90° of rotation from left to right. The parabolic effect is due to the cross-striations on the ribbons rather than the ribbons themselves. Compare this micrograph with figure 31(*a*). (Magn. × 102 000.)

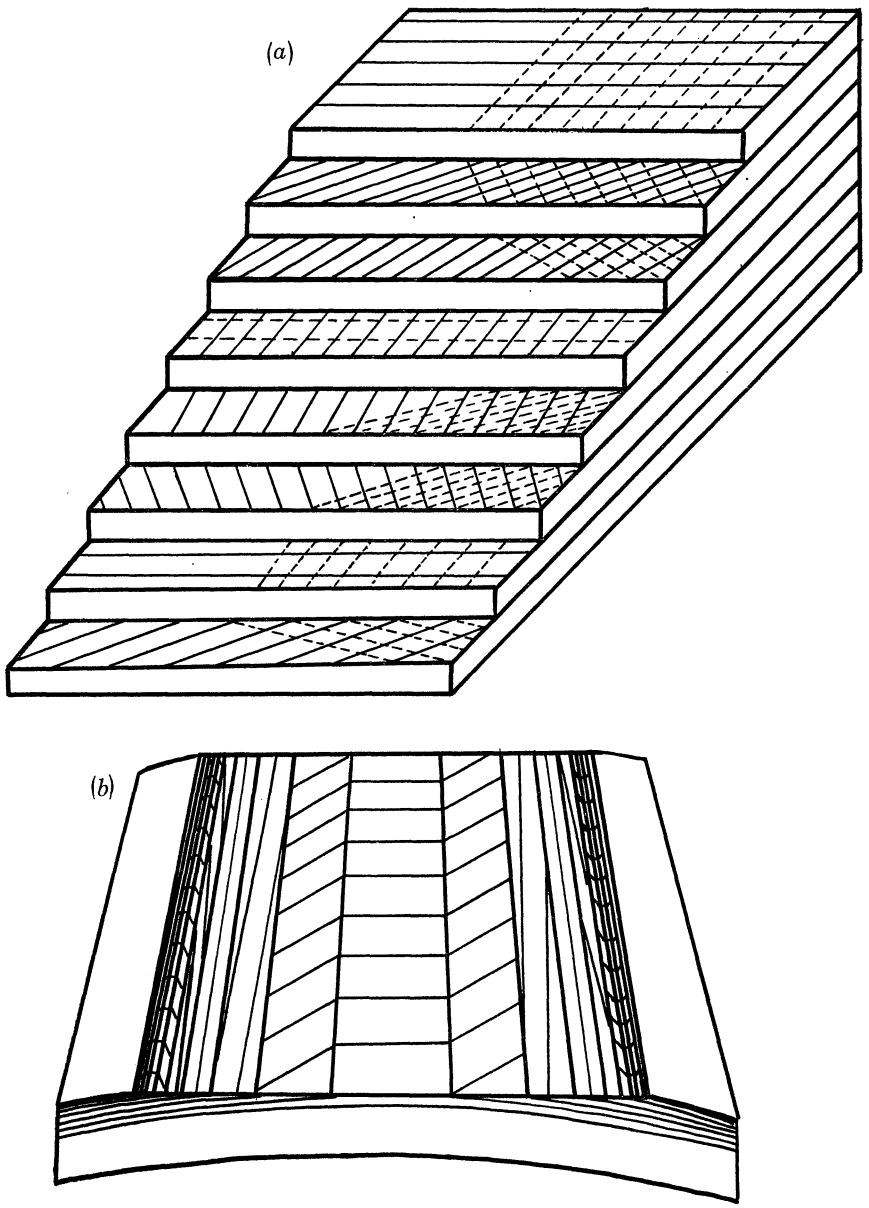

FIGURE 31 (*a*). A conceptual diagram illustrating the derivation of the parabolic patterning in oblique sections of the periostracum. Each step represents a single layer rotated at a fixed progressive angle relative to its fellows immediately above and below. The bands on the steps can in the case of periostracum be taken to either represent the longitudinal axes of the ribbons, which all lie parallel within any one layer, or else the transverse striations on the ribbons. (*b*) A conceptual diagram illustrating in a similar manner to (*a*) the effect of the parabolic artefact of obliquely section a helicoidal structure when the planes or layers are curved rather than flat.

greater degree of irregularity than this. Figures 26, 32, 33 and 34, plates 5 and 6 show sections in which the parabolic lamellae are interrupted by changes in the sense of rotation of the sheets or layers of ribbons composing the lamellae so that instead of a parabolic effect being produced a sigmoid form results from the sectioning (figure 32). In these zones rotation of the sheets progressively through to 90° occurs and then instead of rotation continuing in the same mode, i.e. the same direction, the direction is apparently reversed passing through 90° again to bring the

sheets back to their original position. Reversal of mode of rotation may produce changing direction of parabolicity (figure 33). Lamellar width, where parabolas are interrupted, also seem to vary very considerably. These effects may be more apparent than real resulting from sectioning in a curved or stretched surface (figure 31*b*). However where parabolas are regular there seems to be approximately the same number of sheets per lamella. Some almost orthogonal areas are occasionally seen where fibre sense suddenly becomes unidirectional for some distance (figures 34 and 35, plate 6). We have however not detected any discontinuities or faults in the system and this may be because the sheets are relatively speaking flat without violent curvature. Many of the wider lamella show a fan-like appearance in the distribution of fibrils more suggestive of a decussant mode of organization than the parabolic lamellae (figure 36, plate 6). This effect is probably due to sectioning helicoidal layers which are in a curved rather than flat surface. Such sections often show quite well the superimposed 180° out of phase parabolae due to the cross-striations on the ribbons and also show how well in register the cross-striations tend to be in adjacent layers and ribbons.

In sections which have been cut almost parallel to the lamellae the parabolic layers effect begins to disappear and the cross-striations of fibrils in individual superposed layers appear as systems of parallel lines intersecting one another at acute angles (figure 37, plate 6). In other regions, several layers may be caught in almost planar section where a rapid change in sense of rotation over a short distance has occurred. Figure 38, plate 7, a rather thick section, shows this effect so that the impression of rotation of the layers about an axis at the centre of the photograph is obtained. In these sections made at angles close to the plane of the lamellae, systems of fibrils may be found in which the cross-striations lie on curved arcs rather than parallel straight lines, suggesting an initial conclusion that a fan-like aggregation of sub-units composing the fibrils is possible (figure 39, plate 7). Closer examination of such arrangements reveals however that the curving effects result from sectioning of several layers of closely overlaid ribbons with a very gradual orientation change relative to one another. The intriguing features of such sections is the almost perfect register of the cross-striations in the immediately superposed layers of fibrils. Other areas do, however, occur in which a curved mode of aggregation into sheets does in fact seem to have taken place (figures 40 and 41, plate 7).

Each of the typically parabolic lamellae would seem to contain about 7–8 protein ribbons or sheets of ribbons which therefore gives a rotation of 20–25° between each constituent sheet and makes the helix approximately sixteen fold. However irregularities such as have been described above make layer counting difficult and it seems highly likely that the wider lamellae which are often incomplete contain potentially more layers.

In transverse section (figure 26) the striated fibrils as seen at the apices of the parabolae have a more irregular appearance than their ribbon-like manifestation in longitudinal section would suggest and although they are generally flattened along the curve of the parabola there is still the impression that they may be arranged in bundles. As the ribbons become more obliquely sectioned towards the apex of the parabolae the striated effect is lost and they appear as uniformly dark structures against the lighter background. Tilting however (figures 42–45, plate 8) reveals the striated pattern in these dark bodies.

It seems clear from the sections seen in figures 26, 32, 33 and 46, plates 4, 5 and 8, that the packing of the striated ribbons is not always close, the distance between them seems to vary and what appears to be a matrix of more lightly staining material seems to be present between the ribbons. Closer examination of this matrix reveals that it contains dark densely-staining granules

(about 19–20 nm wide) and it will be seen on examining figures 26 and 47, plates 4 and 8 that these granules are aligned along the dark *a* band of the ribbons and extend in the matrix as a regular geometrical array. A similar effect is seen in reverse in the curiously negatively stained sections (figures 28 and 30).

(iii) *Non-lamellate regions*

The helicoidal arrangement does not extend to all areas of the periostracum. In the inner layers, that is to say those nearest to the shell, the parabolic pattern becomes irregular or breaks down altogether; this also tends to happen in the outer layers (figures 28 and 35). Disorientated ribbons may then be seen in an extensive matrix and there are numerous vacuoles some seen in grazing section.

The matrix, consisting of irregularly rounded granules some 20 nm across (figure 48, plate 8) in a lighter staining background, shows evidence of being hexagonally packed and in many cases these granules which sometimes have lighter centres can be seen to be joined to each other by six fine threads (figures 47 and 48). These fine threads sometimes appear broadened as though they had flattened ribbon-like cross sections or sometimes doubled and often show a fine longitidinal periodicity (figure 48). Although six linking threads per dark centre is typical there are not uncommonly only five and sometimes seven. Often around the vacuoles, but elsewhere also, the hexagonal packing changes to a striated repeat (figures 49–51, plate 9) which can readily be seen to relate to the repeat of the ribbons. There is a direct physical relationship between the hexagonally packed matrix and the isolated striated ribbons which merge smoothly into each

Description of plate 7

Figure 38. This micrograph is of a rather thick section taken almost parallel to the plane of the periostracal sheet. Several layers mutually rotated relative to one another are visible. (Magn. × 157000.)

Figure 39. Fan-like effects resulting from oblique sectioning of super-imposed sheets with only slight relative angular displacement. The register between ribbon striation is a notable feature. (Magn. × 107520.)

Figures 40 and 41. These two micrographs show sections in the plane of the periostracum in which protein sheets are super-imposed giving rise to a plaid effect. An interesting feature of these sections is the apparently truly curved mode of lateral aggregation in the sheets particularly obvious in figure 40. (Magns: figure 40, × 80000; figure 41, × 50000.)

Description of plate 8

Figures 42–45. These are respective tilt pairs of helicoidal lamellar regions of the periostracum intended to show that the non-striated appearance of the material closer to the paraboloid vertices is due to obliqueness of sectioning. Note how tilting causes reappearance of striation in the arrowed areas. Figures 42 and 45: $x = +20°, y = -20°$; figures 43 and 44; $x = -20°, y = -20°$. (Magn. × 56100.)

Figure 46. Transverse section of the striated ribbons. Note their irregular outline and the absence of evidence of sub-unit structure. Large spaces filled by a matrix of granules and threads occur between the ribbons. (Magn. × 86000.)

Figure 47. This electron micrograph shows a non-lamellar region of the periostracum. The field contains striated ribbons and an extensive matrix of dark granules. Note the relation between the granules and the *a* bands of the ribbons (for details see text). (Magn. × 74800.)

Figure 48. (and insets *a*, *b* and *c*) Detail from figure 47 showing the lattice of rounded granules lying between the ribbons. Note the evidence of hexagonal packing of these granules, the fine threads which connect the hexagonally disposed centres (circled areas) and the evidence of striation on some of the connecting threads (arrowheads). In some cases the threads either appear doubled or else as broader ribbons (short arrows). There is a clear smooth transition from the dark *a* bands of the striated protein ribbons into the hexagonal matrix. Threads connect *a* bands to the dark centres. (Magn. × 158000.)

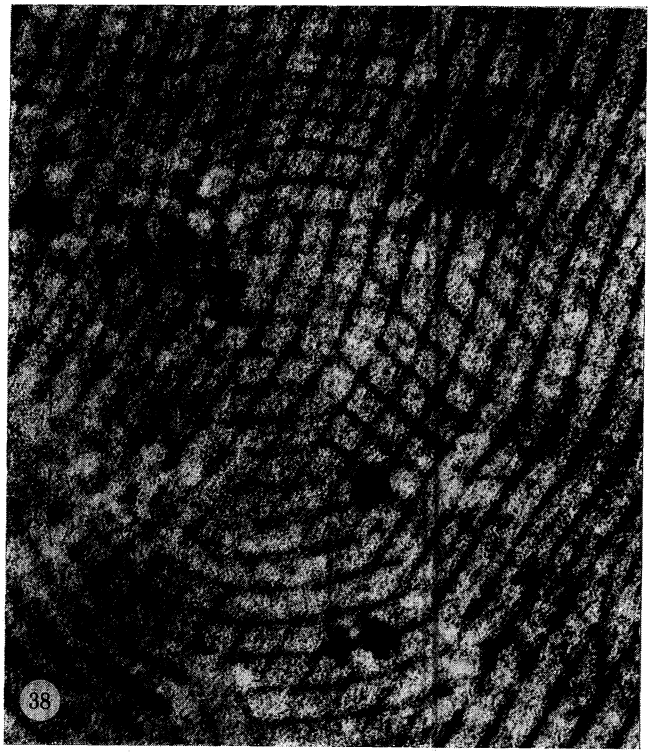

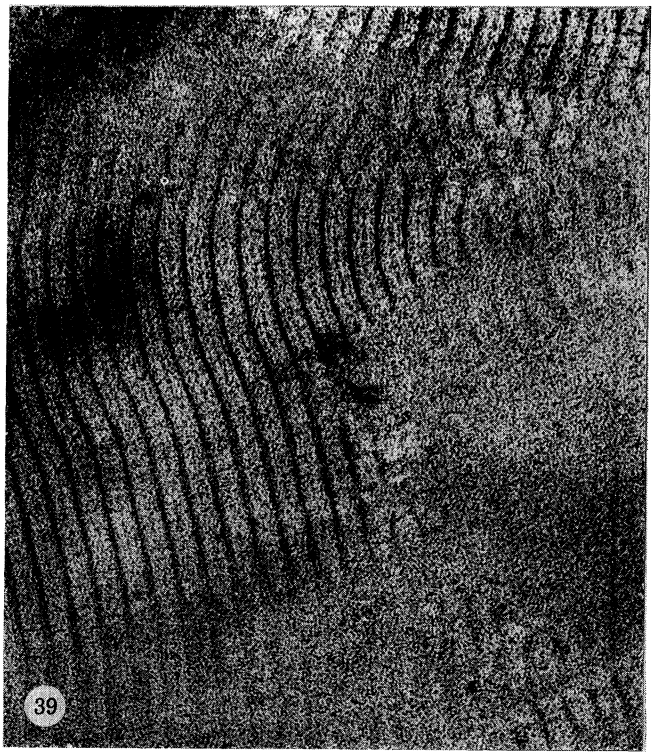

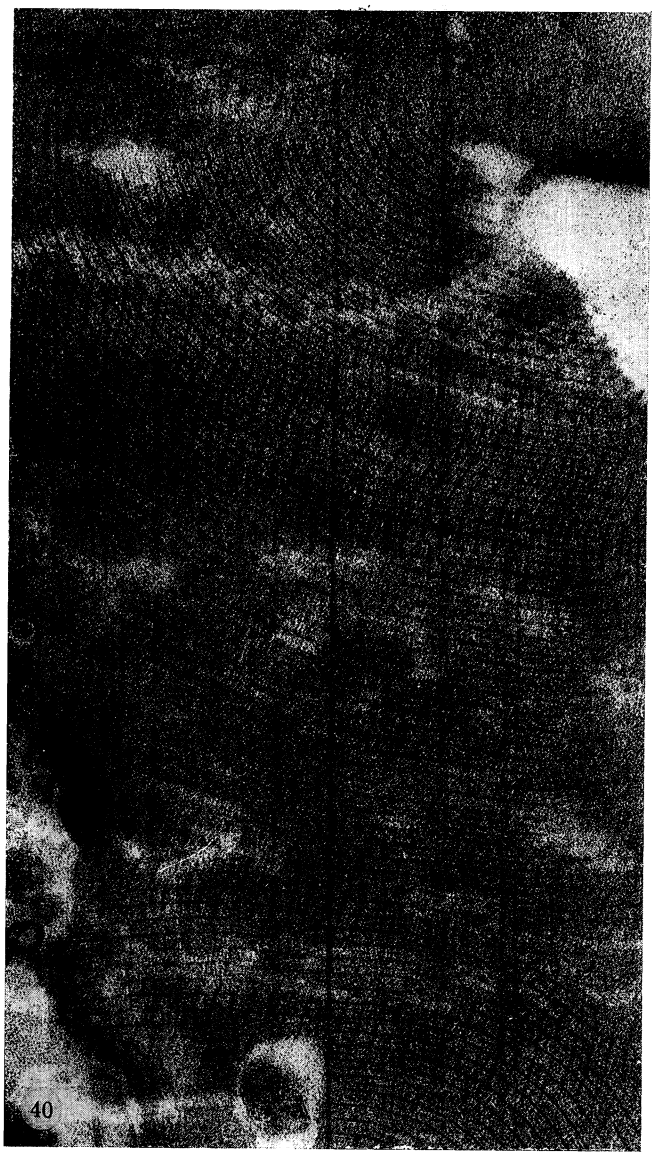

FIGURES 38–41. For description see opposite.

(*Facing p.* 430)

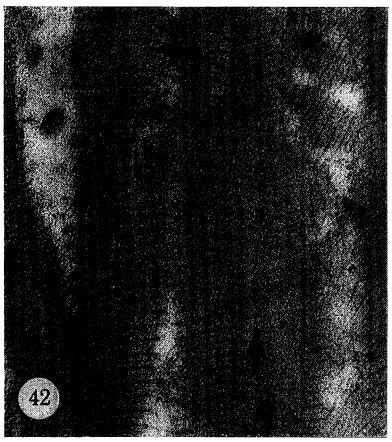

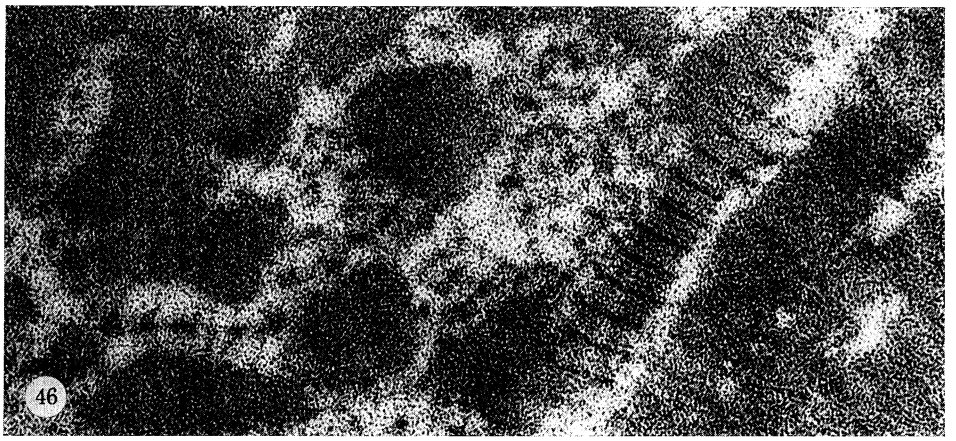

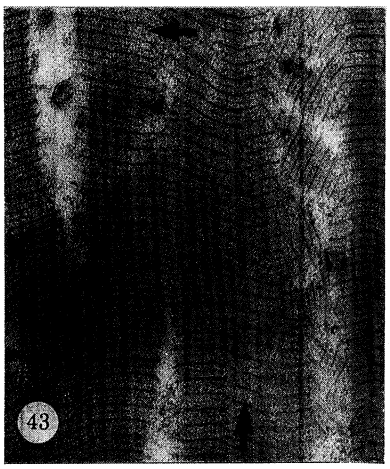

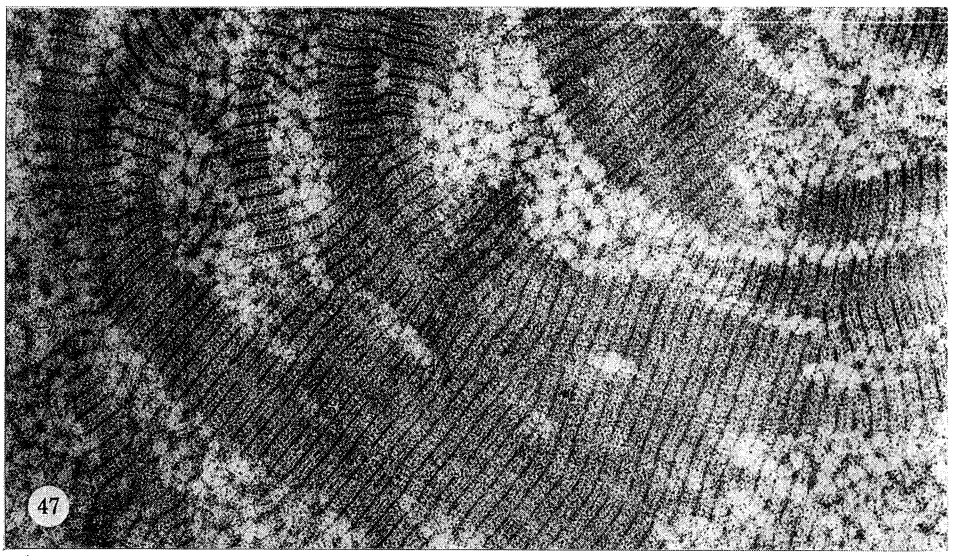

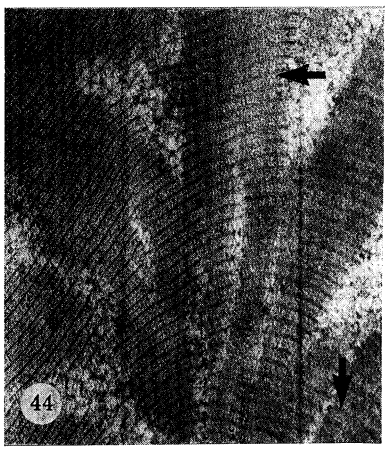

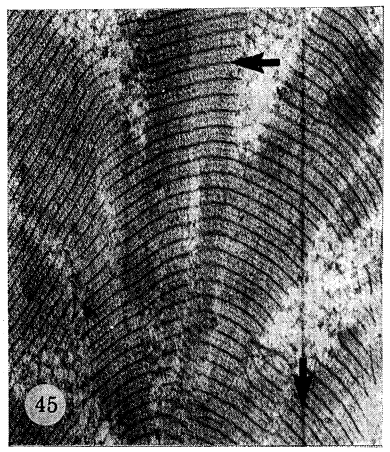

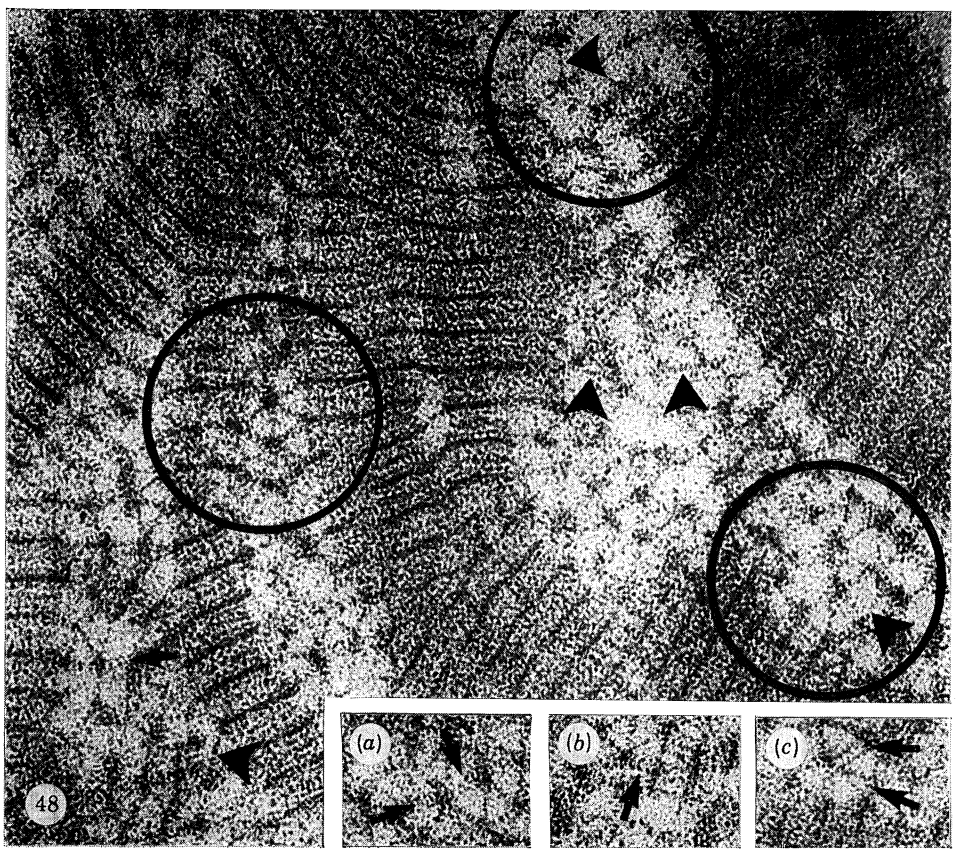

FIGURES 42–48. For description see p. 430.

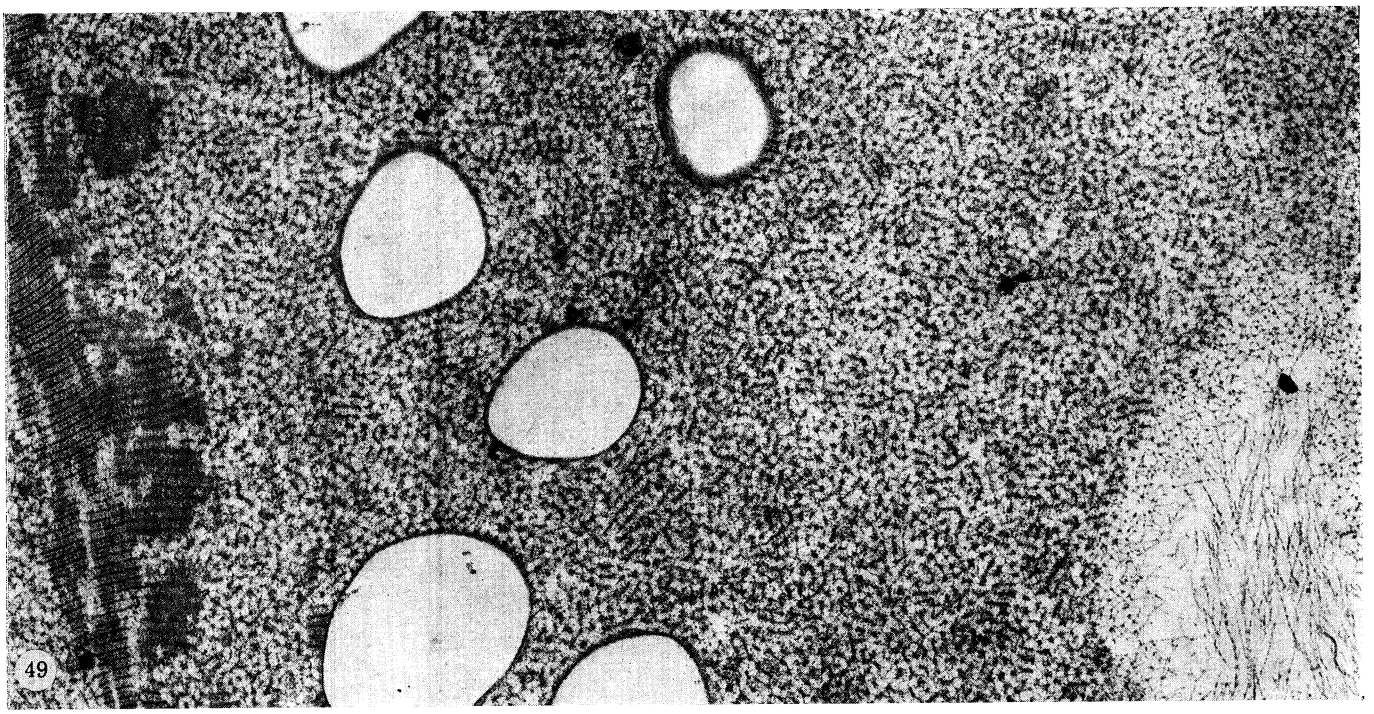

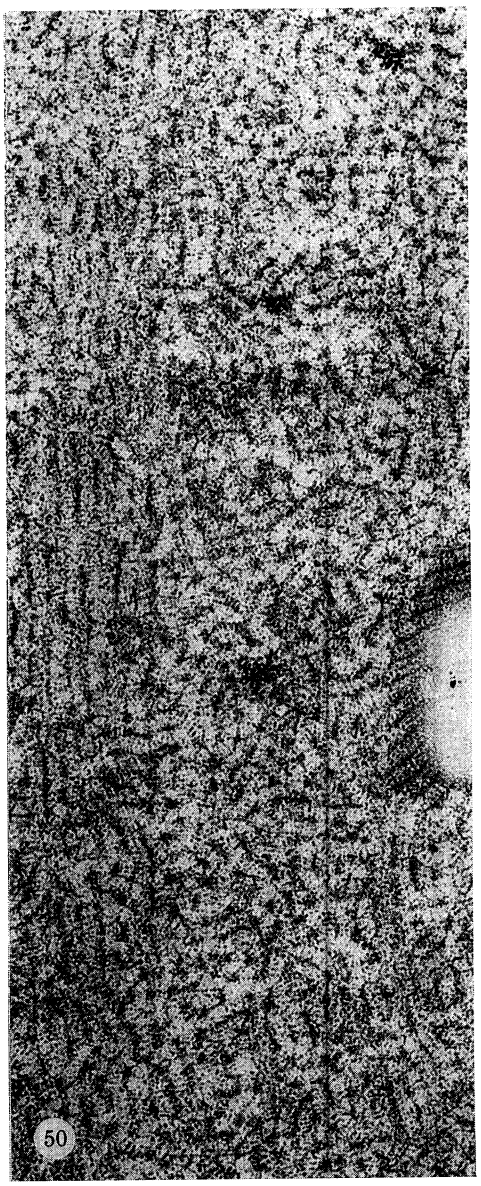

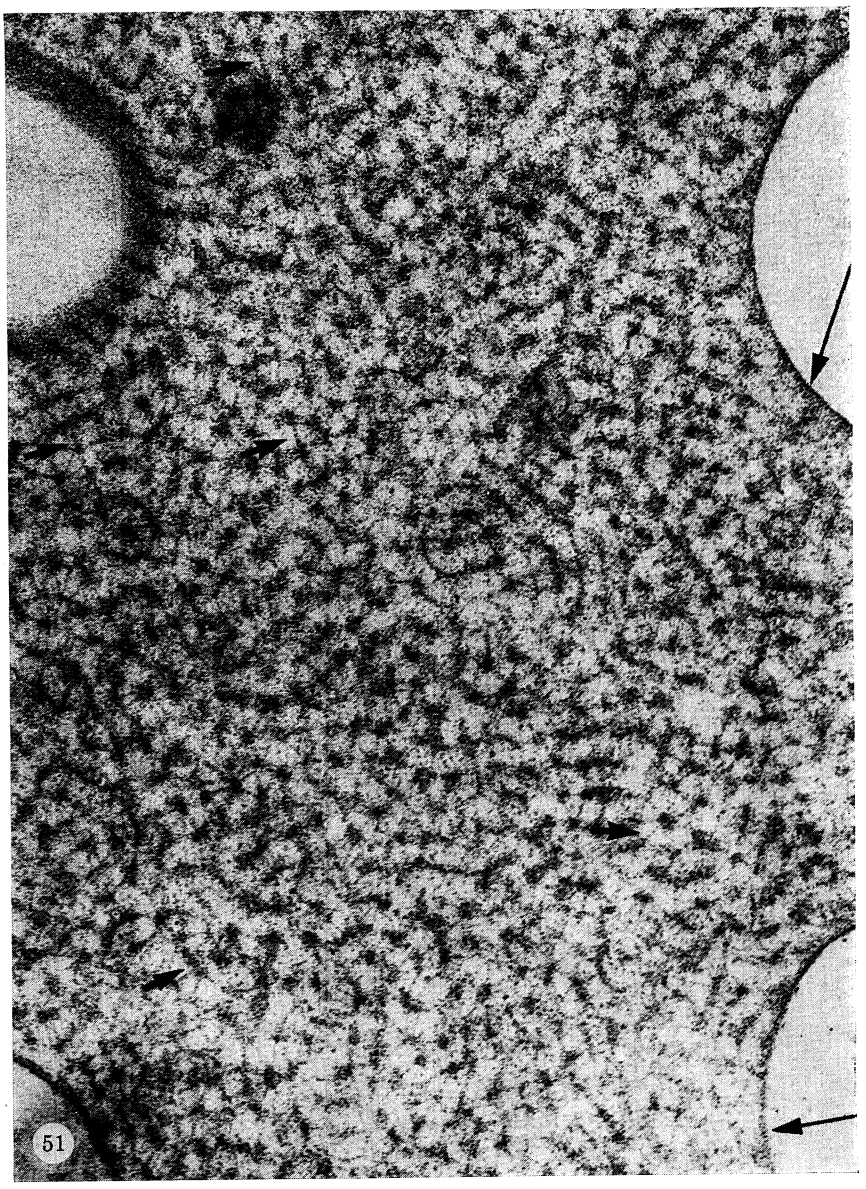

FIGURES 49–51. For description see p. 431.

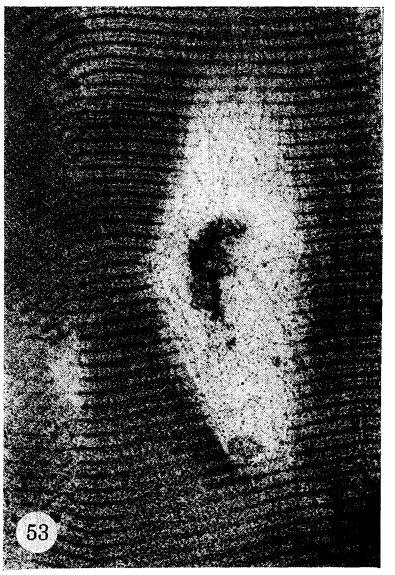

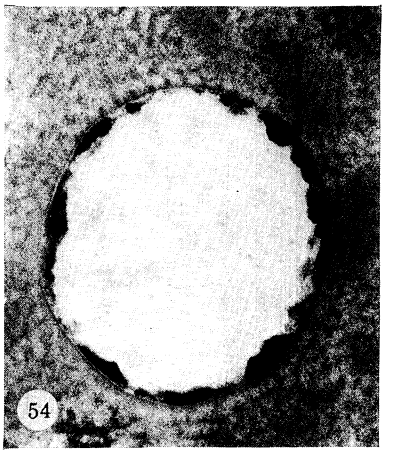

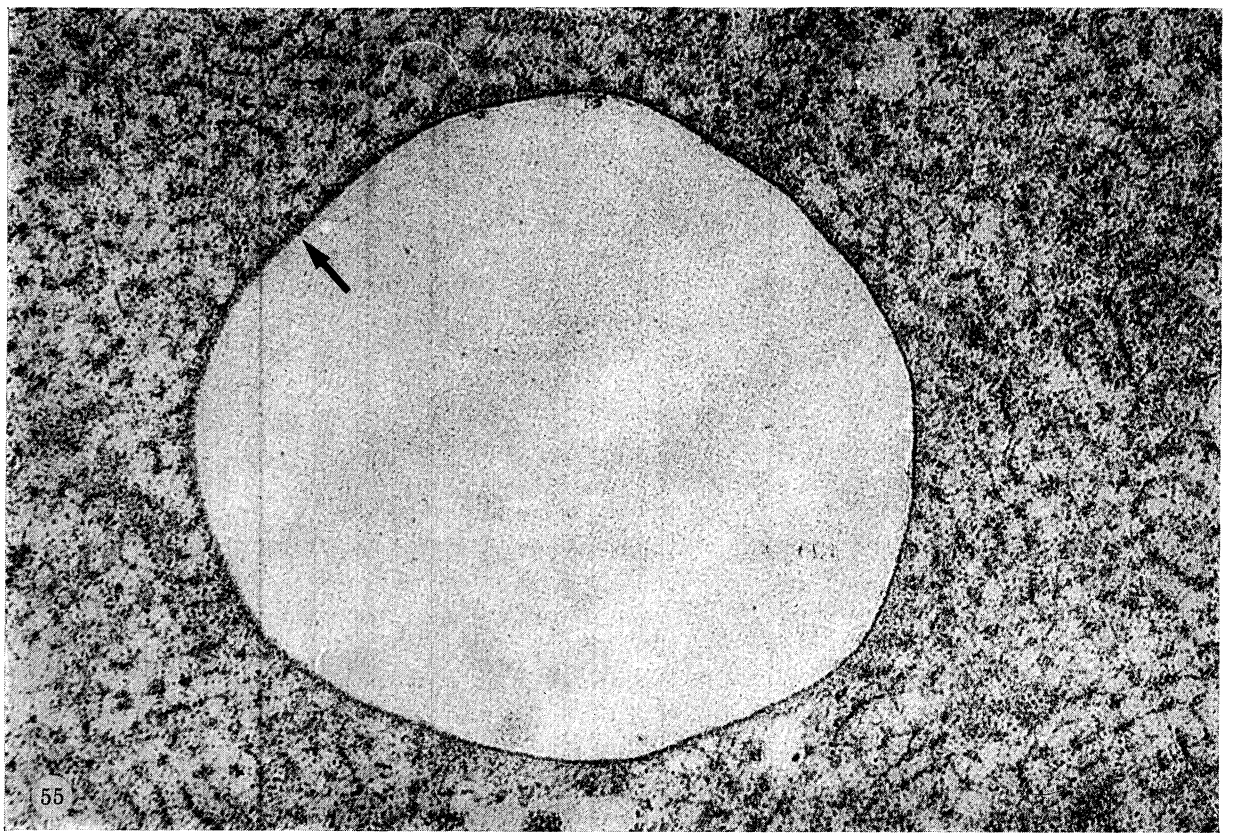

FIGURES 52–55. For description see opposite.

other in these non-helicoidal regions (figures 47–49). The centre to centre separation of the dark centres in the hexagonal matrix is very similar to the major repeat of the ribbons (31–32 nm).

The vacuoles which are round or slightly elliptical are of two types. In one type the vacuole is delimited by a densely stained zone of varying thickness with a regular 37.5 nm repeat and with what has sometimes the appearance of a trilaminar membrane structure lying between the dense material and the matrix/striated material (figures 49, 51, 52 and 54, plates 9 and 10). The effect is very similar to that observed at the innermost layer of the periostracum.

In some cases where the vacuole has been sectioned, in a plane which cuts through it almost exactly perpendicular to its wall, a fine striated appearance is seen in the wall with the striations running around the wall (figures 51 and 55, plates 9 and 10). These striations closely resemble in period and appearance the periodicity observed in the fine connecting fibrils of the hexagonal net (i.e. 4.5 nm).

In the other type of vacuole there is no well defined delimiting zone but the granular matrix merges gradually into the apparently empty zone of the vacuole usually showing organization into the cross-striations typical of the ribbons in the helicoidal layers (figures 50 and 53, plates 9 and 10).

Tilt studies indicate that the hexagonally packed material is not a manifestation of the ribbons cut at an unusual angle. Figures 56–59, plate 11, show that there is little change in their form when the section is tilted, suggesting that the hexagonal packing is three dimensional and not in one plane.

Immediately adjacent to the shell, the periostracum innermost layer presents a rather different appearance. Here there is seen at lower magnification a densely stained limiting layer

---

Description of plate 9

Figure 49. An extensive area of hexagonal matrix with a few ribbons and numerous vacuoles. Note the dark limiting border of the vacuoles and how the matrix tends to change to a striated ribbon mode around them. An area at the bottom right of the micrograph contains more tenuous material; the hexagonal matrix is very sharply defined while at the centre of this vacuole individual threads, which have not aggregated laterally into ribbons, can be seen. (Magn. × 40000.)

Figure 50. A non-helicoidal, non-ribbon region of the periostracum. The hexagonal matrix is less regular here. An area occurs running from top to bottom left where ribbon formation has initiated but not completed. Around the vacuole, seen in grazing section, a striated ribbon has formed. (Magn. × 80000.)

Figure 51. (Detail of figure 49). A hexagonally packed region of the periostracum with several vacuoles. Note how the striations on the connecting fibrils of the matrix centres (short arrows) resemble the striated dense walls of some of the vacuoles (long arrows). (Magn. × 110000.)

Description of plate 10

Figure 52. A mixed area of ribbons, hexagonal matrix, empty vacuoles delimited by a dense zone and spaces containing loose dispersed material. (Magn. × 62500.)

Figure 53. A vacuole or split without a limiting dense zone and containing thin strands of structural protein. (Magn. × 57600.)

Figure 54. A vacuole with a thin dense limiting zone which in this case carries an internal acretion of very dense material separated from it by a lighter zone. There is a superficial resemblance to a trilaminar membrane. (Magn. × 62500.)

Figure 55. A vacuole delimited by a thin dark zone which has a regularly beaded appearance where the sectioning has been exactly normal to the spherical surface but which appears striated (arrow) where the sectioning is oblique. Note the absence around this vacuole of a transition from the hexagonal to ribbon modes of packing. (Magn. × 108800.)

(figure 60, plate 11) approximately 300–350 nm deep. More detailed examination of this layer reveals that it is composed of what appear to be lamellae 20–40 nm deep overlaid in some manner by a general background of darkly staining substance. This layer of material is separated from the major body of the periostracum by a narrow zone of material which on close examination reveals itself as what could be one repeat of the fibrous ribbon material found throughout the periostracum (figures 61 and 63, plates 11 and 12). Where the striated protein ribbons of the general periostracum impinge on the inner layer some changes in geometry are sometimes seen which are not observed elsewhere. In figure 62, plate 11, the units of one of the striated ribbons appears to turn a sharp corner. Also in this region of the periostracum adjacent to the inner layer, a larger periodicity of about 83 nm is sometimes observed in the background to the ribbon periodicity (figure 63, plate 12). It would also appear that the region of periostracum nearer to the shell tend to an orthogonal mode of organization rather than helicoidal (figure 60).

(iv) *Evidence from cleavage studies for a helicoidal mode of organization*

Although the sections of lamellae seen in figures 25, 26, 32 and 33 give definite indications of a helicoidal mode of organization; sections such as that seen in figure 36 do suggest in some degree a type of fan-like arrangement of molecules. Even though this can be explained, within the terms of reference of the helicoidal system other proof for the helicoidal system or alternatively the fan-like system as well would be most desirable to seek. Particularly since recent studies of arthropod cuticle by Dennel (1974) have suggested that decussant systems of fibrils may give rise to parabolic effects mimicing Bouligand parabolicity.

Description of plate 11

Figures 56–59. These micrographs are a tilt series of an identical area and are intended to demonstrate the three dimensional consistency of the hexagonally packed matrix. Note that while the appearance of the striations on the ribbons is affected by tilting, individual dense centres in the matrix are virtually unchanged (arrows). (Magn. × 56100.) (Figure 56: $x = 0°$, $y = 0°$; figure 57: $x = +20°$, $y = 0°$; figure 58: $x = -20°$, $y = 0°$; figure 59: $x = 0°$, $y = +20°$.)

Figure 60. This electron micrograph is of the innermost layers of the periostracum. The densely stained layer is in contact with the shell. Within this are rotated layers of ribbons which seem to be neither helicoidal nor completely orthogonal in disposition. (Magn. × 18900.) The position normally occupied by the shell is denoted S in this and in figures 61–63.

Figure 61. A more detailed view of the dense inner layer of the periostracum showing its lamellar organization and the narrow zone (arrowed) which separates it from the major body of the periostracum. (Magn. × 46000.)

Figure 62. A similar area to figure 61. Note how the thin layer beneath the dense layer appears to be derived either from one repeat of the ribbon laid down at right angles to a ribbon or by aggregation of a repeat rotating gradually around a corner (arrows). (Magn. × 56000.)

Description of plate 12

Figure 63. This micrograph shows vacuolation in the dense layer and either intrusion or inclusion of material, of the same type as the major body of the periostracum, within this layer. Note the impression of a larger scale repeat in the material between the ribbons at the lower left. This may be an artefact of viewing the ribbon repeat obliquely. (Magn × 48000.)

Figure 64. Replica of a cleaved surface of periostracum. All the ribbons run in one direction. (Magn. × 49000.)

Figure 65. A cleaved surface in which more than one layer is revealed. Differences in orientation between layers are apparent (arrows). (Magn. × 64000.)

Figure 66. A cleaved surface showing clear evidence of steady rotational changes in orientation of sheets in overlying layers (orientation indicated by arrows). (Magn. × 30000.)

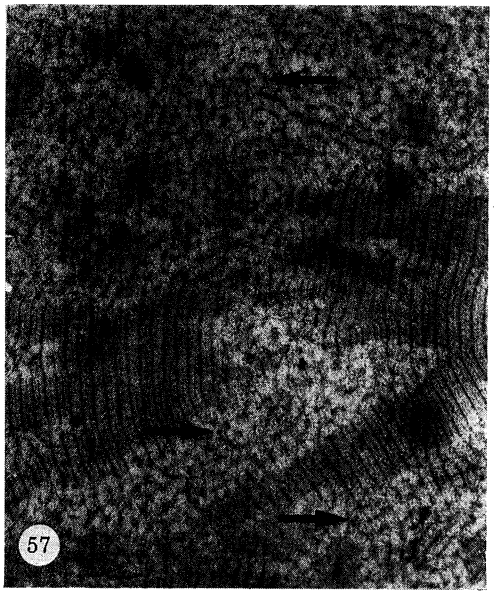

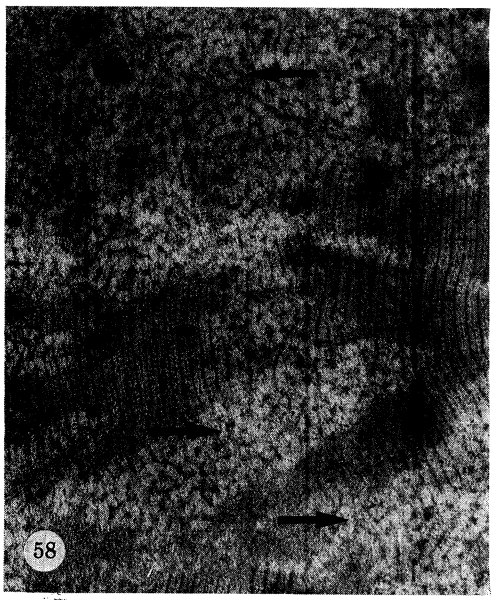

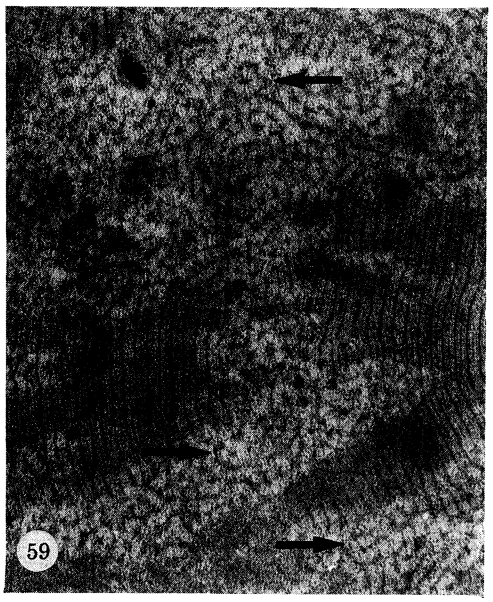

FIGURES 56–62. For description see opposite.

(*Facing p.* 432)

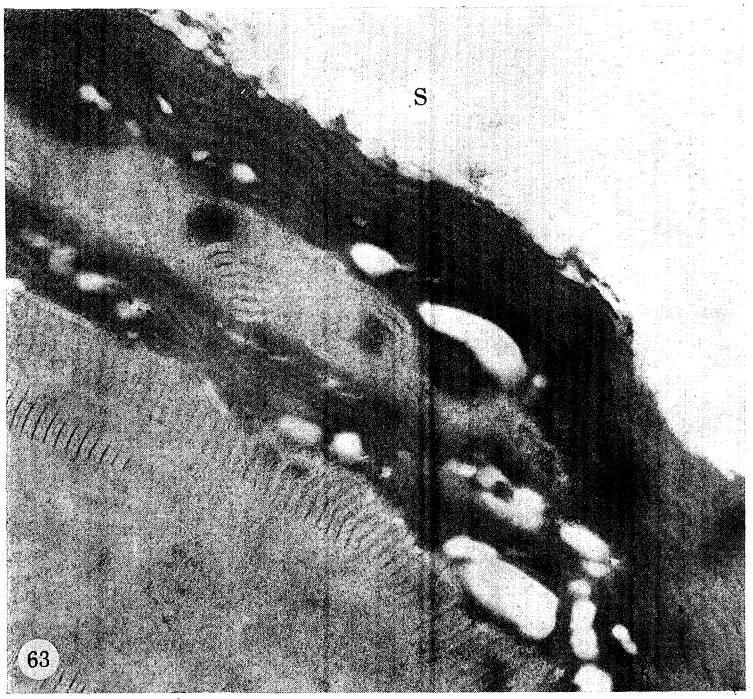

FIGURES 63–66. For description see p. 432.

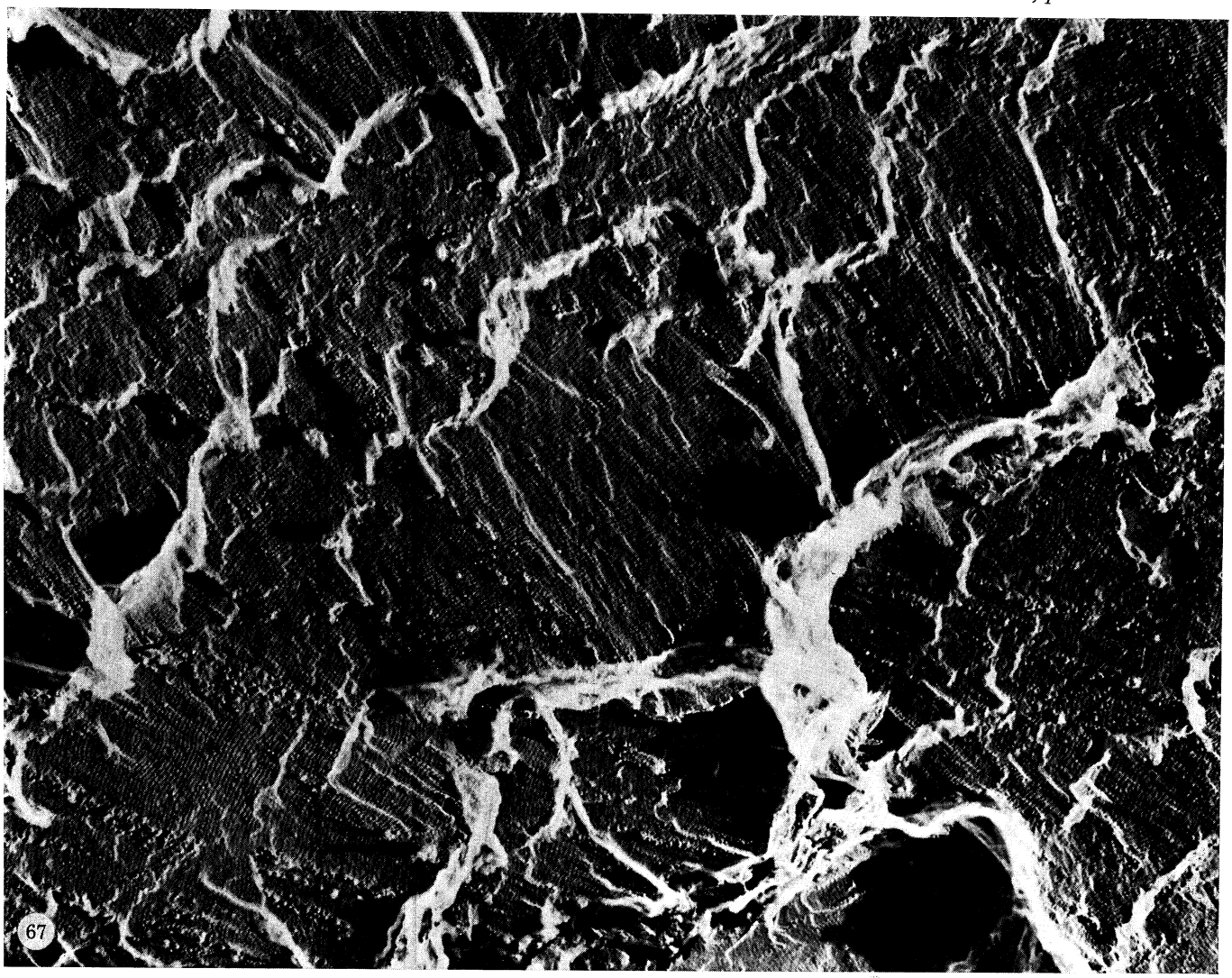

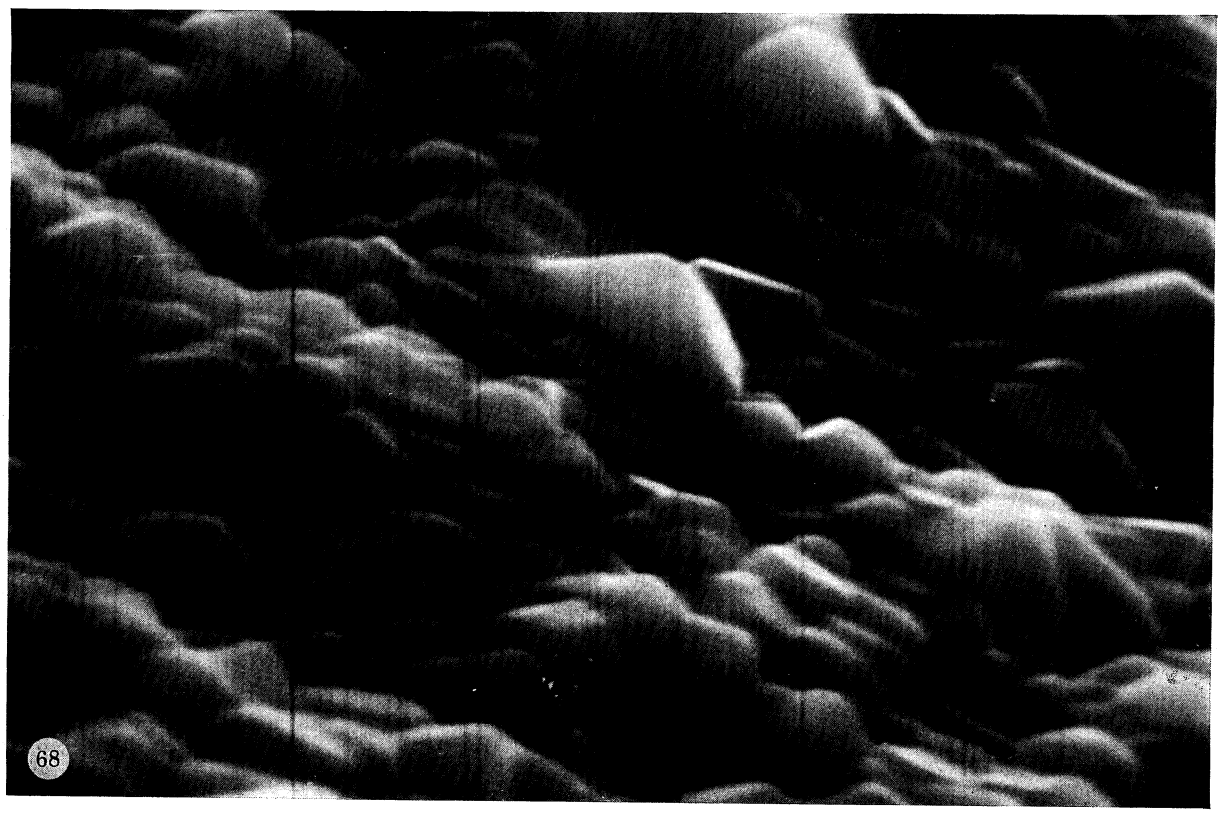

FIGURES 67 AND 68. For description see p. 433.

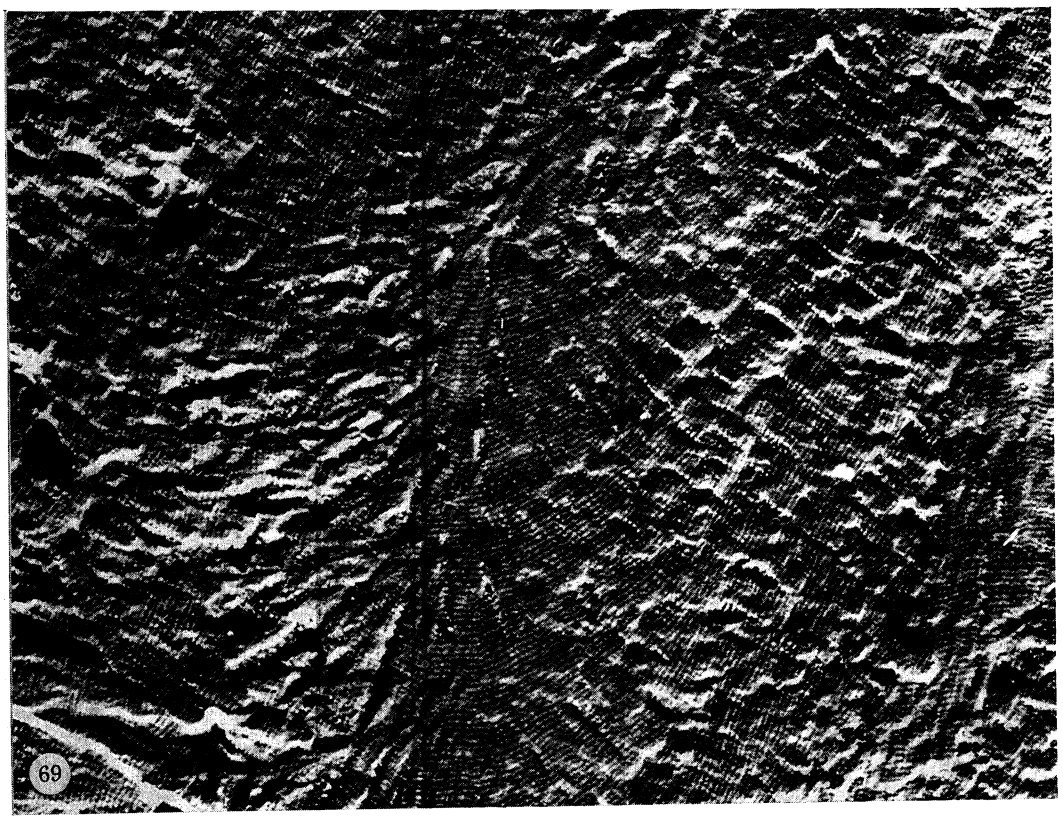

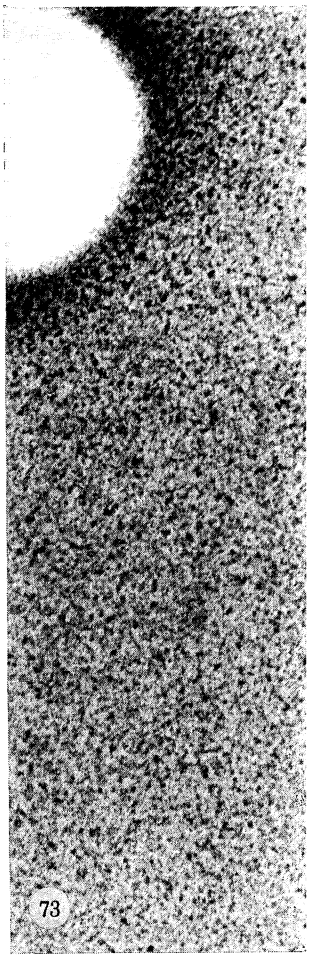

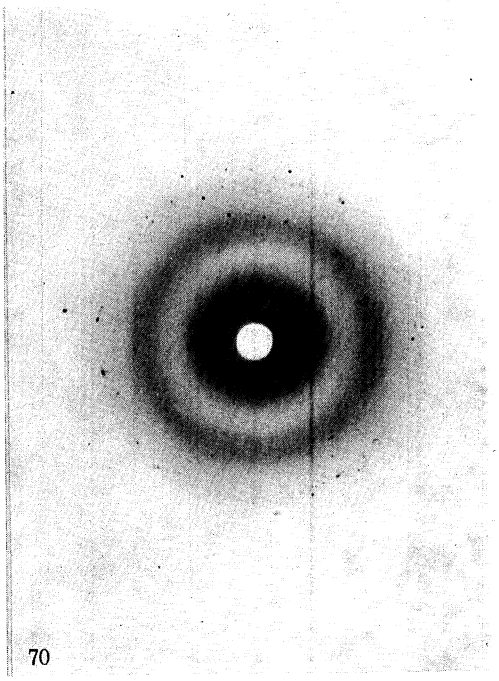

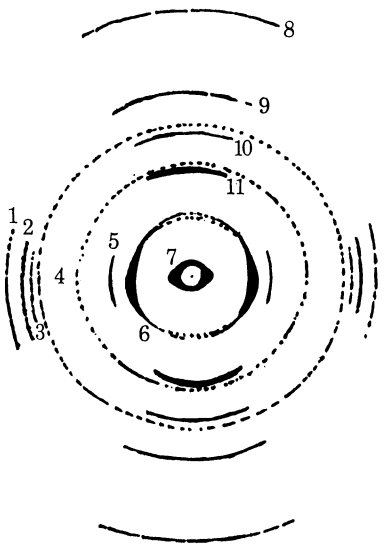

71

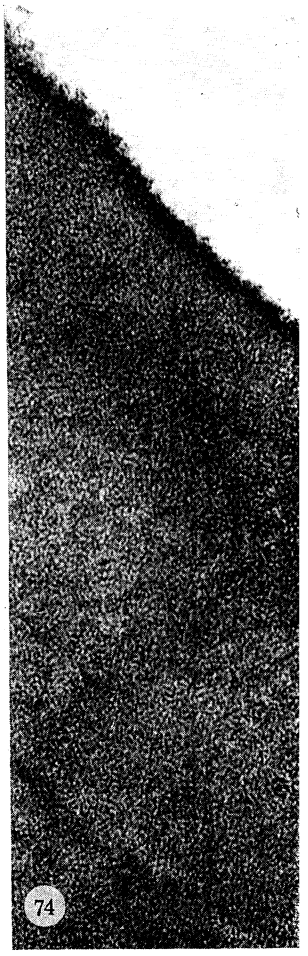

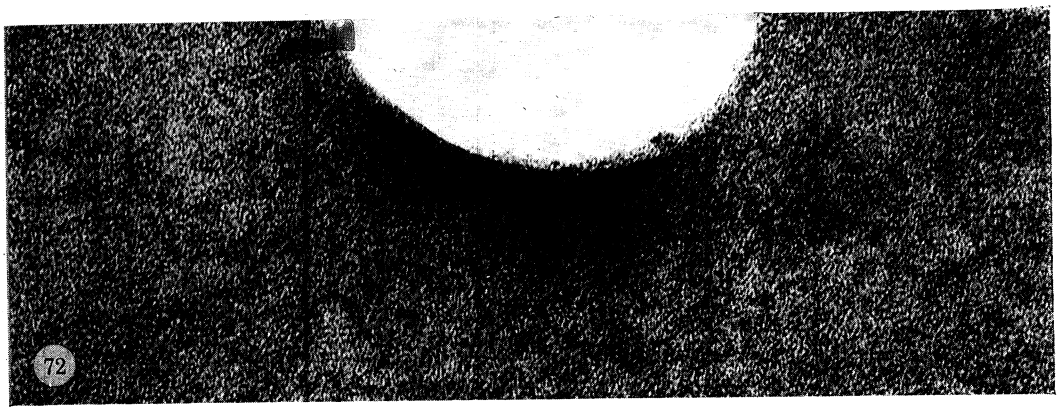

FIGURES 69–74. For description see opposite.

Figure 64, plate 12 is a replica of a cleaved surface of periostracum formed by cementing sheets of periostracum between metal plates and then forcing the plates apart as described in the Methods section. In this figure one layer of a lamella has been revealed, the cross-striations of the individual ribbons comprising the layer can be clearly seen as can the edges of the constituent ribbons. This figure corresponds to the view seen in the sectioned material of figures 29 and 35 cut in the plane of one lamellar sheet. Figure 65, plate 12, is a similar cleaved section. Here cleavage has cut down in a stepwise manner through several lamellae of the periostracum and the protein sheets can be seen at different orientations to one another. In figure 66 (plate 12), a similarly cleaved sheet to that seen in figure 65, there is at the edge of the cleavage zones what appears to be at low magnification a fan-like arrangement of ribbons which on closer examination reveals itself as edge on views of several layers of lamellae with ribbons in successive layers helicoidally disposed. Figure 67, plate 13, reveals the block-like arrangement of units of the periostracum seen also in the stereoscan views of a torn edge of periostracum of figure 68, plate 13.

Figure 69, plate 14, also suggests that the extensive layers of protein molecules which contribute to the lamellae may deviate over larger areas from the parallel arrangement of molecules in the ribbons or sheets. Thus a sheet fans out, the cross-striation being apparently arranged along arcs rather than straight lines. Here again however closer examination suggests that no arc is continuous but may be divided into straight sections of individual segments of ribbons.

X-ray diffraction studies and the conformation of the structural protein

Periostracum which is examined by X-ray diffraction with the beam of X-rays perpendicular to the plane of the periostracal sheet gives a powder diagram with rings spaced around 10 Å† and rather diffusely in the 4.5–5.5 Å region. With the beam parallel to the plane of the periostracum however a poorly orientated pattern of meridional and equatorial arcs is obtained. The spacings and relative intensities obtained from a series of diffraction photographs taken

† 1 Å = 0.1 nm = 10^{-10} m.

Description of plate 13

Figure 67. View of a cleaved surface of periostracum which suggests that the sheets may not be laid down over very large areas continuously but in blocks. (Magn. × 24000.)

Figure 68. Scanning electron micrograph of a fractured and cleaved edge on a periostracal sheet (decalcified). A block-like organization is suggested. (Magn. × 11500.)

Description of plate 14

Figure 69. A cleaved surface of periostracum showing extensive deviation from lateral linearity of ribbon alignment in what appears to be a single sheet. The cross-striations fall on steep curves. (Magn. × 27000.)

Figure 70. X-ray diffraction pattern produced by orientation of strips of periostracum with the beam in the plane of the sheet and the plane along the meridian.

Figure 71. Synthesis of several diffraction patterns to show all observable details. Numbers correspond to those in table 1.

Figures 72–74. These three electron micrographs are of sections of the periostraca of *Solen marginatus*, *Arctica islandica* and *Helix aspersa* respectively. Even at the high magnifications represented here there is no evidence of an organized molecular ultrastructure similar to that found in *Buccinum undatum*. (Magn. × 157500.)

over a range of exposures are given in table 1. Figure 70*a*, plate 14, shows a typical diffraction pattern while figure 71, plate 14, is a synthesis made from several different photographs not all of the same sample. If the fibre is assumed to lie in the plane of the periostracal sheets then the diffraction patterns represent the rotation of this and a second axis about the mutually perpendicular third crystalographic axis which is horizontal in the figures and perpendicular to the plane of the sheets. While the patterns are rather weak, diffuse and poorly orientated there is an overall pattern evident which consists of a strong equatorial reflexion at 9.78 Å, a meridional

TABLE 1. SPACINGS AND RELATIVE INTENSITIES OF REFLEXIONS ON THE DIFFRACTION PATTERN GIVEN BY AN X-RAY BEAM DIRECTED IN THE PLANE OF THE PERIOSTRACAL SHEET

(See figures 70 and 71, plate 27.)

	equatorial/Å		meridional/Å
1	3.45 w	8	2.75 w
2	3.67 w	9	3.57 w
3	4.02 w	10	4.57 w
4	4.63 diffuse ring	11	5.29 m
5	7.31 m–w		
6	9.78 v.s.		
7	18.0 s		

w = weak; m = medium; s = strong; v.s. = very strong.

arc at 5.29 Å and a relatively intense diffuse ring centred around 4.63 Å. This basic diffraction pattern is very reminiscent of that given by an alpha helical protein system such as α-keratin (cf. figure 70*a* and *b*) superimposed upon a non-crystalline globular protein type of diffraction pattern. In fact unstretched α-keratin (hair) gives a meridional arc at 5.18 Å and an equatorial spot at 9.5 Å. If the conformation is that of an alpha helical system then it is probably not that of a simple alpha form since the meridional reflexion is not off axis and is appreciably shorter than 5.4 Å. The indication would be of some sort of coil–coil system but with the major helix less tightly coiled than in the α-keratin system. The packing of the helices would also be slightly less compact than in keratin also. A puzzling feature of the diffraction patterns are a series of sharp equatorial arcs of low intensity (numbered 1, 2, 3, 5 and 7 in figure 71). These are too sharp to be readily related to the poorly orientated protein conformation which gives rise to the dominant intensities of the diffraction pattern. They may represent a lower molecular mass component packed between the fibrils and undetected by microscopy or analysis. Similar types of sharp arced reflexions are seen for example in diffraction patterns of amyloid where they are attributed to lipid (Bonar, Cohen & Skinner 1969). In our case they may originate in polyphenolic material.

DISCUSSION

(*a*) *Ultrastructure of periostraca from gastropod molluscs other than* Buccinum undatum

The periostracum in *Buccinum undatum* is shown in the present study to be a lamellar structure organized from protein ribbons which have a characteristic longitudinal repeat and which are arranged in sheets with the sheet lamellae helicoidally distributed over much but not all of the structure. Gastropod periostraca have not been extensively studied at the fine structural level although the mode of secretion has been examined in some detail (Bevelander & Nakahara

1967; Neff 1972*a*, *b*). However studies of periostraca in three species other than *Buccinum* have been made. Jones (1969) describes the periostracum in *Lymnea peregra* (Muller) as having an outer layer composed of two sets of fibres about 0.5–100 μm diameter and differing chemically. One set rich in serine and glycine is produced from the mantle groove passing at regular intervals over the outer lip and at right angles to it. A second set of fibres is produced parallel to the outer lip and is usually polymerized at a pigmented zone some distance from the lip. These fibres lie beneath the first set and form with it an orthogonal 'open weave' system. At the pigmented zone, underneath the fibres a strip of beta-type protein is reported to be produced at 30 μm intervals upon which calcification as pentagonal plates takes place. It is unfortunate that no published electron micrographs of this interesting study are available.

A different species of *Lymnea* (*Lymnea stagnalis*) studied by Kniprath (1972) appears to have a quite different structure. Here there are three distinct layers of which the outer is protected by a membrane-like lamella reminiscent of that seen in the innermost layer of *Buccinum* periostracum. The outer layer constitutes over half the depth of periostracum and is composed of about twenty strata which are not wholly continuous with each other being separated by gaps which give a loose flexible structure. The strata are made up of largely randomly distributed, poorly organized, fibrillar elements which, around the gaps, may show some linear arrangement of lower order. Beneath this layer is a second layer of homogeneous material which seems to be divided into an outer more electron dense component merging smoothly into a more electron luscent material. Proximal to this second layer is a dense homogeneous layer constituting about 5 % of the depth of the periostracum. It is on this latter layer that the first crystals of calcium carbonate form. Each of the three layers owes its origin to a well defined zone of the mantle epithelium. The outermost layer is secreted by the proximal wall of the periostracal groove and by the microvilli-bearing cells of the immediately adjacent zone of the supramarginal ridge. The second layer derives from the next band of supramarginal cells, which lack microvilli, while the third layer is produced by two or three cells, adjacent to the second zone on the supramarginal ridge, which are rich in alkaline phosphatase and which seem also to contribute the first crystals of calcium carbonate.

Bevelander & Nakahara (1970) describe the periostracum of the prosobranch *Littorina littorea* as being bilayered with an inner relatively homogeneous layer and an outer layer exhibiting a uniform periodicity of 30 nm very similar in appearance to the periodicities seen in *Buccinum* periostracum. As already mentioned in the introduction there is however no evidence for a helicoidal mode of organization in this particular periostracum.

Bevelander & Nakahara (1970) studied the early stages of formation of periostracum as manifested in regenerating shell. Here the newly secreted periostracum seemed to consist 'for the most part of a randomly-arranged network of particles contacting each other by filamentous processes which are embedded in a *gelatinous substrate*'. They also mention, and figure, 'particles undergoing rearrangement to give rise to elongated, fibre-like structures exhibiting a regular periodicity 30 nm. This is exactly the situation found here, as seen for example, in figures 47 or 49. In *Buccinum* however this type of organization is not confined to recently formed periostracum but persists in older material. The older outer periostracum of *Littorina littorea* is composed of a layer of material 4–5 μm thick arranged over short distance in sheets and ribbons with a uniform periodicity of 30 nm. These sheets and ribbons are rather randomly distributed. The dark periodic bands of the ribbons seem to be made up of globular particles and are separated by a 17 nm interperiodic spacing. In transverse section the particles appeared

in a regular lattice arrangement, a feature we have not found in *Buccinum* periostracum even though we have examined many sections. This layer in *Littorina* is derived from a ventral gland composed of large flask-shaped cells located in the mantle margin. The secretory granules of the Golgi apparatus of the ventral gland show a similar periodicity to that in the ribbons and sheets of the periostracum. Neither in the secretory granules or the periostracum is there any evidence of a cholesteric mesophase or helicoidal orientation. The inner layer of the periostracum, 0.4–0.5 μm thick, is derived from cells in a dorsal marginal gland. This layer is relatively homogeneous in appearance with no periodicity but with denser rod-like inclusions and a general similarity of appearance to the inner layer of *Buccinum* periostracum. The thicker outer layer contains many vacuoles resembling those of *Buccinum* periostracum. There seems to be little actual experimental justification for the reference to embedment of the structural protein particles in the early periostracum, of *Littorina littorea*, in a gelatinous matrix since this would imply the presence of two molecular species, a point which has already been discussed earlier in this paper. Certainly it would seem that the hexagonal type of arrangement of particles connected by fine threads is one possible form of organization of the periostracal protein sub-units and that at early stages of aggregation a transition between this form and the striated ribbon mode is possible. Even so it would be difficult to visualize how this transition could take place directly.

(*b*) *The significance of the hexagonal-packed matrix and its relation to the laterally packed ribbons*

In thin sections such as that seen in figures 47 and 48 a common manifestation of the particle matrix is, as already mentioned, one in which a central particle is surrounded by six others connected to it by fine strands. However some arrangements with seven surrounding particles and accompanying strands can be seen both in the sections shown here and in the work of Bevelander & Nakahara (1970) and it seems most likely that a three dimensional array with many more than six particles surrounding each other particle is the true state of affairs. That the dark particles are indeed discrete bodies and not sections of hexagonally packed rods with cross-bridges seems to be clearly indicated by the tilt studies which are shown in figures 56–59. The two forms of packing can also clearly exist in stable form since they are found by us both in mature periostracum as well as at the edges of disrupted ribbons as seen in figure 9. In the latter case the geometrical three-dimensional packing as opposed to the almost two dimensional ribbon mode helps to explain the topological difficulty of the operation which would be involved in placing the isolated but attached sub-units present at the edge of the ribbon seen in figure 9 back in alignment with the ribbon from which they have apparently frayed. Both types of arrangement must therefore be equally susceptible to the chemical process which irrevocably covalently bridges the sub-units to one another. Although in the immature form of the periostracum of *Littorina* and in the mature *Buccinum*, periostracum ribbons and geometrical matrix merging almost imperceptibly are common features, there is always a tendency for a certain amount of non-specific material to obscure details of the structure. The area shown at the top of figure 49 presents an unusual case where although there is not a well formed vacuole the density of polymerizing sub-units has been apparently rather lower than normal. Here around the edges of this area the geometrical packing mode is very clearly defined with the fine connecting threads particularly well displayed. Towards the centre of the zone there are most interestingly displayed the preliminary stages of the aggregation of sub-units into ribbons. Long beaded threads have begun to form and to lie roughly parallel to one another, but total aggregation into ribbons has not taken place. Examination of this area seems to indicate to us two things; one

that the geometrical mode cannot be directly operated upon to produce the ribbon mode without dissociation and re-aggregation and secondly that the ribbons are assembled by end to end aggregation of the sub-units into filaments which are then aggregated *in toto* side by side with adjacent filaments rather than a block lateral side by side assembly of single sub-units, these blocks then being assembled end to end to produce ribbons.

(*c*) *Origin of the vacuoles*

It is noteworthy that a tendency occurs around the periphery of vacuoles for the transition between geometrical matrix modes and ribbon modes to take place (figures 49–53). This shows well in vacuoles caught in grazing section. A number of explanations for this behaviour could be offered. If the more well defined vacuoles were to represent regions of gas bubble entrapment (as their smooth outline suggests) caught during the fluid stage of periostracum secretion then it is likely that the regions around such bubbles might experience a degree of pressure and tension. This could result in an orientating effect on the molecules nearby which might be sufficient to cause the transition to the ribbon mode of organization. Orientation by some mechanical process might then also account for the more general distribution of the ribbon and sheet forms in the periostracum as a whole. It may be significant that the ribbon form tended to predominate in sections of the papillae, regions of the periostracum showing the greatest extent of macroscopic orientation of material.

On the other hand it is possible that the vacuoles may represent regions where cellular or mantle mucinous materials have been trapped or even perhaps where secretion packets of substances, involved in dictating the mode of aggregation and perhaps containing cross-linking materials, have failed to release their contents in anything but a limited manner.

Some of the vacuoles, that is to say those with no obvious boundary at all, seem to have formed where the structural protein sub-units, initially present as a geometrical matrix but as yet not cross-linked perhaps, have aggregated to form the denser ribbon mode leaving an empty region behind (see for example, figure 53). Certainly one might expect that molecule for molecule the lattice of the geometrical matrix would take up more space than the more compact close packed ribbon form.

(*d*) *Distribution of network lattices*

Network lattices of the type observed here are known to occur in other structural protein situations. In Descemet's membrane of bovine cornea, Jakus (1956) has demonstrated a rather disordered centred-hexagonal array of collagen molecules with dense nodes (27 nm diameter) at 107 nm centre to centre spacings connected by finer fibres (10 nm wide) which are often doubled or double edged. The filaments are probably ribbon-like rather than cylindrical. The filaments show a fine banding at 7–25 nm intervals with low peaks every 3 nm. The whole effect is very similar to that observed here. In the case of Descemet's membrane the hexagonal lattice would appear to be extended to only two dimensions, the packing forming sheets which are then superimposed with hexagonal centres in phase (at depths of 27 nm through the depth of the stack of sheets. The internodal spacings in Descemet's membrane are twice the repeat period of stromal collagen fibres. Jakus (1956) suggested an aggregation mode in which two collagens united with unlike ends together; lateral association out of phase producing equivalent filament ends in keeping with the apparent equivalence of the nodes. Part of each collagen unit would be extended to form its half of the internodal filament while the remainder in collaboration with five other units formed a node.

Gross (1956) observed, during the formation of the fibrous long spacing form of collagen aggregate, an intermediate stage in which there were extensive areas of densely stained centres arranged in roughly hexagonal array from which extended thin fibrous processes. These centres which were separated by distances of 150 to 250 nm then transformed via transient 300 nm × 10 nm tactoids to a form with local condensations having the appearance of clouds of dense spheroids again packed hexagonally and from these fibrous long spacing collagen fibrils appeared. Again the effect is very similar to that found in different regions of the periostracum. Filamentous collagen in compact clusters (6–7 nm diameter) with thin cross-bridging filaments and an ill defined 60 nm period are found closely surrounded by a highly structured collagen array in the perispicular spongin fibres from the siliceous sponge *Haliclona elegans* (Garrone & Pottu 1973). The structured array is formed by a stacking of plane triangular networks and has dark nodes with centre to centre spacings of about 12 nm apparently linked by fine threads. In cross-section the different networks are 20 nm apart and apparently linked. The appearance is very similar to that of Descemet's membrane and *Buccinum* periostracum. Similarly Smith & Lauritis (1969) observed 2–4 nm wide reticulated filaments in the mesoglea of the sponge *Cyamon neon* packed in a longitudinally symmetrical hexagonal pattern with centre to centre spacings of 20 μm and connected by finer filaments. Periostracum is not of course collagen but what is of interest is the manner in which structural protein molecules which 'normally' aggregate and pack to form ribbon or fibril units by processes of end to end and side by side binding can also, when given the appropriate conditions, aggregate in a network type of lattice which is presumably energetically favoured. Further examples of this type of network self-assemblage under abnormal *in vitro* conditions involving usually fibrous forms can be seen in the cases of such muscle structural proteins as myosin and tropomyosin–troponin (Nakamura, Streter & Gergely 1971; Greaser *et al.* 1973; Cohen *et al.* 1973). In a very similar situation to molluscan periostracum Williams (1968) examining the fine structure of the brachiopod periostracum in *Waltonia* noted the organization of structural protein, at the surface, into rhomboidally (8 nm) packed rods connected by fine fibrils, with a spacing of about 40 nm. These extended down into labyrinths, in a densely-staining protein matrix, where they showed a transition to a roughly hexagonally packed system of dark centres connected by single or double fine filaments at a spacing of about 50 nm. Clearly where a structural protein is being secreted wholly extracellularly, extra-tissue and extra-animal at an organism/aqueous environment interface there is a strong possibility that environmental fluctuations may vary sufficiently to shift self-assemblage of the quaternary structure from one mode to another outside the control of the secreting organism. This may in part account for the presence of both ribbon and hexagonal lattice forms in the periostracum when it is probable that only one protein is actually involved. On the other hand these different modes of aggregation may well depend on the presence or absence of small amounts of accompanying secretion of other types.

(*e*) *Assembly of ribbons and sheets from coiled-coil molecular systems*

We have already mentioned that we consider the predominant striated sheet-like mode of aggregation which sometimes manifests itself as isolated ribbons and which is usually seen as ribbons in disrupted preparations, as being assembled from the dumb-bell shaped sub-units shown in figure 19. The negatively stained preparations would seem to suggest that assemblage of these asymmetric sub-units is end-to-end with their long axes aligned along the long axis of the ribbon and by in phase lateral aggregation across the ribbon. This results in a symmetrical

repeat striation. As far as we can see there is no sub-unit overlap contributing to the organization of the ribbons, the thickened regions of the banding pattern being satisfactorily accountable for by the globular areas of the sub-units. The presence of two symmetry planes, within the longitudinal repeat, of equal size does not therefore call for explanation by some type of antiparallel packing.

The ribbons observed here either in isolation or in the intact periostracum show many general similarities to a wide range of other proteins having a structural function. They may be compared with collagens, myosin, tropomyosin, paramyosin, fibrin, trichocyst fibrils and egg capsule proteins of some marine gastropod molluscs for example (Bairati 1972; Greaser *et al.* 1973; Nakamura *et al.* 1971; Szent-Gyorgi, Cohen & Kendrick-Jones 1971; Tooney & Cohen 1972; Messer & Ben-Shaul 1971; Flower, Geddes & Ruddall 1969). Although these are clearly different molecules which are most probably not related in any way as episemantides they have in common the features that they exist ultimately as monomers which in the normal course of biological events aggregate in very specific ways to form giant polymeric systems with high degrees of order and paracrystallinity. They are all also capable of existing in a wide variety of polymorphic crystalline and paracrystalline forms which depend for their formation upon relatively small changes in the state of the surrounding medium under *in vitro* conditions. Similarities in fine structural organization of fibrils may be reflected in more fundamental similarities of primary structure and amino acid composition.

Naturally some of the similarities of fibrous structural protein systems of this type are an inevitable consequence of their mode of organization. Given a monomeric sub-unit which is to be assembled into a ribbon or fibril then one would expect some sort of periodic structure to be visible as a result of the repetitive aggregation of the monomer; providing the monomer size does not fall below the resolution limits of the technique used to study it. If the sub-units are markedly asymmetric, i.e. having two axes of symmetry one appreciably longer than the other then the aggregation of the monomers with their long axes along the fibre or ribbon axis will exagerate the repeat effect while overlapping either parallel or antiparallel will contribute to this exageration. Of course it is not a requirement for fibril formation that the sub-units be morphologically asymmetric although physico-chemically they are almost certainly likely to be, as is the case for example of the G-actin to F-actin transition. However, in the majority of cases the sub-unit monomers do display asymmetry, existing as rod shaped entities.

It is common for many of the better known structural protein fibres or ribbons to be assembled from sub-units whose asymmetry and rod-like form is due to a high content of some type of coiled-coil protein chain conformation. Examples of this may be found in the alpha keratins, in some of the polymorphic forms of light meromyosin and tropomyosin (Nakamura *et al.* 1971; Greaser *et al.* 1973), paramyosin (Szent-Gyorgyi *et al.* 1971) and moluscan egg capsule proteins (Flower *et al.* 1969) which are all alpha helical type proteins and in the various manifestations of the collagens including the regular collagens as well as ovokeratin and elastoidin (Bairati 1972; Bailey 1968; McGavin 1962).

In some instances fibres may be elaborated from globular units, as is the case for the natural form of F-actin or certain *in vitro* aggregation states of flagellin (Hanson & Lowy 1963; Champness & Lowy 1968; Cohen 1966). In other cases the monomeric sub-unit of the fibres or ribbons may combine rod-like and globular regions as is found for myosin, fibrinogen and probably the monomeric form of the periostracal protein (Cohen 1966; Tooney & Cohen 1972). On the basis of our accumulated data from electron microscopy X-ray diffraction and amino acid

analysis (Hunt 1971 and table 3 of this paper) we would feel that as a protein type among structural proteins, periostracum most closely resembles fibrinogen–fibrin at the molecular level.

Although we have not yet succeeded in isolating the preperiostracum monomeric protein from the glandular regions of the mantle edge and examining it electron microscopically, the appearance of the polymeric protein in ribbons and sheets under conditions of negative staining (see figures 6–16) does strongly suggest that we are dealing here with a protein of part globular, part rod-like, morphology and the evidence already cited would also suggest that the monomer has a dumb-bell form of globular units of unequal size connected by rods. In this case there are two larger globular regions at the extremities of the monomer with a pair or perhaps a trio of smaller globular units separated from the larger units and one another by thin rods. One large and one small globular unit form a pair symmetrically related to the other pair by a symmetry axis running normal to the thin rod and third globular unit connecting the two small globular units. In the case of fibrinogen there are three globular units connected by two thin rods (Hall & Slayter 1959, 1963). Here again the larger units lie at the extremities of the 47.5 nm long molecule with this time the single small globular unit lying on the axis of symmetry normal to the long axis of the molecule. The resemblance between the two molecules is striking. Dimensionally fibrinogen is some 20 nm longer than the periostracum monomer and must pack more closely in the fibrin polymer than does the polymeric periostracin because the monomers are not as easily visualized as in periostracum (Karges & Kuhn 1970; Belitser, Morjakov & Varetskaya 1971). The situation in the fibrin polymer is also complicated by the fact that assembly into the fibrin ribbon seems to involve an overlapping aggregation (Tooney & Cohen 1972). Fibrin has a marked axial repeat of 22.5 nm and while shrinkage of the molecule has been proposed to account for the smaller axial period relative to the dimension of the monomer recent evidence strongly favours a half-staggered arrangement (Tooney & Cohen 1972).

Periostracum differs from fibrin however in that the aggregation of fibrinogen seems to be self-limited to the formation of ribbons of relatively restricted width under most conditions while periostracum protein seems capable of aggregation into sheets which are not only of great extent but also show continuity of structure, manifested as unbroken lengths of the longitudinal periodicity extensively in register extending laterally for considerable distances (figures 29 and 35). This type of well ordered aggregation into large sheets is also characteristic of certain of the collagens *in vivo* and can be demonstrated with most collagens *in vitro*. Thus the collagen of the fin rays of elasmobranch fishes, elastoidin, very clearly illustrates this point (McGavin 1962). Two-dimensional collagen sheets with two-dimensional order have been obtained by dialysis of acid citrate extracts of young rat skin collagen (Gross 1956). Although these sheet systems show two-dimensional order they also tend to show slight curvature along the lateral period, of the same type seen in some of the periostracal sheets (figures 40 and 41), as though there was some degree of strain in the system.

If the fish collagen ichthycol is treated in solution with large quantities of acid glycoprotein and then dialysed an aggregation form is produced (Gross 1956) which rather closely parallels some of the periostracal manifestations such as are seen, for example, in figures 40 and 41. Here the main collagen period was reproduced in two dimensions with a plaid pattern which could have been produced by one sheet folding over in a direction 45° to the banding. The banding was curved and the same skew was observed in all cases and in the example shown by Gross no

nonplaid overlap could be detected so that the plaid did not in fact have the appearance of folding.

It seems more likely that one layer of collagen molecules was being laid down above another under sufficiently rigorously dictated conditions of self-assembly as to maintain a constant angle between the layers. It is this type of behaviour which probably dictates helicoidal assembly in periostracum.

All these points merely serve to illustrate the observation that there are a large number of systems of structural protein now known, in which there exist the potential for steady growth into crystalline or paracrystalline arrays of high order. The type of array for any particular molecular system may vary quite radically, depending upon the *in vitro* conditions employed to bring about aggregation, as one can see from the different forms which can be produced from the basic collagen unit both *in vitro* and *in vivo*. Some type of coiled-coil rod-like element in the molecular sub-unit seems to be almost a prerequisite for this sort of behaviour.

(*f*) *Origins of the helicoidal cholesteric system*

In periostracum we see two main modes of aggregation, the ribbon mode extending in three dimensions as the lamellate helicoidal mode and the hexagonal or geometrical mode also extending in three dimensions. Because we lack *in vitro* information we do not as yet know what conditions cause the transition between these two rather different modes. Even so, the changes in condition must be relatively slight since both modes frequently merge smoothly into each other. Apart from these two very distinctive modes of organization other variants also occur, these mostly being departures to a lesser or greater extent from the ribbon-helicoidal mode. There must be rather specific physico-chemical features, spatially distributed on the flat faces of the ribbons or sheets which assemble from the dumb-bell sub-units, which bring about complementary binding of further sub-units so that the next sheet to form immediately below has the molecular axes of the sub-units, from which it forms, directed at a specific angle to those of the sub-units in the first formed sheet. Clearly there exist some conditions under which these binding sites are modified sufficiently to alter this angle because we see alterations in the pitch of the helices, orthogonal forms and alterations in the helical sense (figures 32–34). This must indicate that there are a number of binding sites just involved in directionality of binding on the faces of sheets in a stack of sheets. To assemble such a helical system as we have here from assymetric small rod-like sub-units suggests a sophisticated chain of physico-chemical events.

Binding sites must exist on the dumb-bell shaped sub-units directed along three mutually perpendicular axes; this must be the case since order in the periostracum extends in three dimensions. One would feel that these binding sites might be most likely to be located on the globular regions of the sub-units while the rod zones provide sufficient rigidity to maintain the specific spatial distribution of the binding sites. Fine structural evidence would suggest that linear aggregation somewhat precedes side-by-side aggregation of the sub-units since separate chains of sub-units have been seen (figure 49) while tapering of ribbons is also observed (figures 47 and 49). Formation of a large enough ribbon or sheet is then presumably a prerequisite for further aggregation along the third axis at right angles to the surface of the ribbon sheet in a further layer one molecule deep. It seems a likely possibility that the binding sites for this latter aggregation do not become available until the first two sets of binding sites (i.e. those distributed at right angles in the plane of the sheet) have been filled, either because the act of building to the first sets actually exposes or releases the third set or because binding of one sub-unit to the face

of a sheet required sites on two or more laterally related sub-units in the sheet or a combination of such circumstances.

As we have already mentioned, helicoidal systems assembled from macromolecules are quite common in biological systems while wholly synthetic forms are also known, e.g. in polyethylenes (Keller & O'Connor 1958). Their distribution occurs across the whole spectrum of the 'living' world from virus inclusions in cells through protozoans to animals and higher plants. Nucleic acids, polysaccharides and proteins all seem to be capable, when given appropriate conditions, of 'crystallization' in helicoidal form. Bouligand has prepared a comprehensive list of such systems involving twisted fibrous arrangements (Bouligand 1972). The type form in a low molecular mass liquid crystal system is of course the helicoidal structure which salts of cholesterol give rise to (Friedel 1922). Helicoidal structures are often therefore referred to as being in the cholesteric state even when they are not true liquid crystals, i.e. cholesteric mesophases. Neville and his associates have studied helicoidal structure in a number of biological systems, principally arthropodan (Neville 1967; Neville & Luke 1969*b*; Neville, Thomas & Zelazny 1969; Neville & Caveney 1969). Neville & Luke (1969*a*, *b*) have noted that while an insect is bilaterally symmetrical the sense of rotation of the helicoidal regions of the cuticle is the same on both sides of the insect and this is regarded as contributing evidence for the self-assembly of the helicoidal cuticle by a crystallization process. They comment that helicoidally organized cuticle could be self-assembled as a liquid crystal in the deposition zone immediately adjacent to the epidermal cells, becoming stabilized to a solid crystalline state shortly afterwards. Neville & Luke make the important point that such a liquid crystal translation model would render easy a change from preferred nematic orientation to helicoidal cholesteric orientation by a simple dependance upon solvent state. Cases are known for *in vitro* systems, e.g. poly-γ-benzyl-L-glutamate where a solvent change can change the helical sense from clockwise to anticlockwise and where an appropriate balance of two solvents can induce a preferred nematic phase (Robinson 1961). Neville & Luke also note that variations in simple factors can alter the rate of rotation in a cholesteric system, such as solvent and solute concentrations and temperature.

There seems no reason why periostracum also should not be deposited from cholesteric liquid crystals of protein secreted by the cells of the periostracal groove at the mantle edge. Control of conditions is likely to be more difficult where secretion has to take place in a liquid environment of not necessarily exactly constant salinity and hydrogen ion concentration and where temperature may vary considerably. It might be expected therefore that, in the period between secretion of the liquid crystal and its transition to a solid crystalline mode, fluctuating conditions in the environment might make those obtaining at that time felt as variations in the helical sense or transition to a nematic or some other mode of crystallization. The helices in periostracum are as we have seen in fact much less regular than in arthropod cuticle varying considerably in pitch and number of layers per turn of helix and also changing sense frequently or failing to complete a full turn of helix and in some cases deteriorating to complete disorder. An important consideration also must be the fact that the time scale involved in the deposition of periostracum is very much longer than it is for arthropod cuticle the periostracal sheet being extended at its edges in a slow and irregular manner. The rate of this process and the manner in which it is seasonally pulsed over period of months rather than hours or days is evidenced by the seasonal growth lines in the underlying shell whose growth is coupled to the growth of the periostracum.

As we have already mentioned the presence of ribbon-like forms of protein aggregation with

regularly repeating striations or proteins in hexagonal arrays seems to go hand in hand with the protein having a fibrous form with some type of rod-like element originating in a coiled conformation of the polypeptide chains. Similarly, helicoidal organization at the macromolecular level seems also to require fibrous elements (this seems self-evident) but in the case of protein systems there is no evidence to suggest that this necessarily must also involve chains in helical conformations. Table 2 lists the amino acid compositions of proteins which are known to be involved in structural systems with a helicoidal mode of organization. This list is at present rather limited but would seem to indicate that proteins potentially capable of being in the beta rather than some form of coiled or globular conformation, i.e. those with elevated contents of small side chain amino acids such as glycine and/or serine or high apolar content are possibly excluded from participating in helicoidal cholesteric organization (probably by virtue of their strictly parallel or antiparallel modes of assembly into stacks of sheets) and that in protein systems this may be a feature of either coiled-coil fibrous protein or tektin systems with structure originating in regular linear aggregation of globular units. Of course one might reasonably ask why all alpha proteins do not Bouligand. Keratins on the basis of composition ought to. Other factors must operate as well!

(*g*) *Periostraca in molluscs other than gastropods*

Periostraca are not of course confined to gastropod molluscs; they occur also in some form or other covering the shells or shell analogues of other molluscan groups. It is however only in the case of the lamellibranchs that we have any concrete information regarding detailed ultrastructure and composition of the periostracum.

Usually the periostracum in lamellibranchs consists of two or more layers. Those of *Fabulina nitidula* and *Mercenaria mercenaria* consisting of two layers (Kawaguti & Ikemoto 1962; Neff 1972*a*), *Mytilus edulis* and *Macrocallista maculata* three layers (Dunachie 1963; Bevelander & Nakahara 1967 while there are four in *Solemya parkinsonii* (Beedham & Owen 1965). The outer layers are usually thinner than the inner; in *Fabulina* the thicknesses are 0.6 and 1.4 μm respectively (Kawaguti & Ikemoto 1962).

As already mentioned most bivalve periostraca show little fine detail when examined ultrastructurally (Kawaguti & Ikemoto 1962; Kawakami & Yasuzami 1964; Bevelander & Nakahara 1967). Figures 72, 73 and 74 are typical of amorphous periostraca. In *Mercenaria mercenaria*, however, the periostracum has been shown to have a more complex organization (Neff 1972*a*). In this species the periostracum is composed of two layers, a thin electron-dense pellicle (also noted by Bevelander & Nakahara 1967) in *Macrocallista* and in *Pinctada fugata* by Wada (1968) and a homogeneous protein layer. This latter layer Neff calls the periostracum proper. The pellicle which is secreted in the curvature at the base of the periostracal groove in a space between the basal cell and the first intermediate cell, originates first of all as a unit membrane-like structure composed of two electron dense lamellae 3 nm wide and separated by a space 4 nm wide. Distal to the point of its appearance electron-dense particles are deposited on the outside of the pellicle which as more are added, moving distally, become tightly packed. These particles are slightly elongated and pack with their long axes perpendicular to the pellicle surface forming a layer 20–30 nm thick with two to three cross-striations parallel to the pellicle surface. The periostracum proper originates in the periostracal groove opposite the first cells of the general inner surface of the outer fold, its thickness increasing distally away from the site of its appearance. The innermost layer of the periostracum always appears slightly roughened and

TABLE 2. AMINO ACID COMPOSITIONS OF PROTEINS KNOWN TO EXHIBIT HELICOIDAL ORGANIZATION AT SOME STAGE OF SECRETION

(For comparison amino acid compositions of typical α-helical coiled-coil protein and β-pleated fibroin are included.)

amino acid†	*B. undatum* periostracum	*B. undatum* egg capsule	*Salmo salar* egg chorion	*Acheta domestica* egg shell	*Sphodromantis centralis* oothecal protein	*Erpobdella octoculata* egg capsule	*Ephydatia fluviatilis* gemmule wall	*Scyliorhinus caniculus* egg capsule	human haemoglobin (beta) sickle-cell anemia	non-helicoidal as far as present knowledge shows: α keratin fraction epidermis	non-helicoidal as far as present knowledge shows: mean value silk-fibroins
hydroxyproline	35	0	0	0	0	0	82	9	0	0	0
aspartic acid	126	132	85	71	95	111	120	110	48+41 asparagine	91	47
threonine	101	56	66	15	31	55	39	56	48	40	11
serine	93	94	55	342	54	83	49	62	34	111	104
glutamic acid	99	167	139	161	214	102	77	67	48+20 glutamine	140	18
proline	48	9	140	22	19	156	99	79	48	14	7
glycine	90	55	54	34	55	91	201	160	89	164	326
alanine	58	77	74	25	147	70	39	65	103	67	362
cysteine	10	6	30	33	0	16	24	12	14	6	1
valine	64	71	57	145	32	44	43	52	130	40	19
methionine	7	2	—	trace	0	1	5	trace	7	13	4
isoleucine	37	65	43	52	24	30	17	33	0	35	11
leucine	74	95	69	33	65	35	42	35	123	92	18
tyrosine	7	trace	34	9	38	54	37	80	21	28	40
phenylalanine	34	46	38	9	19	24	15	32	55	36	7
lysine	63	91	52	13	101	74	34	71	75	51	6
histidine	14	3	14	13	27	8	24	31	62	10	7
arginine	40	31	48	23	50	42	43	45	21	61	7

TABLE 2 (*cont.*)

apolar residues‡	405	418	475	320	361	450	456	456	548	448	750
small side chain residues§	241	226	183	401	256	244	289	287	226	342	792
acid residues‖	225	299	224	232	309	213	197	177	96 (157 counting amide)	231	65
basic residues¶	117	125	114	49	178	124	101	147	158	122	20
molecular configuration	α-helical	α-helical	no data	on basis of electron microscopy and molecular mass probably globular	α-helical	globular and coiled-coil possibly α-helical	spongin a form of collagen	collagen?	globular	α-helical	β-pleated sheets
situation	extracellular	intra- and extracellular	extracellular	extracellular	secretion packets within gland; not ootheca	extracellular	extracellular	precursor secretion in cells of oviduct	in sickle-cell anemia erythrocytes		
reference	this paper	Hunt 1971; N. R. Price & S. Hunt, unpublished	S. Hunt, unpublished data	Furneaux 1970; Furneaux & Mackay	Rudall & Kenchington 1971; Kenchington & Flower 1969, Neville & Luke 1971	Knight & Hunt 1974*a*	Vos 1974	Knight & Hunt 1974*b* and unpublished data	recalculated from Dayhoff & Eck 1968, Ingram 1957, Dobler & Bertles 1968	Baden & Goldsmith 1972	Hunt 1970*b*

† Residues per 1000 total amino acids.
‡ Proline, glycine, alanine, valine, isoleucine, leucine, phenylalanine.
§ Serine, glycine, alanine.
‖ Aspartic acid, glutamic acid.
¶ Lysine, histidine, arginine.

sometimes more electron dense than the rest of the homogeneous protein. The general appearance of the periostracum in this species is similar to that found in *Macrocallista maculata* by Bevelander & Nakahara but differs from that seen in *Pteria martensii* or *Pinctada fucata* (Tsujii 1968; Wada 1968).

(*h*) *Implications of composition for differences between molluscan periostraca*

Clearly the structure of periostraca at the fine structural level, where molecular organization is likely to be evident, is going to be importantly influenced by the chemical composition of the material, which in the case of gastropod and lamellibranch periostraca is probably principally protein, at the molecular level. Beedham & Truman (1968, 1969) note that the bulk of the cuticle in the Aplacophora and Placophora (homologous with the periostracum of more highly evolved forms) is made up of a mucoid complex which they suggest is mainly glycoprotein, described as being technically glycoprotein but with high mucopolysaccharide and low protein content not stabilized by cross-linking. In the case of the Placophora there is beneath this in the cuticle a layer of apparently tanned protein more typical of periostracum; this layer is absent in the Aplacophora. It is unlikely that glycoprotein as mucins or acid mucopolysaccharides play any very important rôle in the structure of gastropod and lamellibranch periostraca however. Neutral polysaccharide is reported as being present in the periostraca of all of twelve genera of gastropod on the basis of the PAS reaction but alcian blue and toluidine blue gave no evidence of the presence of acid mucopolysaccharides (Meenakshi, Hare, Watabe & Wilbur 1969). Degens, Spencer & Parker (1967) find varying amounts of glucosamine and galactosamine in both gastropod and lamellibranch periostraca. It seems likely that the neutral polysaccharide present in gastropod periostraca at least, is present largely as oligosaccharide prosthetic groups associated covalently with the structural protein. The monosaccharides present and the generally low level of monosaccharide content (Hunt 1970*a*) supports this view, although very small amounts of chitin are evidently also present (S. Hunt, unpublished results). Meenakshi *et al.* (1969) found the chitosan test to be consistently negative for gastropod periostraca. Even so chitin may well be present and even an important component in the periostraca of other groups (Peters 1972). Hunt (1973) has identified chitin both by chemical and X-ray diffraction methods in the periostracum of the lamellibranch *Lutraria lutraria* although the actual amounts involved are rather small. It seems probable that the most important structural component of gastropod and lamellibranch periostracum is structural protein and one would feel that the variability of periostracal organization, which is as we have seen particularly evident in gastropod periostraca, will originate in variability of these proteins.

The amino acid compositions of molluscan periostraca have been investigated by a number of authors and analyses are available for a wide range of gastropod and lamellibranch species (reviews by Wilbur & Simkiss 1968; Hunt 1970*a*). In general glycine accounts for 40% or more of the amino acids of marine and fresh-water lamellibranchs and of fresh-water and terrestrial gastropods (Meenakshi *et al.* 1969; see also Degens *et al.* 1967) while marine gastropods contain much less glycine and elevated contents of polar amino acids such as aspartic acid and glutamic acid. Moreover the amino acid compositions of at least one gastropod periostracum apparently showed environmental sensitivity with glycine contents in the fresh-water species *Potamopyrgus* decreasing with increasing salinity of the culture medium (Meenakshi *et al.* 1969). This may point to the presence of more than one protein. Meenakshi *et al.* (1969) also noted a relation between environment (and hence amino acid composition) and numbers of

layers in gastropod periostraca. Fresh-water species had two layers, terrestrial species a single layer and marine species a single or incomplete layer. These authors presented no photographic evidence for this latter observation but it rather sounds as if the thinner innermost layers have been neglected or not observed in this tally. The observation is still however of considerable interest.

Elevated glycine contents in proteins tend to be diagnostic of some type of structural protein. If the levels lie between about 30 and 60 % and large quantities of proline and/or hydroxyproline are not present then it is likely that some form of beta conformation with the protein in sheets at the molecular level such as are found in the silks will be found (Lucas & Rudall 1968). Such arrangements on a large scale tend to be ultrastructurally amorphous although when disrupted they may appear as rather structureless ribbons with only the direction of the individual fibres obvious. The presence of elevated levels of proline and possibly hydroxyproline will be likely to result in a collagen type of helical conformation with the molecules forming rods; such conformations are not confined to tissue collagens but are present in certain silks rich in glycine and proline (Rudall & Kenchington 1971). These conformations will tend to assemble into regularly repeating linear structures, clearly visible at the ultrastructural level, unlike the beta conformation. Levels of glycine above 60 %, in the absence of quantities of imino acids, will have the potentiality of adopting one of the polyglycine conformations. Polyglycine I is an extended beta chain conformation similar to the silk fibroins while polyglycine II adopts a form of three-fold helix with all chain senses parallel and hydrogen bonded into a potentially infinite hexagonal lattice (Ramachandran 1967). It is instructive to compare the composition of the periostracum of *Arctica islandica* (marine lamellibranch) with that of the silk of the solomon seal sawfly (table 3) (Degens *et al.* 1967; Lucas & Rudall 1968). It is not likely that either form of polyglycine conformation will present a very well ordered appearance at the ultrastructural level although the direction and general direction of fibres should be visible particularly in disrupted preparations. As the content of glycine (and alanine and serine) decreases in a structural protein the likelihood of beta conformation being adopted decreases and the likelihood of a globular or alpha helical, possibly coiled-coil, rod-like conformation increases. As we have already commented, where a structural protein system is involved such alpha helical or globular or hybrid rod-globular proteins tend to assemble into linear structures as ribbons or fibres with characteristic regular linear repeats readily visualized at the ultrastructural level. Examples of this are found in F-actin, fibrin, paramyosin, tropomyosin, trichocyst fibrils and many other cases. A comparison between composition, conformation and fine structure is made in table 3.

In molluscan periostraca we have a separation into roughly two ultrastructural situations: one in which the periostracum shows evidence of considerable molecular order with a regular linear repeat appearing on constituent ribbons or sheets; the other in which there is very little visual evidence of order the structure being perhaps layered but otherwise amorphous or at most slightly fibrous in appearance (figures 72–73, plate 14). The former situation, as far as our limited experience shows, obtains in marine gastropods the latter in fresh-water and terrestrial gastropods and marine lamellibranchs. We can couple to this observation the evidence of amino acid analysis which shows that marine gastropod periostraca have low glycine contents and amino acid compositions characteristic of globular or alpha helical coiled-coil rod-shaped proteins while the periostraca of fresh-water gastropods and marine lamellibranchs have elevated glycine contents and amino acid compositions characteristic of proteins in beta conformations or possible polyglycine conformations. We know also that in one marine gastropod

TABLE 3. CHARACTERISTICS OF BUCCINUM PERIOSTRACAL PROTEIN COMPARED WITH OTHER STRUCTURAL PROTEINS WHICH HABITUALLY AGGREGATE AS FIBRES, RIBBONS OR SHEETS WITH A REGULAR LONGITUDINAL REPEAT

(The structural proteins of periostraca of a marine lamellibranch and a terrestrial gastropod are also included and compared with a structural protein known to adopt polyglycine II conformation and a molluscan structural protein known to be in a beta conformation.)

amino acid†	*Buccinum* periostracum	F-actin	fibrinogen	paramyosin	tropomyosin	Trichocyst fibril (dino-flagellate)	*Buccinum* egg capsule	*Arctica islandica* periostracum	*Phymatocera aterrima*	*Helix aspersa*	*Buccinum* operculum
hydroxyproline	35	0	0	0	0	0	0	0	0	0	0
aspartic acid	126	96	119	140	106	78	132	16	76	20	140
threonine	101	80	62	44	28	49	56	5	3	15	21
serine	93	69	80	48	48	57	94	23	34	22	100
glutamic acid	99	108	119	207	252	102	167	13	7	47	32
proline	48	47	60	2	2	44	9	25	8	28	17
glycine	90	78	90	20	18	103	55	669	662	511	299
alanine	58	84	50	132	123	107	77	21	15	79	148
cysteine	10	10	26	0	24	0	6	14	0	0	0
valine	64	51	42	34	31	75	71	11	20	103	26
methionine	7	27	20	13	24	23	2	20	0	31	0
isoleucine	37	74	44	27	34	51	65	21	22	45	7
leucine	74	73	65	130	106	95	95	12	34	32	36
tyrosine	7	38	36	22	18	29	trace	70	57	30	57
phenylalanine	34	33	34	7	6	48	46	13	1	17	13
lysine	63	54	75	72	139	33	91	19	21	7	41
histidine	14	21	20	5	7	13	3	6	11	0	37
arginine	40	49	54	99	54	43	31	33	29	7	27

TABLE 3 (*cont.*)

apolar residues‡	405	440	385	352	320	521	418	772	762	815	546
small side chain residues‡	241	231	220	200	189	267	226	713	711	612	547
acid residues‡	225	204	238	347	358	180	299	29	83	67	172
basic residues‡	117	124	149	176	200	89	125	58	61	14	105
molecular configuration	α-helical probably coiled + globular	globular	globular + α-helical rod	α-helical coiled-coil	α-helical coiled-coil	no data		no data	polyglycine II	no data	× -β-pleated
fibre axis major repeat	*ca.* 30 nm non-overlap	fibre composed of beads at 50 nm; double helix with 36 nm crossover	225 nm overlap	—	various *in vitro* ribbon aggregates principle repeat 56 nm overlap	65–70 nm	92–93 nm overlap	non	non	non (in *Helix* pomatia)	non
sub-unit	●–•–•–● 26 nm long	● 50 nm diameter	●–•–● 475 nm long	——140 nm	—— 40 nm	no data	—— 45 nm	non	extended 'fibres'	non	non
reference	Hunt 1971	Carsten 1965; Hanson & Lowy 1963	Steiner 1965; Hall & Slayter 1963	Kominz *et al.* 1958; Szent Gyorgyi *et al.* 1971	Carsten 1968; Sobieszek & Small 1973	Messer & Ben-Shaul 1971	Hunt 1971 (N. R. Price, unpublished)	Degens *et al.* 1957	Lucas & Rudall 1968	Meenakshi *et al.* 1969	Hunt 1971

† Residues/1000 total residues.
‡ As for table 2.

(*Buccinum*), that the protein of the periostracum is in the alpha helical conformation. In this organism therefore we might have predicted from the structure, by analogy with such proteins as fibrin or tropomyosin, that the amino acid composition might be low in small side-chain amino acids and that the diffraction pattern might be that of an alpha helical system.

The amorphous appearance of the periostraca of fresh-water and terrestrial gastropods and marine lamellibranchs is in keeping with their constituent proteins having a beta structure as their amino acid compositions suggest. At present however diffraction data are lacking to confirm this opinion. It is perhaps worth noting that gastropod opercula are composed of a protein containing about 30 % glycine (table 3) in the presence of elevated contents of alanine and serine (Hunt 1970*a*, 1971). This protein is tanned and histochemically resembles lamellibranch periostracum. Like periostracum too it is largely amorphous at the fine structural level except for layering and some slight evidence of fibrous organization rather like that seen in the periostracum of *Lymnaea stagnalis* by Kniprath (1972). This protein is in an unusual form of beta pleated conformation well orientated in a plane perpendicular to that of the plane of the operculum (S. Hunt, unpublished data). Thus we may have reasonable cause to predict a beta conformation for glycine rich periostraca and their amorphous fine structural appearance need not necessarily imply a lack of organization at the molecular level. In fact the infrared spectrum of *Helix* periostracum tends to confirm the predictions based on amino acid analysis and ultrastructure (figure 74, plate 14); the amide absorption bands agree with values for known β-proteins and the spectrum is remarkably similar to that for *Buccinum* operculum (S. Hunt, unpublished data.)

(*i*) *Stabilization of periostracal proteins*

Histochemical evidence presented by several authors renders it likely that many molluscan periostraca have their proteins stabilized by tanning (Kessel 1940; Trueman 1949; Beedham & Owen 1965; Wada 1964; Beedham 1958, 1965; Brown 1950; Meenakshi *et al.* 1969; Hillman 1961). Most of this earlier evidence rests upon solubility and staining properties of the material, i.e. absence of solubility in reagents other than hypochlorite, strong positive responses to such tests for diphenols as argentaffin and upon high contents of phenolic amino acids especially tyrosine. In fact tyrosine contents vary widely and can be as high as 18 % (residues) or as low as 0.4%. Dihydroxyphenylalanine is sometimes present but by no means always, as is also the case with dihydroxyphenylalanine oxidase (Degans *et al.* 1967; Hillman 1961). Moreover the presence of tyrosine and dihydroxyphenylalanine in hydrolysates of periostracal protein may not provide a particularly useful indicator of the involvement of these compounds in the stabilization of the structure since it is most likely that they would have been modified by the tanning process in an irreversible manner. It is much more important therefore to examine periostracal scleroprotein hydrolysates for aromatic products derived perhaps from altered aromatic amino acids. The strong pigmentation of some periostraca relative to others may not be a good indicator; for example the deep bluish brown of *Mytilus* periostracum relative to that of another bivalve *Lutraria* is almost certainly due to the polymerization of halogenated amino acids and not to cross-linking. S. O. Andersen (personal communication) has isolated bromotryptophane from the periostracum of *Mytilus edulis*; a suitable precursor of the purple pigmentation of this particular material. It will be necessary also to determine whether all periostraca are subject to the same processes of tanning and stabilization. S. O. Andersen again (personal communication) has isolated arterenone, a compound implicated in the stabilization of insect

cuticular protein, from the periostracum of *Mytilus*. We in this laboratory however have failed to detect this and related compounds in *Buccinum* periostracum. Possibly gastropod periostraca are stabilized by mechanisms different from those in lamellibranchs. The presence of halogenated tyrosines in *Buccinum* periostracum does however suggest that the protein is at some stage in contact with a system capable of oxidizing a halide ion such that available tyrosines become substituted. This could point to the presence of a phenol oxidase system and perhaps therefore to a measure of phenolic or quinone cross-linking. Certainly hydrolysates of periostracum from *Buccinum* when chromatographed on columns of Sephadex G15 reveal a content of a wide range of aromatic compounds both benzenoid and heterocyclic other than tyrosine, phenylalanine, tryptophane and halogenated tyrosines. Some of these may be tryptophane degradation products but several compounds with characteristics of diamino-diphenols also appear to be present. We are at present pursuing this problem intensively.

(*j*) *Periostraca analogues in invertebrates other than molluscs*

Periostracum-like structures appear in organisms other than molluscs in similar situations and it is probably worth comparing therefore these with the molluscan materials since the biological problem which has been solved, namely the secretion under water of a scleroprotein sheet covering an external inorganic skeleton and acting as a locus for 'shell' deposition, is essentially the same.

In brachiopods the situation is broadly analogous to that found in molluscs. The periostracum originates on the inner side of the outer mantle lobe by a 'conveyor belt' system of growth involving the migration of transient cells from an intramarginal generative zone towards the tip of the lobe (Williams 1968). Periostraca of two different types occurring in articulate brachiopods have been described by Williams (1968). In the rhynchonellid *Notosaria nigricans* the first material to be produced is a continuous film of mucopolysaccharide up to 100 nm thick and it is beneath this layer that the true periostracum is laid down. Immediately beneath the mucopolysaccharide layer there is formed a so-called outer bounding membrane upon which rests a layer of short cylindrical units with distally rounded heads. These rods 20 nm thick and 35 nm tall stand 40 nm apart in a 75° rhombic array and show a 2.5 nm periodicity suggestive of a compressed coil. The membrane on which the rods rest is a triple layered structure 14 nm thick rather reminiscent of the trilaminar structures which bound some of the vacuoles in the *Buccinum* periostracum or which lie on the innermost face of the latter structure. Beneath this so-called membrane the periostracum of *Notosaria* consists of a 600 nm thick layer of vacuolated glycoprotein the vacuoles being again bounded by membrane-like structures and again very much resembling the vacuoles of *Buccinum* periostracum. At a later stage of development fibrils appear in the glycoprotein layer which are sporadic continuations of an erect mat of fibres 30 nm deep distributed at 10 nm intervals and resting on an inner bounding membrane similar to the outer membrane. Clearly this type of periostracum is far more complex than any of the molluscan ones that we have examined. In terebratulid articulate brachiopods the structure of the periostracum is similar to that of the rhynchonellids but differs in detail. In *Waltonia* there is a rod-like outer layer very similarly arranged to that of *Notosaria* but with the rods being of widely differing lengths extending deep into labyrinths in the immediately proximal layer and connected to one another by fine fibrils which at lower levels alter to a roughly hexagonal net. We have already mentioned the similarities of this organization to certain features of *Buccinum* periostracum. The glycoprotein layer of *Notosaria* is in *Waltonia* represented by a densely

osmophilic protein layer which forms the labyrinths mentioned above. Large vacuoles are also present in this layer and once again they are bound by trilaminate membranes very similar in appearance to the limiting zones seen around many of the vacuoles of the *Buccinum* periostracum. In *Waltonia* the triple layered structure of the inner basal membrane is obscured by internal and external thickening to a depth of up to 250 nm. It is worth noting how in the periostraca of gastropods and brachiopods the innermost layers which are in contact with the calcified material differ quite radically from the major part of the periostracum.

TABLE 4. AMINO ACID COMPOSITIONS OF SOME 'PERIOSTRACAL' PROTEINS OF NON-MOLLUSCAN ORIGIN

Compare with table 3 for molluscan periostraca

	Brachiopoda. Jope (1969)			*Bryozoa* (*Ectoprocta*) Hunt 1972
	Articulata (*Terebratulida*)		*Inarticulata* (*Lingulida*)	*Cheilostoma*
amino acid†	*Laqueus*	*Waltonia*	*Lingula*	*Flustra foliacea*
hydroxyproline	0	trace	29	0
aspartic acid	135	146	87	143
threonine	16	33	45	38
serine	75	71	66	89
glutamic acid	47	75	47	105
proline	52	30	76	67
glycine	324	288	228	300
alanine	37	70	116	80
cysteine	13	11	28	0
valine	26	45	44	20
methionine	1	trace	9	0
isoleucine	12	38	23	11
leucine	20	45	34	28
tyrosine	59	0	35	12
phenylalanine	61	44	37	19
lysine	28	37	27	13
histidine	32	11	9	0
arginine	64	53	63	75
Apolar residues‡	532	560	558	525
small side chain residues‡	436	429	410	427
acid residues‡	182	221	134	248
basic residues‡	124	101	99	88

† residues/1000 total residues
‡ as for table 2

Williams (1968) visualizes a prototypic brachiopod periostracum as a triple-layered membrane with a distal mat of fibrils beneath an impersistent layer of mucopolysaccharide. He suggests that the membrane might originally have been secreted as the only exoskeletal cover of the prototypal brachiopod and that later in the evolution of the phylum this might have served as a seeding sheet for an evolving mineralized shell. This view compares in an interesting way with that of Beedham & Trueman (1969) for the prototypic molluscan periostracum with a development through an evolutionary sequence of protective mucoid complex, enhancement of protective value by incorporation of tyrosine-rich protein, tanning of protein and subsequent utilization of this now sclerotized material for deposition of nacreous calcified layers. In the Placophora a mucoid periostracum with a thin underlying tanned protein layer still persists (Beedham & Trueman 1969) and thus, although the nature of the brachiopod and gastropod periostraca may seem rather divergent, there may well be thematic links at earlier stages of molluscan evolution.

Bryozoans also have an outer organic cover to the exoskeleton which is termed a periostracum and which is secreted at the growing edges or tips of the colony (Taverner-Smith & Williams 1972). In *Membranipora* for example the external cover of the periostracum is formed as a triple-unit membrane-like structure consisting of outer and inner electron-dense layers about 3.5 and 4.5 nm thick respectively and separated by an electron-luscent zone about 5.5 nm thick (Taverner-Smith & Williams 1972). The external surface of the outer layer carries a filamentous brush of bulbous headed rods 18 nm high and 7.0 nm wide. The main periostracal layer is divided into two zones of approximately equal thickness. The electron-luscent groundmass of the outer zone contains linear trails of dense particles lying approximately parallel to the outer surface. The inner zone contains more evenly distributed particles. Histochemical tests suggest that the periostracum is composed of mucopolysaccharides, protein and chitin. An analysis of the exoskeletal material not susceptible to aqueous extraction from *Flustra foliacea* by Hunt (1972) indicates that approximately 90 % of the material is structural protein with the remainder chitin.

Brachiopod and bryozoan periostraca both contain structural proteins rich in glycine and dicarboxylic amino acids. For example the periostracum of *Laqueus californianis* (Brachiopoda, Articulata) contains 324 and 135/1000 total residues of glycine and aspartic acid respectively (Jope 1967) while the periostracum of *Flustra foliacea* (Bryozoa, cheilostoma) contains 300 and 143/1000 total residues of glycine and aspartate respectively (Hunt 1972). Table 4 compares the chemical compositions of some 'periostracal' proteins. Clear similarities to marine lamellibranch and fresh-water and terrestrial gastropod periostraca although less so to marine gastropods can be seen in the brachiopod and bryozoan periostraca although the ultrastructural organizations are clearly in some ways more complex in the latter groups than in even the most complex gastropod periostraca. None of these structures from brachiopods or bryozoans has a lamellate helicoidally organized periostracum such as we have described in *Buccinum* but then the amino acid compositions suggests that a beta conformation for the protein might be more favoured and as we have already seen, the presence of such protein tends not to give rise to highly ordered periostraca in molluscs. One might feel from these comparisons with other groups that the beta type protein (high glycine) solution to the problem of provision of a periostracum with its associated implications for the calcification process is evolutionarily more common than the use of a helical protein.

(*k*) *General conclusions*

Periostraca would appear therefore to be extracellular cuticular structures which have evolved in several different invertebrate groups to shield a naked epithelium. A later stage seems to have been the development of a mineralized phase beneath the cuticle. Whether the cuticle evolved in response to a requirement for mechanical protection or as a means to waterproofing it must have influenced the further evolution of the animals involved quite radically. Loss of a respiratory surface epithelium over extensive areas of body must have been a decisive factor in gill development and evolution in the mollusca (Stasek 1972).

On this view the subsequent development of a mineral shell would clearly render the original status of the periostracum to a large extent obsolete. We see however periostraca remaining in molluscs and brachiopods as what are not apparently vestigial structures although they may be better developed in some species than in others. The rôle of the periostracum must therefore have changed in those groups where a mineralized shell is now present. It seems an attractive

hypothesis to suggest that mineralization may have been a consequence of the development of a structural protein cuticle overlying a secretory epithelium. The presence of a relatively impermeable barrier between the surrounding sea and the epithelium has provided a micro-environment into which proteins, mucopolysaccharides and mineral ions can be secreted and in which nucleation and crystallization can take place under controlled conditions. Large stable mineralized structures can potentially form under these conditions without continual disturbance of the initial stages of growth by the flux of the external medium. In this sense then the rôle of the periostracum has not changed. It still protects, it is still a barrier to the environment. The protection offered is now however more subtle in its consequences although less subtly it may still serve to protect the completed shell from chemical and mechanical attack. Whether this barrier to the environment is more than a passive structure is a question probably worth asking at the present stage of our knowledge of structural proteins and of the processes of calcification in molluscs.

The process by which the shell is deposited beneath the periostracum is a complex one, usually considered to be mediated almost entirely by the cells of the epithelia in the mantle folds and adjacent regions, with perhaps the periostracum acting as a template nucleating the mineral crystallization in its initial stages. Few authors (Taylor & Kennedy 1969) comment upon the possibility that the periostracum may influence surface architecture of shells but this is perhaps implicit in the last stated function. It is however more generally suggested that crystal type and mineralogical organization are complex variables under the influence of environmental conditions acting both directly and through variation in the composition of the shell organic matrix. More recently it has been suggested that the periostracum has a more active wider physiological rôle to play in mineralization. Digby (1968) feels that the periostracum, functioning in conjunction with the mantle, may be capable of bringing about a gradient of pH across its opposite faces. This is achieved by virtue of internal electrode action coupled to the streaming of salt water through the structure. It is suggested that periostraca have significant semi-conductive properties. The electrochemical gradient generated by these means is then supposed to bring about calcium carbonate deposition on the inner face of the periostracum. A disadvantage of this theory is that it is not clear how the mechanism would function in fresh-water and terrestrial species.

Recent work on the dielectric properties of polypeptides of determined amino acid composition synthesized in sheet form should enhance our knowledge of the way in which structures such as periostraca could potentially behave physiologically. Tredgold & Hole (1976) have shown that glycine–alanine–serine co-polymers in the beta pleated sheet form have much higher dielectric constants (in the dry state) than their side chain compositions might have suggested. This arises from dipole movements associated with peptide bond displacement and looseness and could suggest physico-chemical potential for mediating directional movement of ions. The point is that even glycine-rich natural structural protein sheets, such as form some periostraca, may not be as inert as their composition might suggest, while those containing more polar amino acids may be capable of very complex electrochemical behaviour.

A puzzling feature of what emerges from this and other studies of molluscan periostraca reviewed here, is the variability in their structure and composition. This is most evident when the marine, fresh-water and terrestrial species are compared. In most of the gastropods examined we observe (Meenakshi *et al.* 1969) a dramatic change from aspartic acid-rich proteins to those rich in glycine when the move into fresh-water is made. This pattern is maintained in the

transition to a land habitat. Although fine-structural data is more limited, it would appear that organization also changes dramatically in these circumstances. In contrast, bivalve periostraca appear to be similar in marine and fresh-water species; both are high in glycine and fine-structurally similar to fresh-water gastropod periostraca.

It is clear therefore that whatever function periostraca may have in recent molluscan species this can be fulfilled by the glycine-rich protein system in any environment, whether it be marine, fresh-water or terrestrial. If this were not so then the marine bivalves would suffer a disadvantage from their possession of such a periostracum and there is no evidence to suggest that this is so. Moreover there are occasional marine gastropod species which do appear compositionally to have high-glycine, low-aspartic acid, periostraca; *Nassarius obsoletus* is an example. So equally a high-aspartic acid protein may not be an absolute constraint imposed upon the marine gastropods for their success. These observations then clear the way to look at the anomalous position of the high-aspartic acid, tectin assembled, periostraca of the marine gastropods. We might now conclude that such a structure may not confer special advantage to the group in a marine environment, above that of a periostracum assembled from a glycine-rich protein, but may prove a distinct disadvantage in the fresh-water or terrestrial environment. Why should this be so?

There seem to be two possible answers to this question. First, the more polar periostracum may have difficulty in functioning physiologically, as a means of generating electrochemical gradients or as a crystallization template, in media of low ionic strength or greatly reduced water content. We have however already pointed out the difficulties in envisaging the application of the former function (if it exists at all in any molluscan group) in a terrestrial situation. Secondly, and to our minds more probably, the problem may be associated with the difficulty in assembling, in fresh-water or air, a structural unit of the type described in this paper. The tectins we know of from other sources, which build up into fibrous protein polymers, appear almost always to do this in physiological media at relatively high ionic strengths. Fibrous actin, the myosin thick filament, the fibrin clot, viral coats and microtubules all assemble in situations either within the cell or in physiological fluids. Such self-assembly, and we might include collagens in these systems, must depend upon elaborate dispositions of binding sites on molecular surfaces and it may be that the process requires fine control of pH and ionic composition to be fully effective. In fact the variations observed in the fine structural organization of *Buccinum* periostracum may reflect the difficulty in maintaining precise control in an extracellular and extraorganism situation. It may therefore not be possible to maintain control over self-assembly in fresh-water or air. The process may even be quite impossible.

The silks, which are extracellular structural protein systems largely secreted into air or to a lesser extent fresh-water (trichopteran and certain dipteran larvae), tend to be of the type where a macroscopic structure is generated by interaction at the secondary and to a lesser extent tertiary levels of organization and where quaternary assemblage is of lesser importance. This is the sort of situation which seems to obtain in periostraca of fresh-water and terrestrial gastropods or marine and fresh-water bivalves.

Whether or not these hypotheses are correct we still have to explain how the transition from marine to fresh-water gastropod periostracal types has been achieved. The present state of knowledge of the genetic control of protein synthesis would suggest that it is highly unlikely that the aspartic acid-rich proteins in the marine gastropod periostracum will be homologous with the glycine-rich proteins of other forms. While the triplet code specifying aspartic acid can be

readily changed to that for glycine or alanine by a change in the bases at the second letter it would require an improbably large number of such mutations to change a protein with many aspartic acid residues to one with many glycines. Given sufficient time and a strong evolutionary advantage this could take place but since the change postulated radically affects protein conformation the possibility that intermediate stages in the change might produce periostracal proteins with unfavourable properties seems a high one. It seems more likely then that the major protein of the marine gastropod periostracum originates in a gene different to, and not homologous with, the gene whose expression is the protein of the periostraca of the fresh-water and terrestrial species. Now marine bivalves have periostraca closely resembling those of non-marine gastropods moreover the lamellibranchs and gastropods probably arose at around the same time (gastropods probably slightly earlier) in the marine environment from a common ancestral root. Thus we might reasonably conclude that the periostracal proteins of the non-marine gastropods are not only compositionally but evolutionarily capable of being homologous with those of the bivalve molluscs and could represent expression of a gene of common origin. This gene, while present in marine gastropods, may have lain dormant until the transition to fresh-water or else may be expressed only briefly during the life cycle of the marine species perhaps in the larval stages. The sensitivity of composition, in marine gastropod periostraca, to environmental changes may then be understandable in terms of the activity of this unusually unexpressed genetic function.

The periostracum of this marine gastropod is thus exposed as a structure whose complexity exists not only in its architecture. This complexity has facets reflecting problems of self-assembly, of environmental and genetic influences upon structure, of evolutionary relations and of function. Like many other macromolecular products, destined for use outside the cell, the periostracum speaks vigorously of the dynamic versatility of the biological secretion process and in speaking asks as many fascinating questions as it answers.

We would like to thank the Science Research Council for financial assistance with this study (Grant No. B/RG/0893 3). We would also like to thank Mrs J. Greenwood for much valuable technical assistance and Mr N. R. Price for a wealth of helpful discussion.

References

Baden, H. P. & Goldsmith, L. A. 1972 The structural protein of epidermis. *J. invest. Derm.* **59**, 66–76.

Bailey, A. J. 1968 The nature of collagen. In *Comprehensive biochemistry* (ed. M. Florkin & E. H. Stotz), vol. 26B, pp. 297–413. Amsterdam: Elsevier.

Bairati, A. 1972 Collagen: An analysis of phylogenetic aspects. *Boll. Zool.* **39**, 205–248.

Beedham, G. E. 1958 Observations on the non-calcareous component of the shell of lamellibranchia. *J. Micr. Sci.* **99**, 341–357.

Beedham, G. E. 1965 Repair of shell in species of *Anodonta*. *Proc. zool. Soc. Lond.* **145**, 107–124.

Beedham, G. E. & Owen, G. 1965 The mantle and shell of *Solemya parkinsoni* (Protobranchia: Bivalvia). *Proc. zool. Soc. Lond.* **145**, 405–430.

Beedham, G. E. & Trueman, E. R. 1968 The cuticle of the Aplacophora and its evolutionary significance in the Mollusca. *J. Zool.* **151**, 215–231.

Beedham, G. E. & Trueman, E. R. 1959 The shell of the chitons and its evolutionary significance in the Mollusca. *Proc. Malacol. Soc. Lond.* **38**, 550–551.

Belitser, V. A., Morjakov, V. Ph. & Varetskaya, T. V. 1971 Medium dependent structure modifications of reconstituting fibrin. *Biochim. biophys. Acta* **236**, 546–549.

Bevelander, G. & Nakahara, H. 1967 An electron microscope study of the formation of the periostracum of *Macrocallista maculata*. *Calc. Tissue Res.* **1**, 55–67.

Bevelander, G. & Nakahara, H. 1970 An electron microscope study of the formation and structure of the periostracum of a gastropod *Littorina littorea*. *Calc. Tissue Res.* **1**, 5–12.

Bonar, L., Cohen, A. S. & Skinner, M. M. 1969 Characterization of the amyloid fibril as a cross β protein. *Proc. Soc. exp. Biol. Med.* **131**, 1373–1375.

Bouligand, Y. 1965*a* Sur une architecture torsadée répandue dans de nombreuses cuticles d'arthopodes. *C.r. hebd. Séanc. Acad. Sci., Paris.* **261**, 3665–3668.

Bouligand, Y. 1965*b* Sur une disposition fibrillaire torsadée commune à plusieurs structures biologiques. *C.r. hebd. Séanc. Acad. Sci., Paris.* **261**, 4864–4867.

Bouligand, Y. 1972 Twisted fibrous arrangements in biological materials and cholesteric mesophases. *Tissue Cell* **4**, 189–217.

Brown, C. H. 1950 A review of the methods available for the determination of the types of forces stabilizing structural proteins in animals. *Q. Jl. microsc. Sci.* **91**, 331–339.

Carsten, M. E. 1965 A study of uterine actin. *Biochemistry* **4**, 1049–1054.

Carsten, M. E. 1968 Tropomyosin from the smooth muscle of the uterus *Biochemistry* **7**, 960–967.

Champness, J. N. & Lowy, J. 1968 The structure of bacterial flagellae. In *Symposium on fibrous proteins* (ed. W. G. Crewther), pp. 106–114. Australia: Butterworths.

Cohen, C. 1966 Architecture of the α-class of fibrous proteins. In *Molecular architecture in cell physiology* (ed. T. Hayashi & A. G. Szent-Gyorgyi), pp. 169–190. New Jersey: Prentice Hall.

Cohen, C., Caspar, D. L. D., Johnson, J. P., Naus, K., Margossian, S. S. & Parry, D. A. D. 1973 Tropomyosin-troponin assembly. *Cold Spring Harb. Symp. quant. Biol.* **37**, 287–297.

Dakin, W. J. 1912 Buccinum. *Liverpool marine biology committee memoirs*, no. 20. London: Williams & Norgate.

Dayhoff, M. O. & Eck, R. V. 1968 *Atlas of protein sequence and structure*, pp. 123–163. Maryland: National Biochemical Research Foundation.

Degens, E. T., Spencer, D. W. & Parker, R. H. 1967 Paleobiochemistry of molluscan shell proteins. *Comp. Biochem. Physiol.* **20**, 553–579.

Dennel, F. L. S. 1974 The cuticle of the crabs *Cancer pagurus* L. and *Carcinus maenas* L. *Zool. J. Linn. Soc.* **54**, 241–245.

Digby, P. S. B. 1968 The mechanism of calcification in the molluscan shell. In *Studies in the structure, physiology and ecology of molluscs* (ed. V. Fretter). Symposia of the Zoological Society of London and the Malacological Society of London, no. 22. London: Academic Press.

Dobler, J. & Bertles, J. F. 1968 The physical state of haemoglobin in sickle-cell anemia erythrocytes *in vivo*. *J. exp. Med.* **127**, 711–716.

Dunachie, J. F. 1963 The periostracum of *Mytilus edulis*. *Trans. R. Soc. Edinb.* **65**, 383–411.

Flower, N. E., Geddes, A. & Ruddall, K. M. 1969 Ultrastructure of the fibrous protein from the egg capsule of the whelk *Buccinum undatum J. Ultrastruct. Res.* **26**, 262–273.

Friedel, M. G. 1922 Les états mésomorphes de la matiére. *Annls Phys.* **9**, 273–474.

Furneaux, P. J. S. 1970 O-Phosphoserine as a hydrolysis product and amino acid analysis of new laid eggs of the house cricket. *Acheta domesticus* L. *Biochim. biophys. Acta.* **215**, 52–56.

Furneaux, P. J. S. & Mackay, A. L. 1972 A crystalline protein in the chorion of insect egg shells. *J. Ultrastruct. Res.* **38**, 343–359.

Garrone, R. & Pottu, J. 1973 Collagen biosynthesis in sponges: Elaboration of spongin by spongocytes. *J. Submicr. Cytol.* **5**, 199–218.

Greaser, M. L., Yamaguchi, M., Brekke, C., Potter, J. & Gergely, J. 1973 Troponin sub-units & their interactions. *Cold Spring Harb. Symp. quant Biol.* **235**, 235–244.

Gross, J. 1956 The behaviour of collagen units as a model in morphogenesis. *J. biophys. biochem. Cytol.* **2**, 261–273.

Hall, C. E. & Slayter, H. S. 1959 Fibrinogen molecule. Its size, shape and mode of polymerization. *J. biophys. biochem. Cytol.* **5**, 11–16.

Hall, C. E. & Slayter, H. S. 1963 Molecular features of fibrinogen and fibrin. In *5th International Congress on Electron Microscopy*, vol. 2 (ed. S. R. Breese, Jr), pp. 0–3. New York: Academic Press.

Hanson, J. & Lowy, J. 1963 Structure of F-actin and of actin filaments isolated from muscle. *J. molec. Biol.* **6**, 46–60.

Hillman, R. E. 1961 Formation of the periostracum in *Mercenaria mercenaria*. *Science N.Y.* **134**, 1754–1755.

Hunt, S. 1970*a* *Polysaccharide-protein complexes in invertebrates*. London: Academic Press.

Hunt, S. 1970*b* Amino acid composition of silk from the pseudoscorpion *Neobisium maritimum* (Leach): A possible link between the silk fibroins and the keratins. *Comp. Biochem. Physiol.* **34**, 773–776.

Hunt, S. 1971 Comparison of three extracellular structural proteins from the whelk *Buccinum undatum*. The periostracum, operculum and egg capsule. *Comp. Biochem. Physiol.* **40** B, 37–46.

Hunt, S. 1972 Scleroprotein & chitin in the exoskeleton of the ectoproct *Flustra foliacea*. *Comp. Biochem. Physiol.* **43** B, 571–577.

Hunt, S. 1973 Chemical & physical studies of the chitinous siphon sheath in the lamellibranch *Lutraria lutraria* L. and its relationship to the periostracum. *Comp. Biochem. Physiol.* **45** B, 311–323.

Hunt, S. & Oates, K. O. 1970 Fibrous protein ultrastructure of gastropod periostracum (*Buccinum undatum* L.) *Experientia* **26**, 1196–1997.

Ingram, V. M. 1957 Gene mutations in human haemoglobin: The chemical difference between normal and sickle cell haemoglobin. *Nature, Lond.* **180**, 376–328.

Jakus, M. A. 1956 Studies on the cornea-II. The fine structure of Descemet's Membrane. *Biophys. biochem. Cytol.* **2**, 243–252.

Jones, T. 1969 Aspects of calcification in gastropods. *Proc. malacol. Soc., Lond.* **38**, 549–550.

Jope, M. 1967 The protein of brachiopod shell-I. Amino acid composition and implied protein taxonomy. *Comp. Biochem. Physiol.* **20**, 593–600.

Jope, M. 1969 The protein of the brachiopod shell-III. Comparison with structural protein of soft tissue. *Comp. Biochem. Physiol.* **30**, 209–224.

Karges, H. E. & Kuhn, K. 1970 The cross-striation pattern of the fibrin fibril. *Eur. J. Biochem.* **14**, 94–97.

Kawaguti, S. & Ikemoto, N. 1962 Electron microscopy on the mantle of the bivalved gastropod *Fabulina nitidula*. *Biol. J. Okayama Univ.* **8**, 1–20.

Kawakami, I. K. & Yasuzami, G. 1964 Electron microscope studies on the mantle of the pearl oyster *Pinctada martensii* Dunker. Preliminary report. The fine structure of the periostracum fixed with permanganate. *J. Electron Microsc.* **13**, 119–123.

Keller, A. & O'Connor, A. 1958 General discussion. *Faraday Soc. Disc.* **25**, 207–208.

Kenchington, W. & Flower, N. E. 1969 Studies on insect fibrous proteins: the structural protein of the ootheca in the praying mantis, *Sphodromantis centrolis Rehn. J. Microsc.* **89**, 263–281.

Kessel, E. 1940 Uber den feineren Bau des Mytiliden Periostracum erschlossen aus der Optik. *Z. Morph. Okol. Tiere.* **36**, 581-594.

Knight, D. P. & Hunt, S. 1974*a* Molecular and ultrastructural characterization of the egg capsule of the leech *Erpobdella octoculata* L. *Comp. Biochem. Physiol.* **47** A, 871–880.

Knight, D. P. & Hunt, S. 1974*b* Fibril structure of collagen in egg capsule of dogfish. *Nature, Lond.* **249**, 379–380.

Kniprath, E. 1792 Formation and structure of the periostracum in *Lymneaa stagnalis. Calc. Tissue Res.* **9**, 260–271.

Kominz, D. R., Saad, F. & Laki, K. 1958 Chemical characteristics of annelid, molluscan and arthropod tropomyosins; *Conference on Chemical Muscular Contraction*, 1957, pp. 66–76. Tokyo: Igakn Shoin.

Locke, M. 1964 The structure and formation of the integument in insects. In *Physiology of insecta*, vol. 3 (ed. M. Rockstein), pp. 379–470. New York, Academic Press.

Lucas, F. & Rudall, K. M. 1968 Extracellular fibrous proteins: the silks. In *Comprehensive biochemistry*, vol. 26 B (ed. M. Florkin & E. H. Stotz), pp. 475–558. Amsterdam: Elsevier.

McGavin, S. 1952 The structure of elastoidin in relation to that of tendon collagen. *J. molec. Biol.* **5**, 275–283.

Meenakshi, V. R., Hare, P. E., Watabe, N. & Wilbur, K. M. 1969 The chemical composition of the periostracum of the molluscan shell. *Comp. Biochem. Physiol.* **29**, 611–620.

Messer, G. & Ben-Shaul, Y. 1971 Fine structure of trichocyst fibrils of the dinoflagellate *Peridinium Westii. J. Ultrastruct. Res.* **37**, 94–104.

Nakamura, A., Streter, F. & Gergely, J. 1971 Comparative studies of light meromyosin paracrystals derived from red, white and cardiac muscle, myosins. *J. cell. Biol.* **49**, 883–898.

Neff, J. M. 1972*a* Ultrastructural studies of periostracum formation in the hard shelled clam *Mercenaria mércenaria* (L.) *Tissue Cell* **4**, 311–326.

Neff, J. M. 1972*b* Ultrastructure of the outer epithelium of the mantle in the clam *Mercenaria mercenaria* in relation to calcification of the shell. *Tissue Cell* **4**, 591–600.

Neville, A. C. 1967 Chitin orientation in cuticle and its control. In *Advances in insect physiology*, vol. 4 (eds. J. W. L. Beament, J. E. Treherne & V. B. Wigglesworth), pp. 213–286. London: Academic Press.

Neville, A. C. & Caveney, S. 1969 Scarabaeid beetle exocuticle as an optical analogue of cholesteric liquid crystals. *Biol. Rev.* **44**, 531–562.

Neville, A. C. & Luke, B. M. 1969*a* Molecular architecture of adult locust cuticle at the electron microscope level. *Tissue Cell* **1**, 355–366.

Neville, A. C. & Luke, B. M. 1969*b* A two-system model for chitin-protein complexes in insect cuticles. *Tissue Cell.* 1, 689–707.

Neville, A. C. & Luke, B. M. 1971 Form optical activity in crustacean cuticle. *Comp. Biochem. Physiol.* **17**, 519–526.

Neville, A. C., Thomas, M. G. & Zelazny, B. 1969 Pore canal shape related to molecular architecture of arthropod cuticle. *Tissue Cell* **1**, 183–200.

Peters, W. 1972 Occurrence of chitin in mollusca. *Comp. Biochem. Physiol.* **41** B, 541–550.

Preston, R. D. 1971 Negative staining and cellulose microfibril size. *J. Microsc.* **93**, 7–13.

Ramachandran, G. N. 1967 Structure of collagen at the molecular level. In *Treatise on collagen*, vol. 1 (ed. G. N. Ramachandran), pp. 103–183. New York: Academic Press.

Robinson, C. 1961 Liquid crystalline structures in polypeptide solutions. *Tetrahedron*, **13**, 219–234.

Robinson, C. 1966 The cholesteric phase in polypeptide solutions and biological structures. *Molec. Crystals* **1**, 467–494.

Rudall, K. M. & Kenchington, W. 1971 Arthropod silks: The problem of fibrous proteins in animal tissues. *A. Rev. Entomol.* **16**, 73–96.

Smith, V. E. & Lauritis, J. A. 1969 Cellular origin and fine structure of mesoglea in a marine sponge *Cyamon neon* de Laubenfels. *J. Microsc.* **8**, 179–188.

Sobieszek, A. & Small, J. V. 1973 The assembly of ribbon shaped structures in low ionic strength extracts obtained from vertebrate smooth muscle. *Phil. Trans. R. Soc. Lond.* B **265**, 203–212.

Stasek, C. R. 1972 The molluscan framework. In *Chemical zoology*, vol. 7 (ed. M. Florkin & B. T. Scheer), pp. 1–41. New York: Academic Press.

Steiner, R. F. 1965 *The chemical foundations of molecular biology*, pp. 168–193. Princeton: Van Nostrand.

Szent-Gyorgyi, A. G., Cohen, C. & Kendrick-Jones, J. 1971 Paramyosin and the filaments of molluscan 'catch' muscle. II. Native filaments: Isolation and characterization. *J. molec. Biol.* **56**, 239–258.

Taverner-Smith, R. & Williams, A. 1972 The secretion and structure of the skeleton of living and fossil bryozoa. *Phil. Trans. R. Soc. Lond.* B **264**, 98–159.

Taylor, J. D. & Kennedy, W. J. 1969 The influence of the periostracum on the shell structure of bivalve molluscs. *Calc. Tissue Res.* **3**, 274–283.

Tooney, N. M. & Cohen, C. 1972 Microcrystals of a modified fibrinogen. *Nature, Lond.* **237**, 23–25.

Tredgold, R. & Hole, P. N. 1976 Dielectric behaviour of dry synthetic polypeptides. *Biochim. biophys. Acta* **443**, 137–142.

Trueman, E. T. 1949 The ligament of *Tellina tenuis*. *Proc. zool. Soc. Lond.* **119**, 717–742.

Tsujii, T. 1968 Studies on the mechanism of shell and pearl formation. X. The submicroscopic structure of the epithelial cells on the mantle of the pearly oyster, *Pteria* (*Pinctada*) *martensii* (Dunker). *Rep. Fac. Fish Pref. Univ. Mie.* **6**, 41–57.

Vos, L. de. 1974 Étude ultrastructural de la formation et de l'eclosion des gemmules d'*Ephydatia fluviatilis* L. Thése de doctorat. Faculté des Sciences. Université Libre de Bruxelles.

Wada, K. 1964 Studies on the mineralization of the calcified tissue in molluscs. VII. Histological and histochemical studies of organic matrices in shells. *Bull. natn. Pearl Res. Lab.* **9**, 1078–1086.

Wada, K. 1968 Electron microscopic observations of the formation of the periostracum of *Pinctada fucata*. *Bull. natn. Pearl. Res. Lab.* **13**, 1540–1560.

Wilbur, K. M. & Simkiss, K. 1968 Calcified shells. In *Comprehensive biochemistry*, vol. 26 A (ed. M. Florkin & E. H. Stotz), pp. 229–295. Amsterdam: Elsevier.

Williams, A. 1968 Significance of the structure of the brachiopod periostracum. *Nature, Lond.* **218**, 551–554.

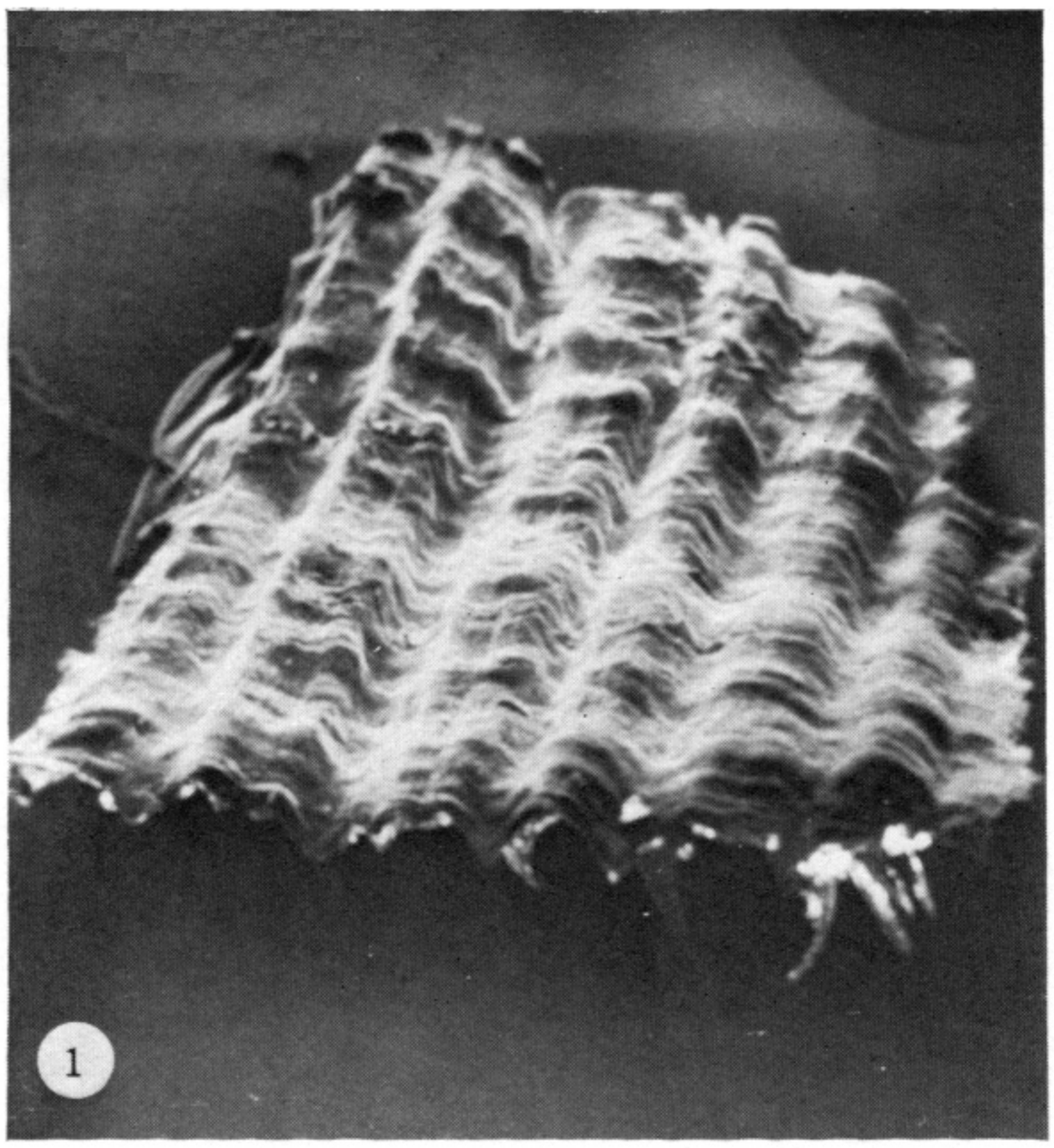

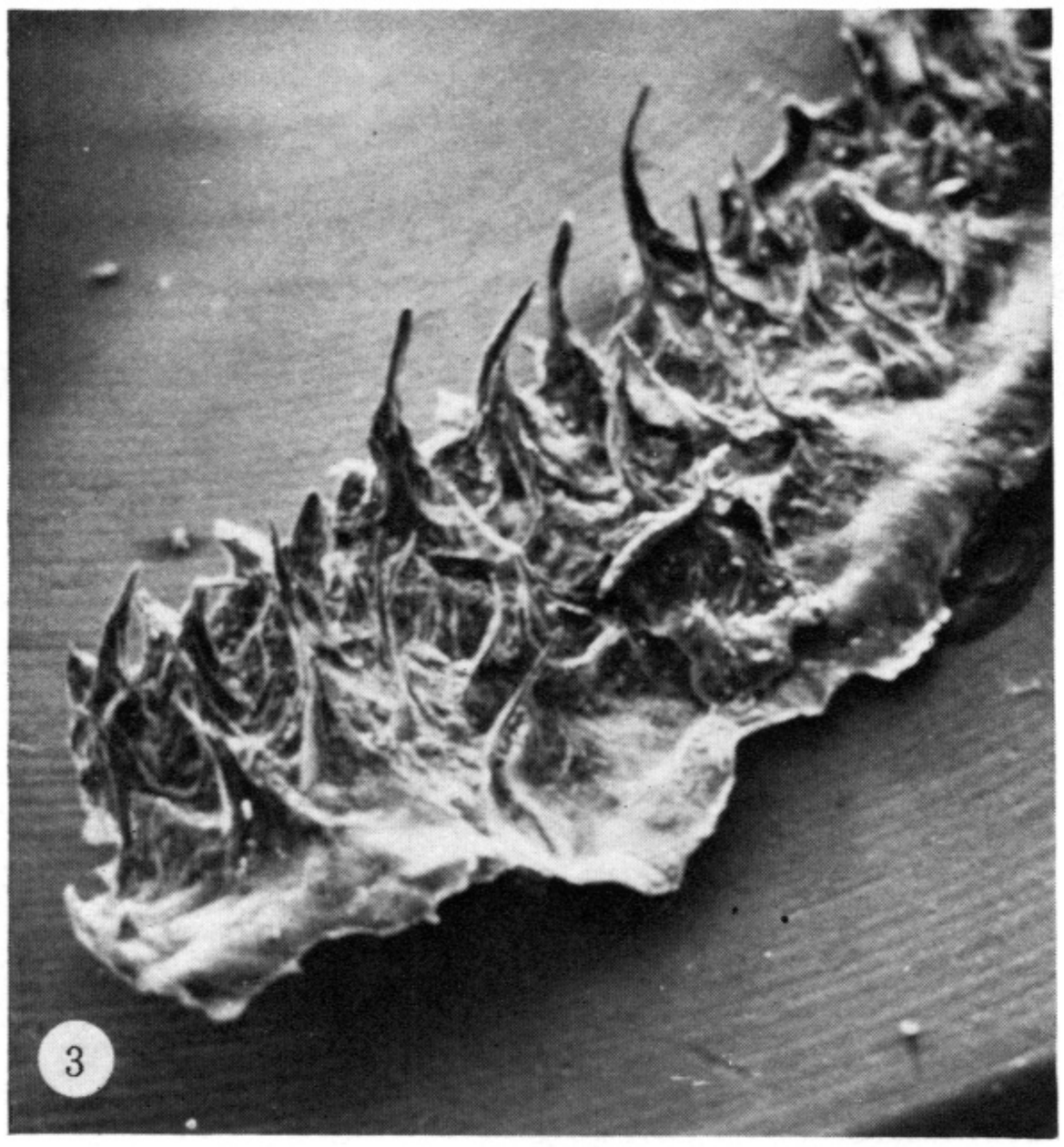

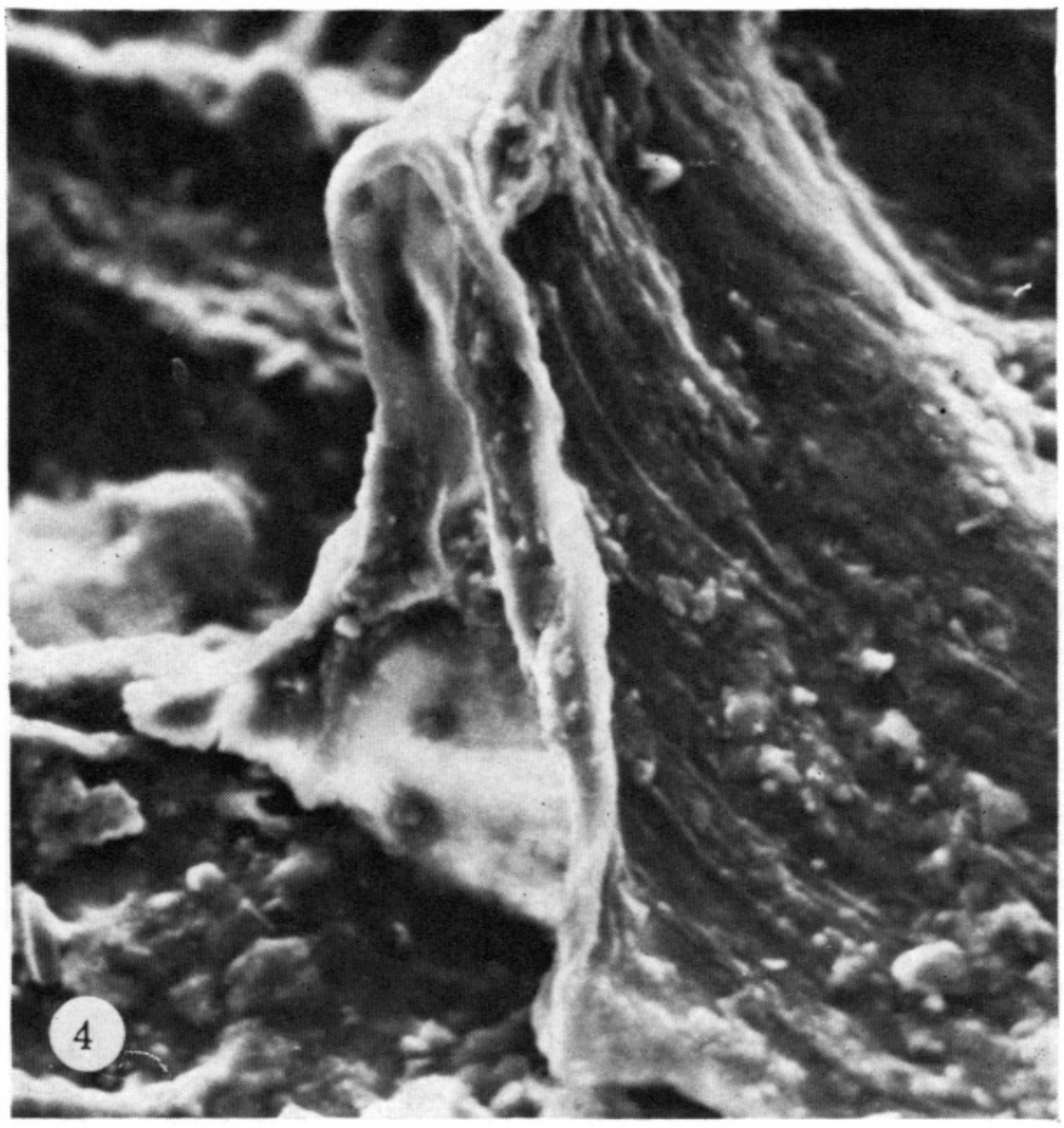

FIGURES 1–5. For description see opposite.

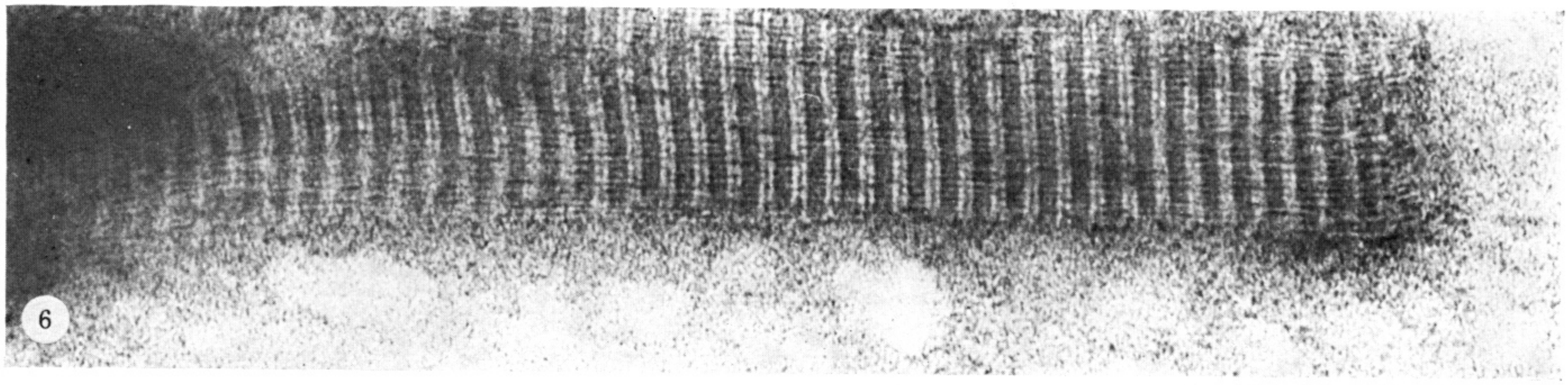

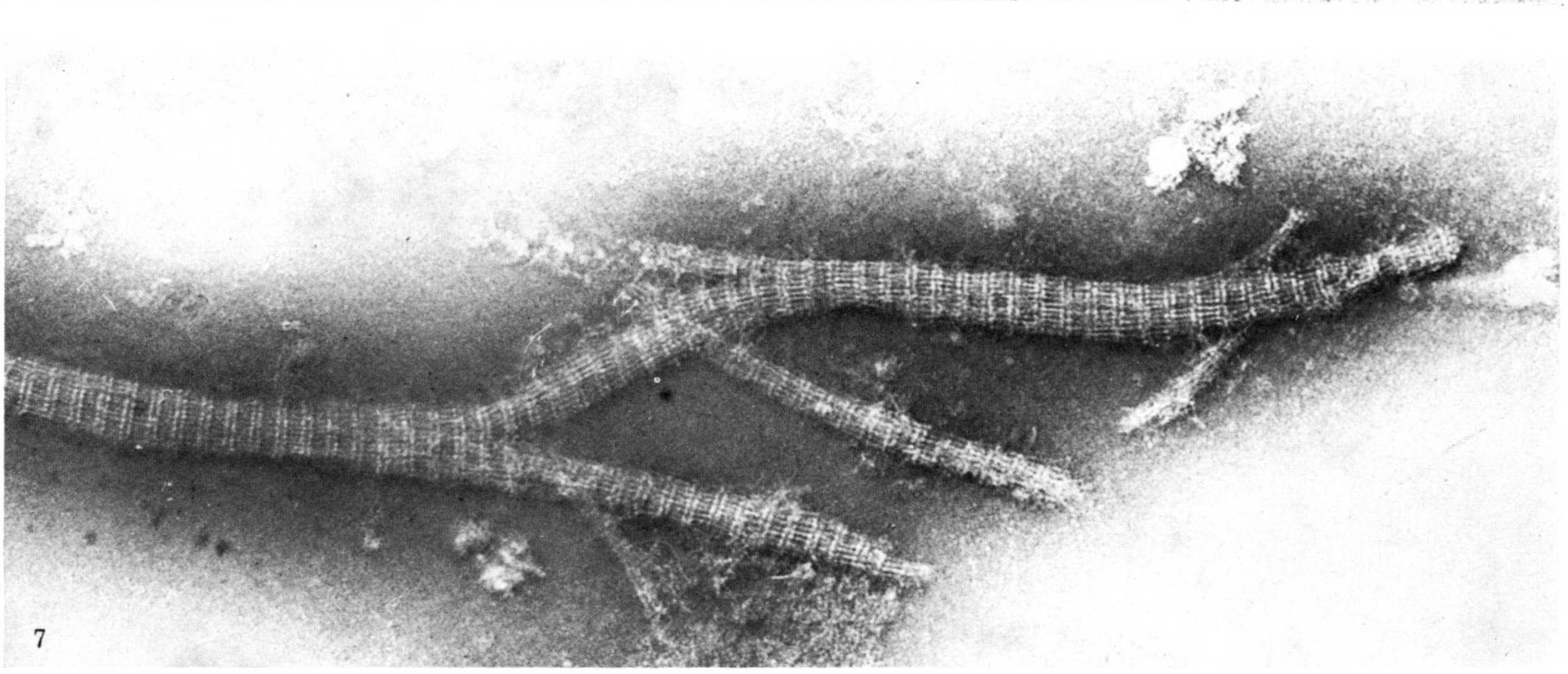

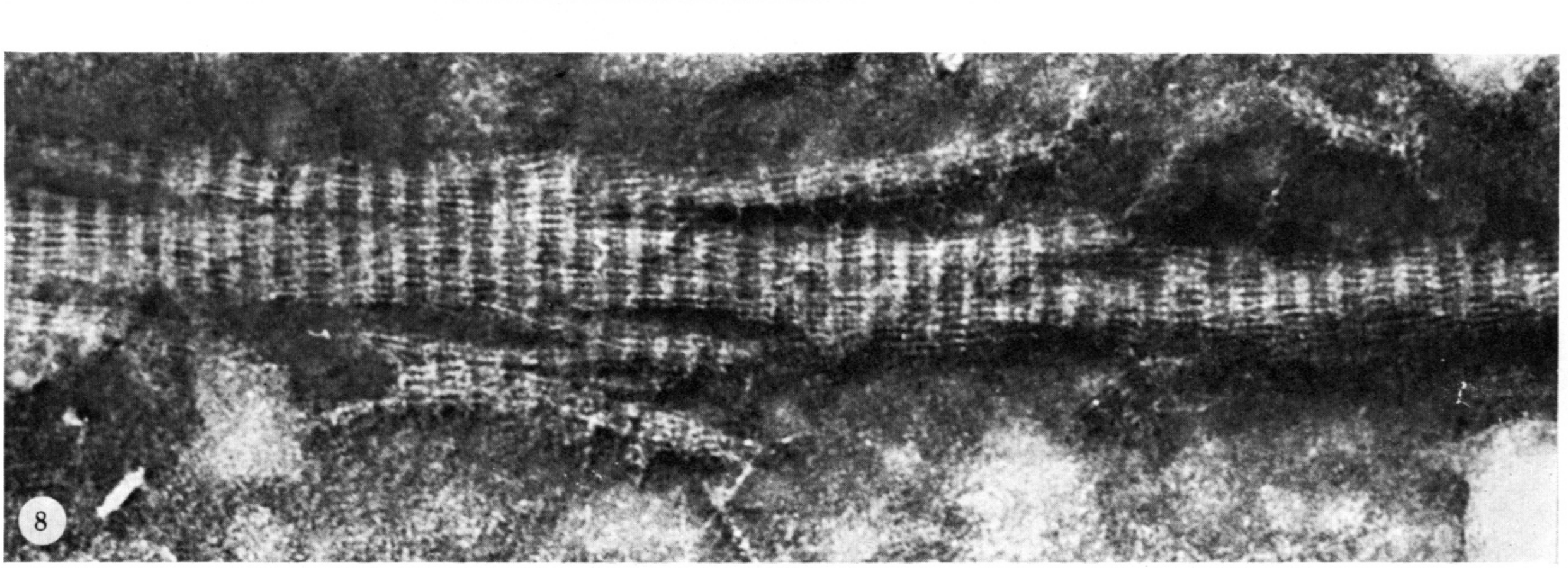

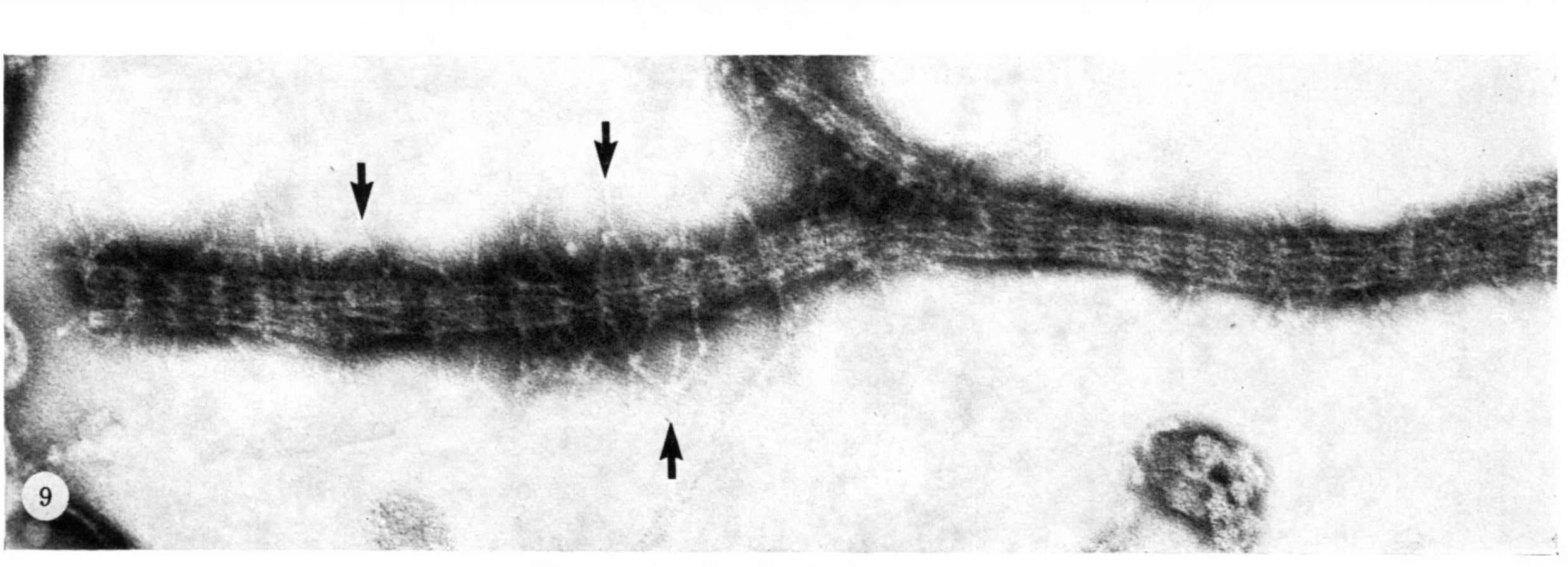

FIGURES 6–9. For description see opposite.

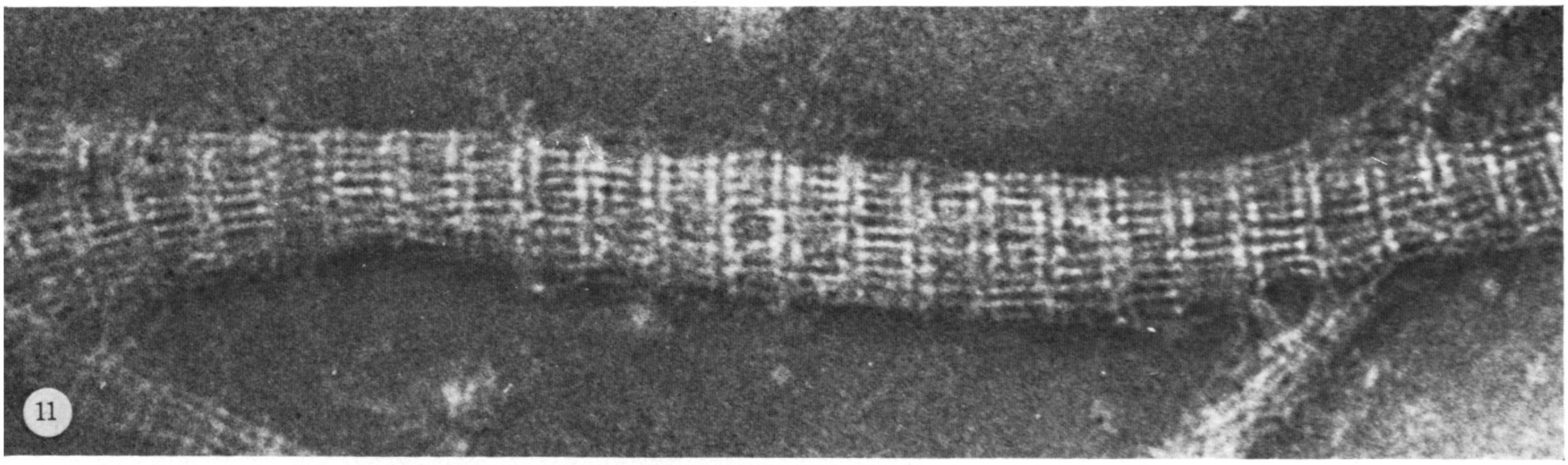

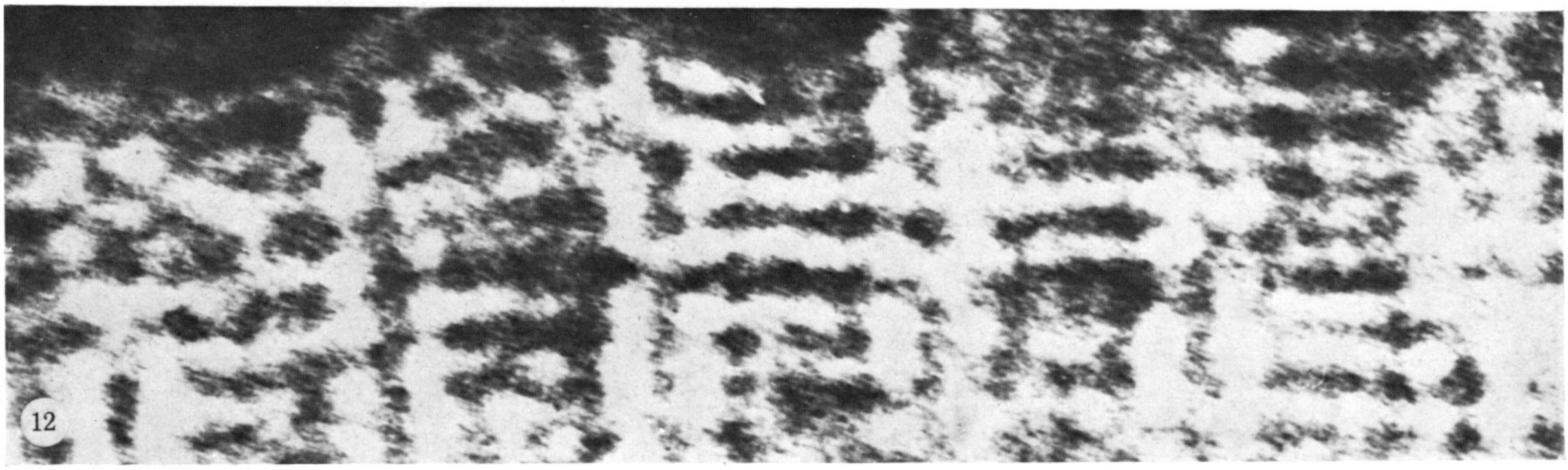

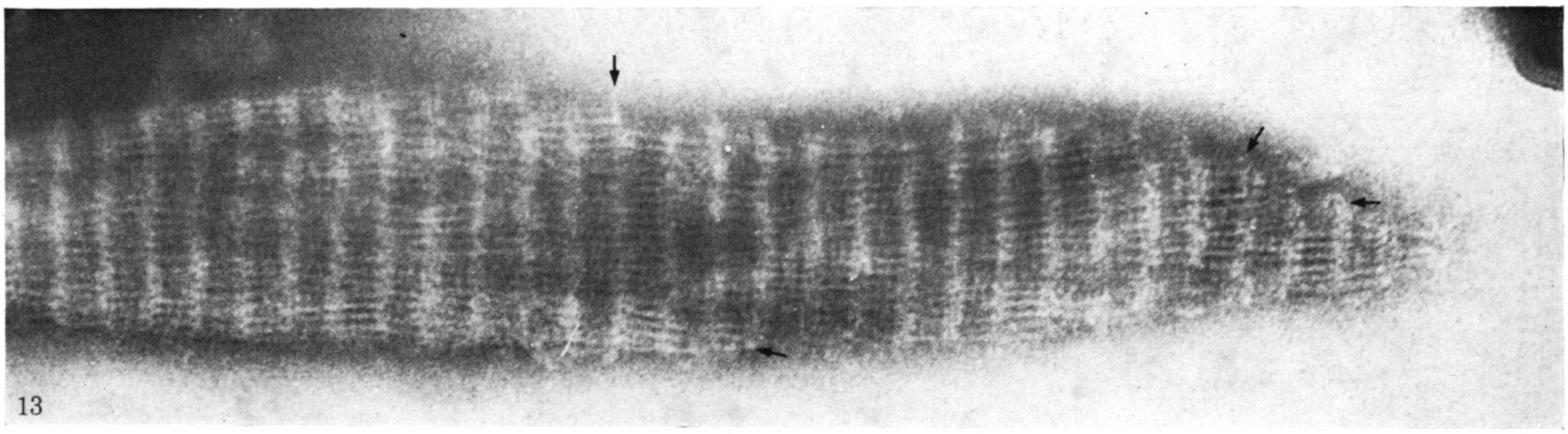

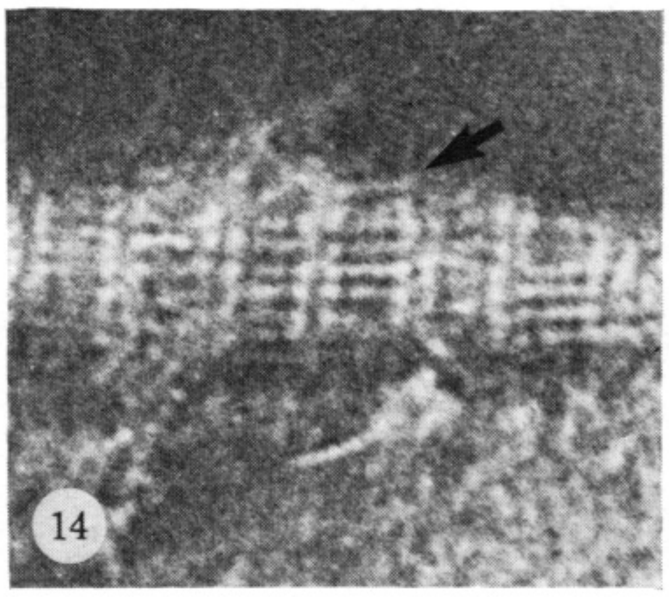

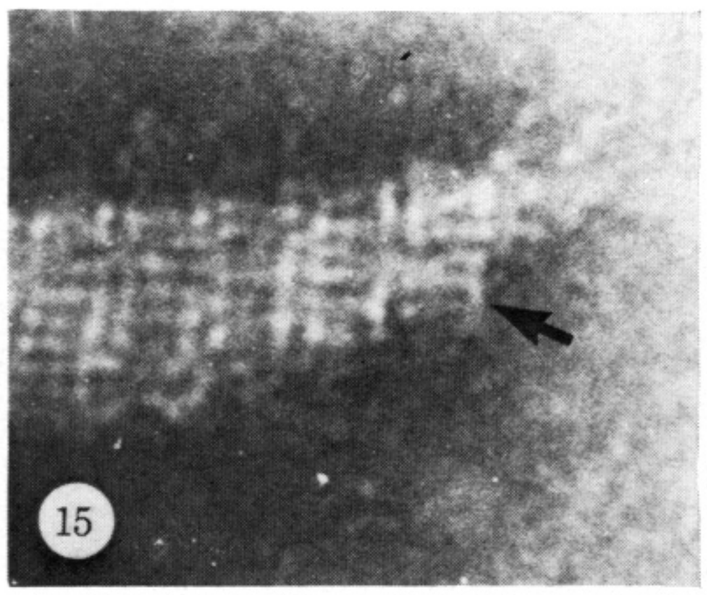

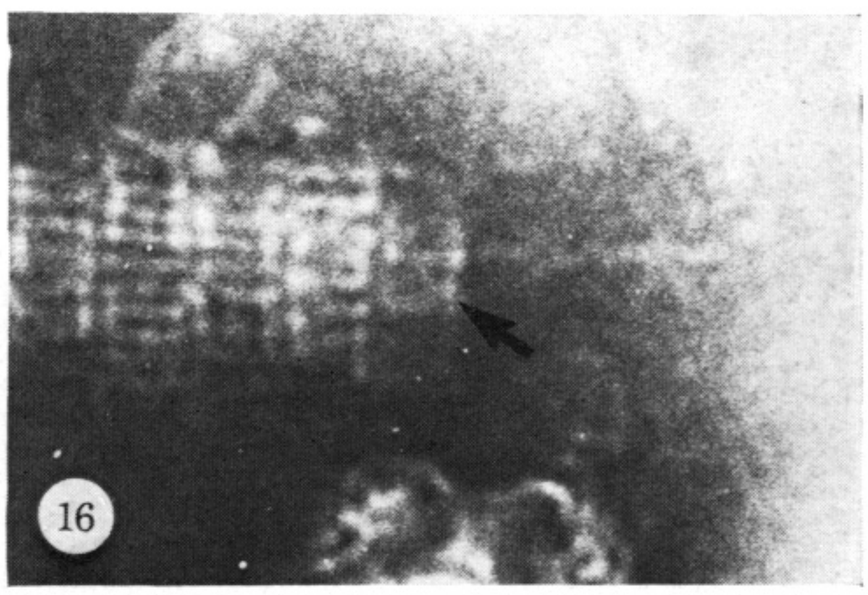

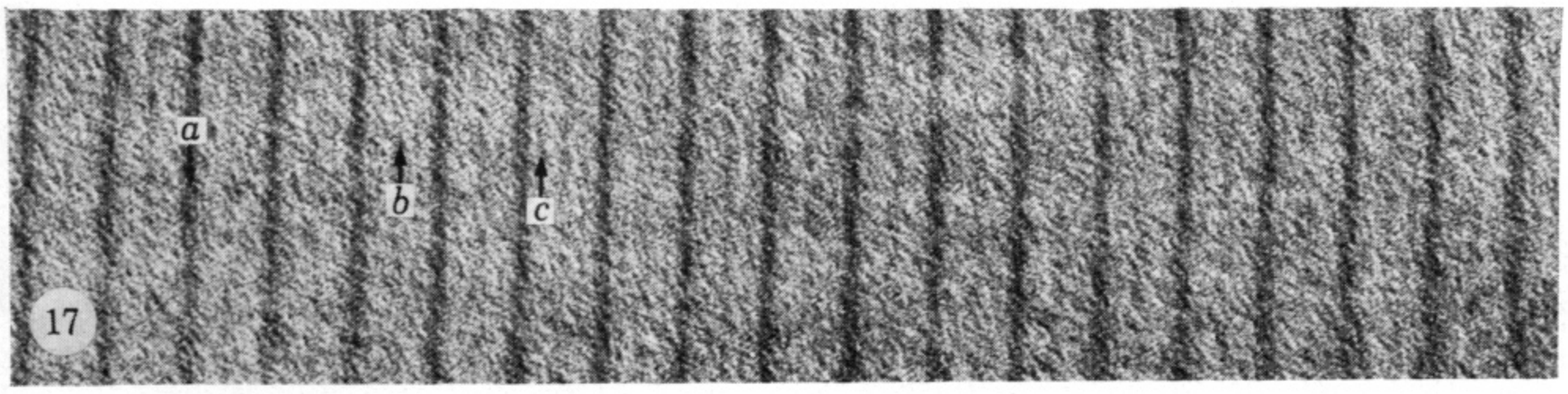

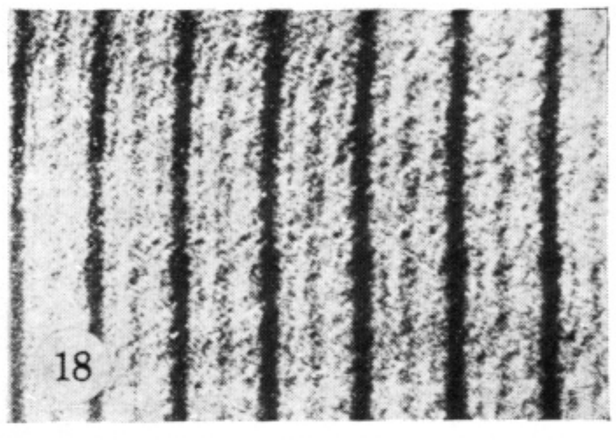

FIGURES 11–18. For description see opposite.

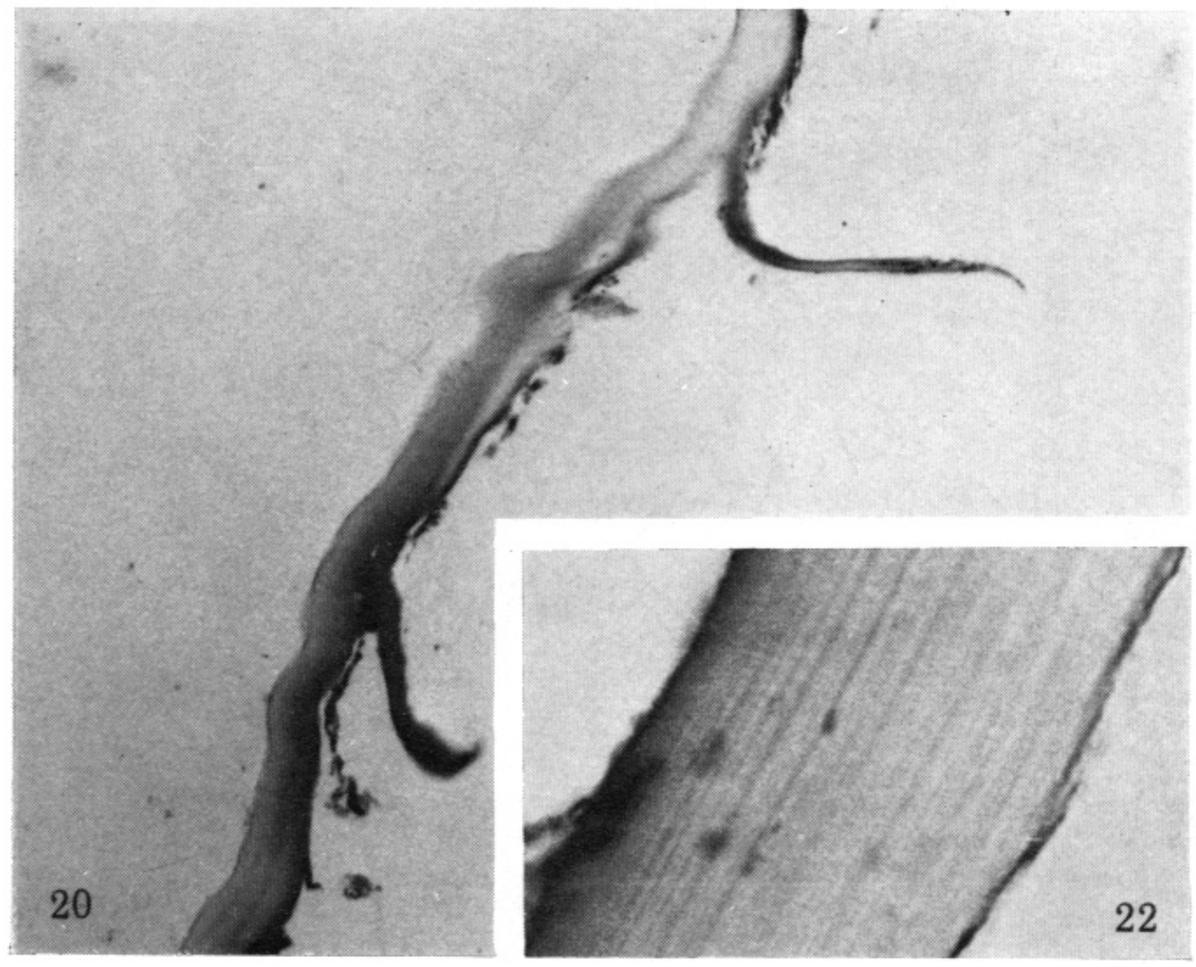

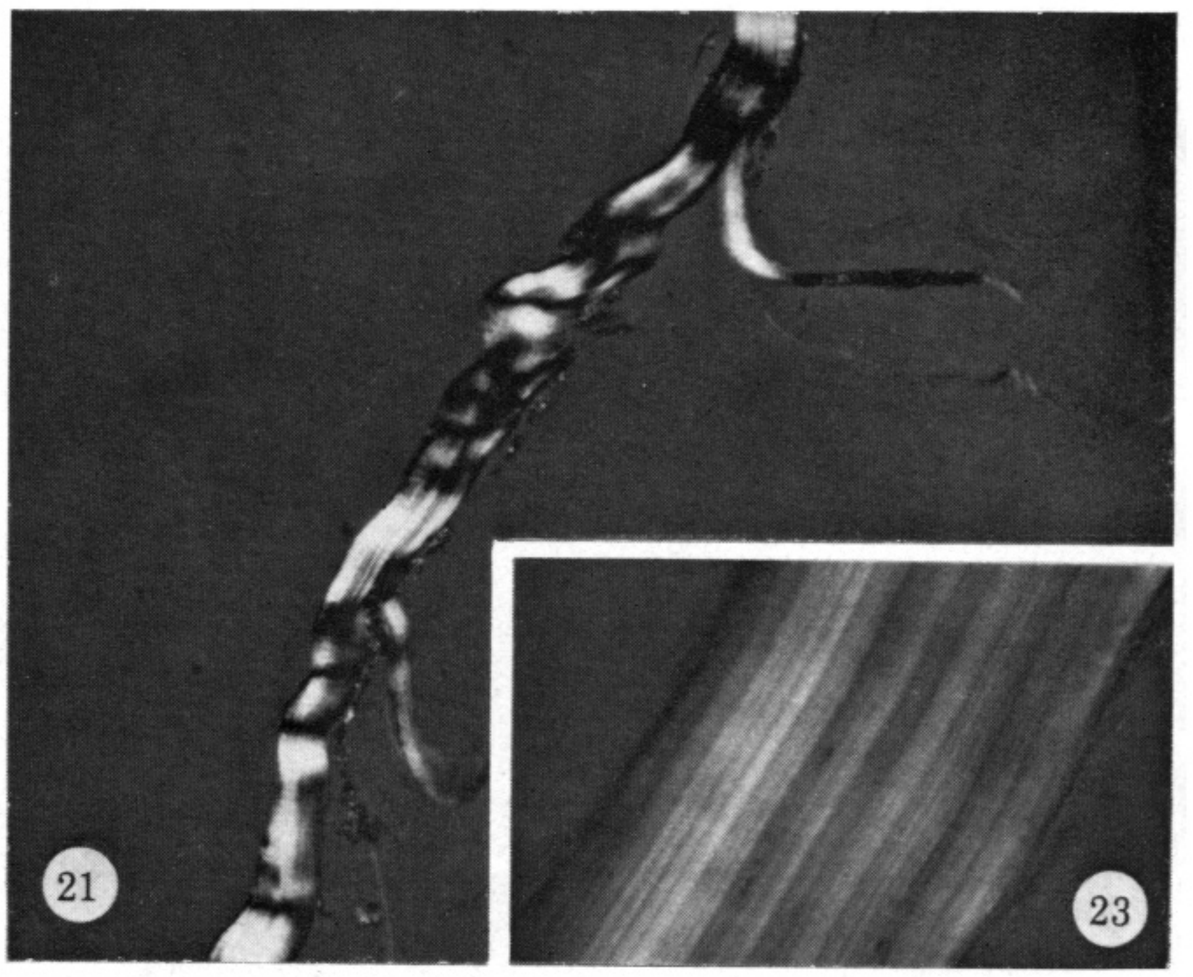

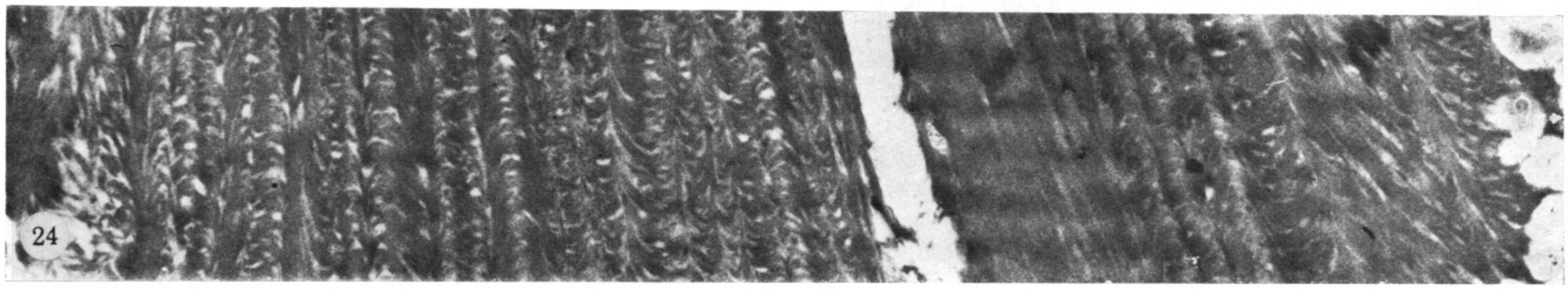

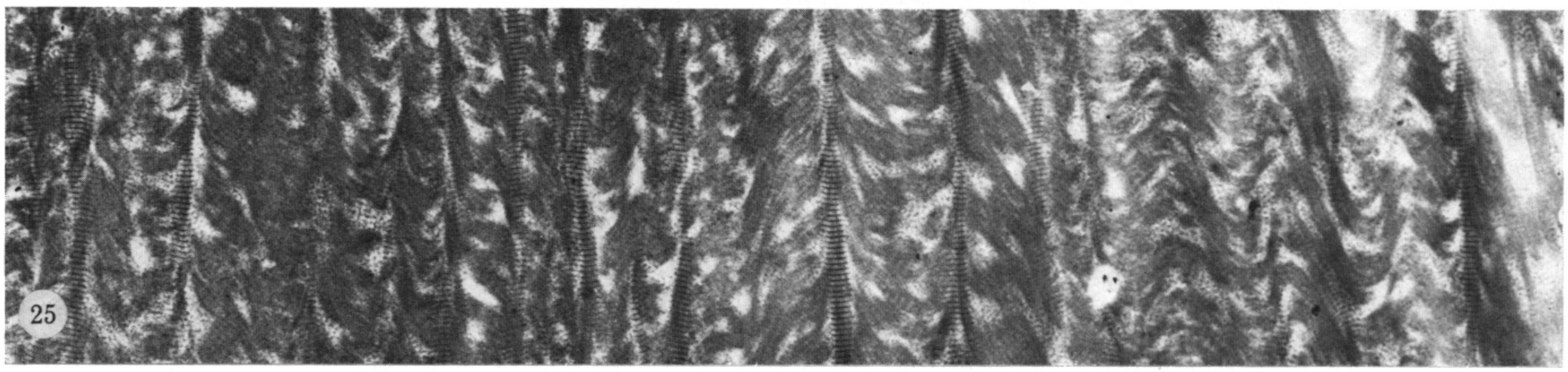

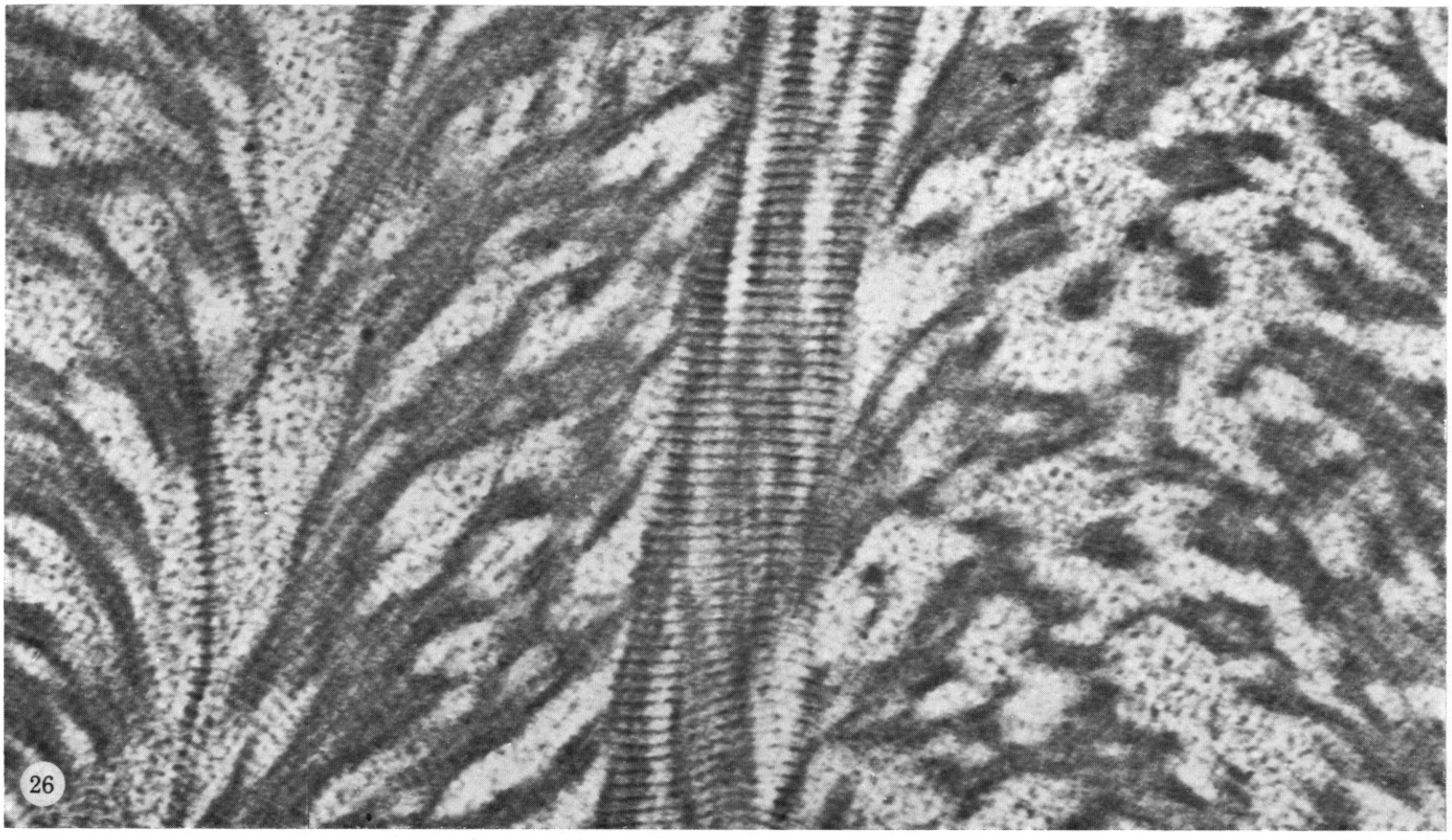

FIGURES 20–26. For description see p. 426.

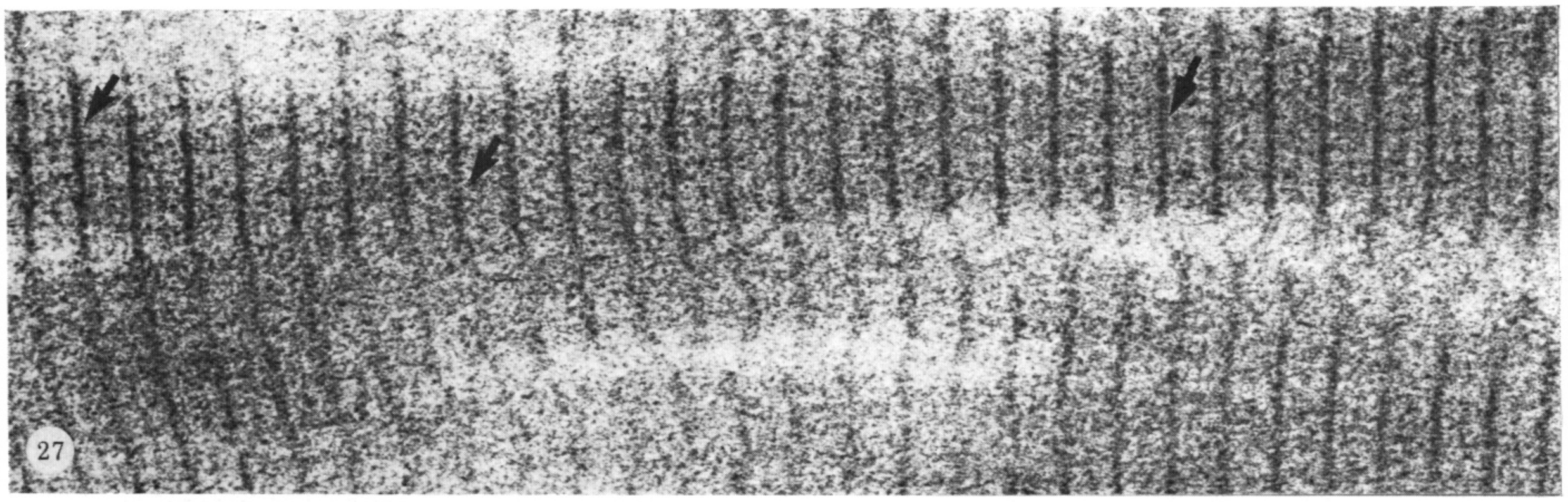

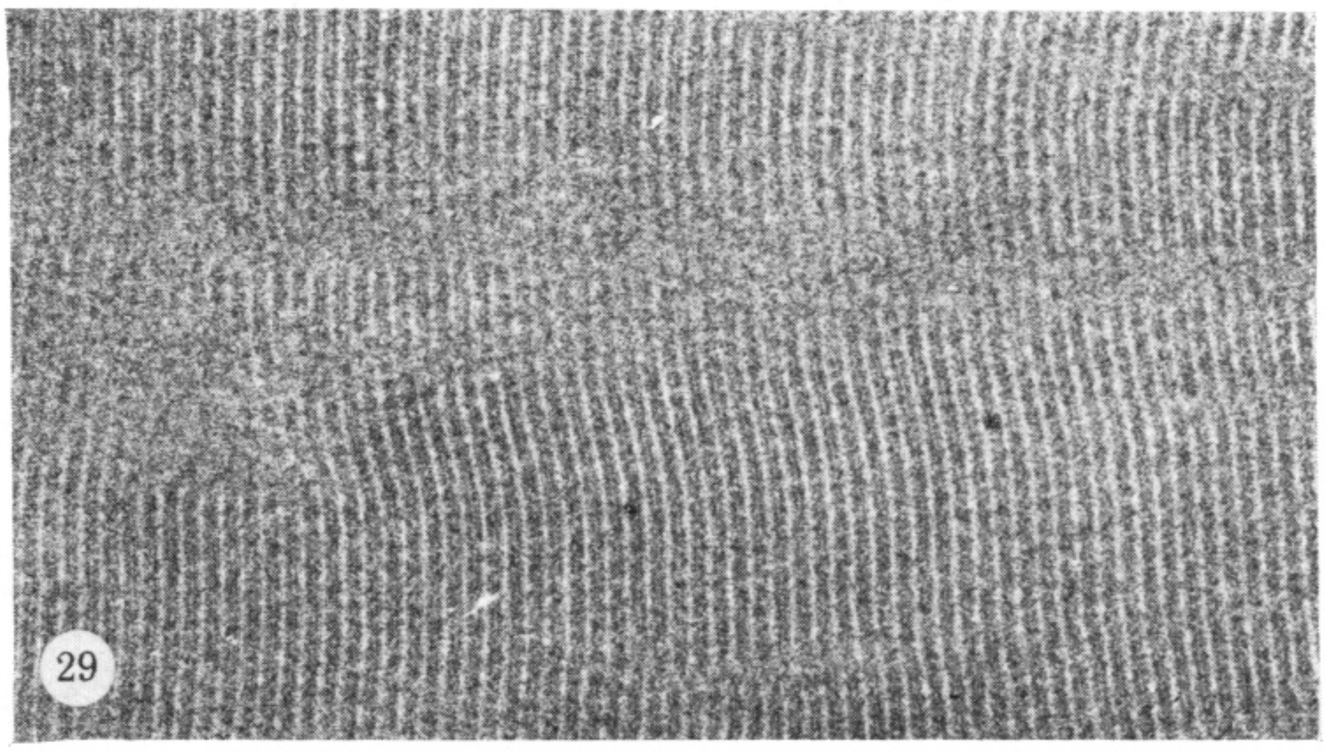

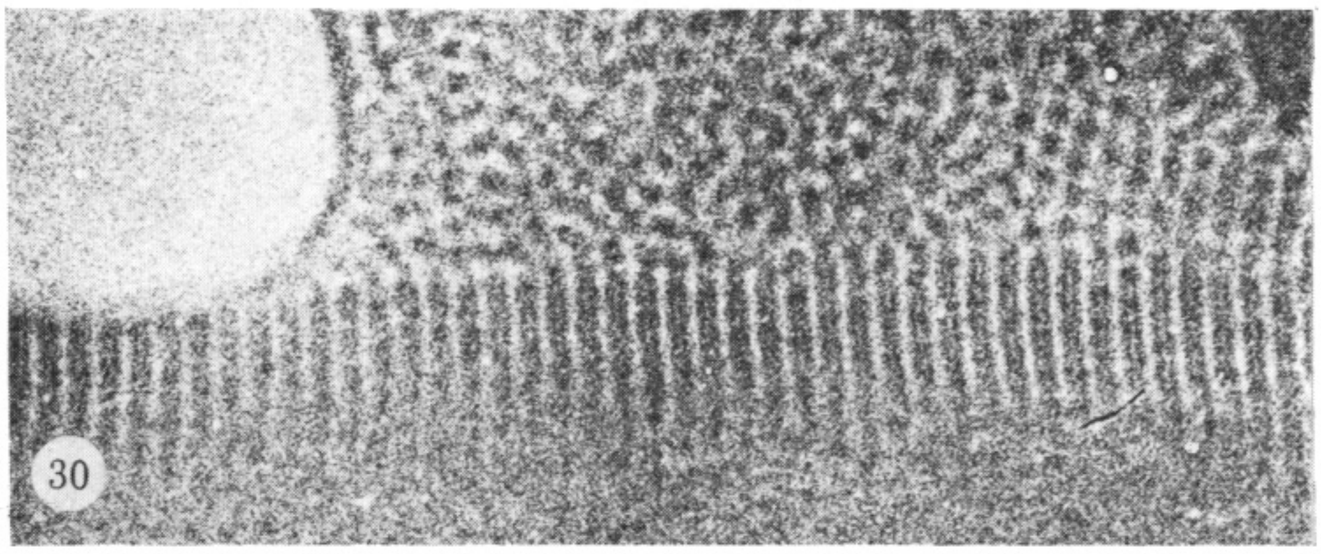

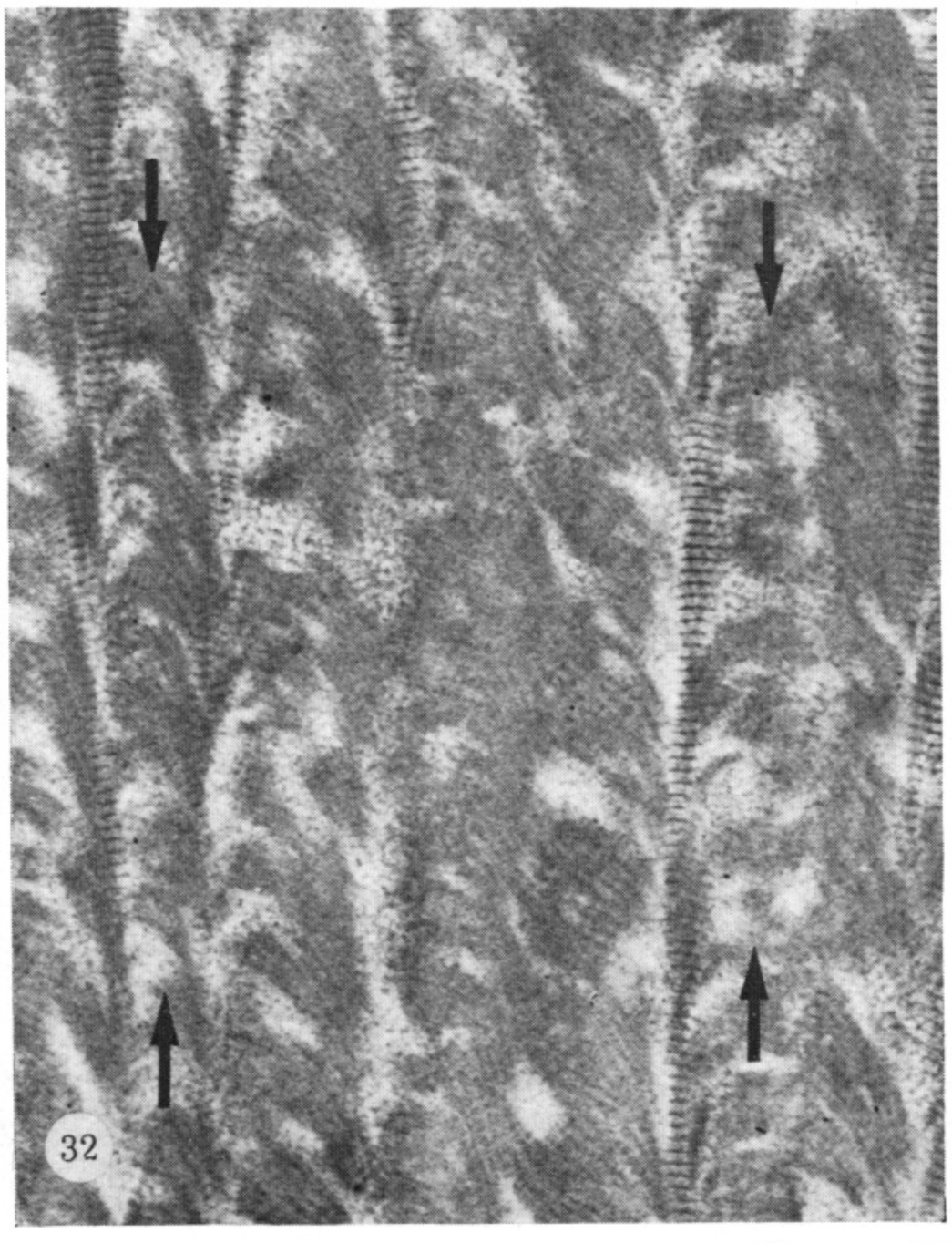

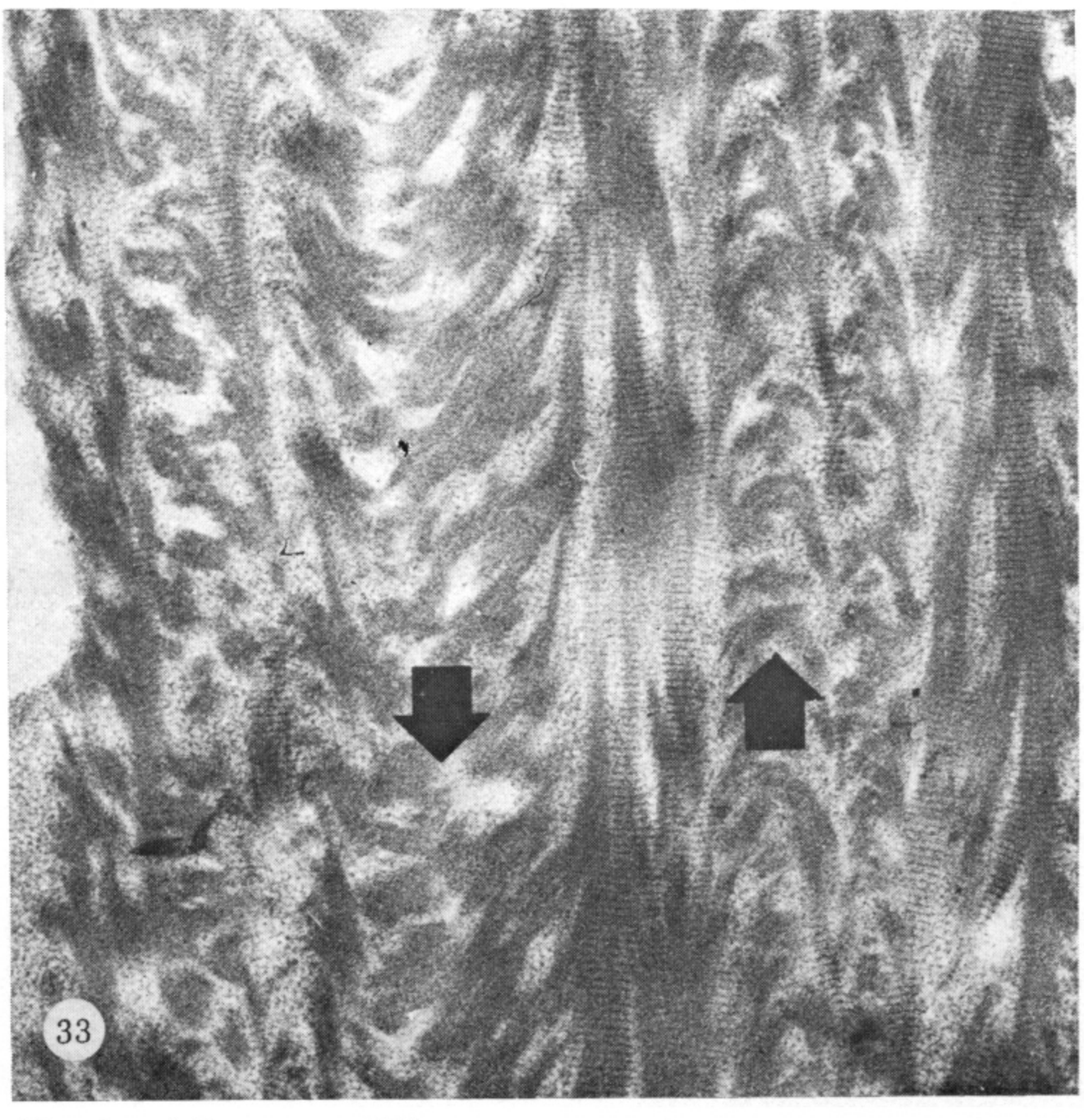

FIGURES 27–33. For description see p. 427.

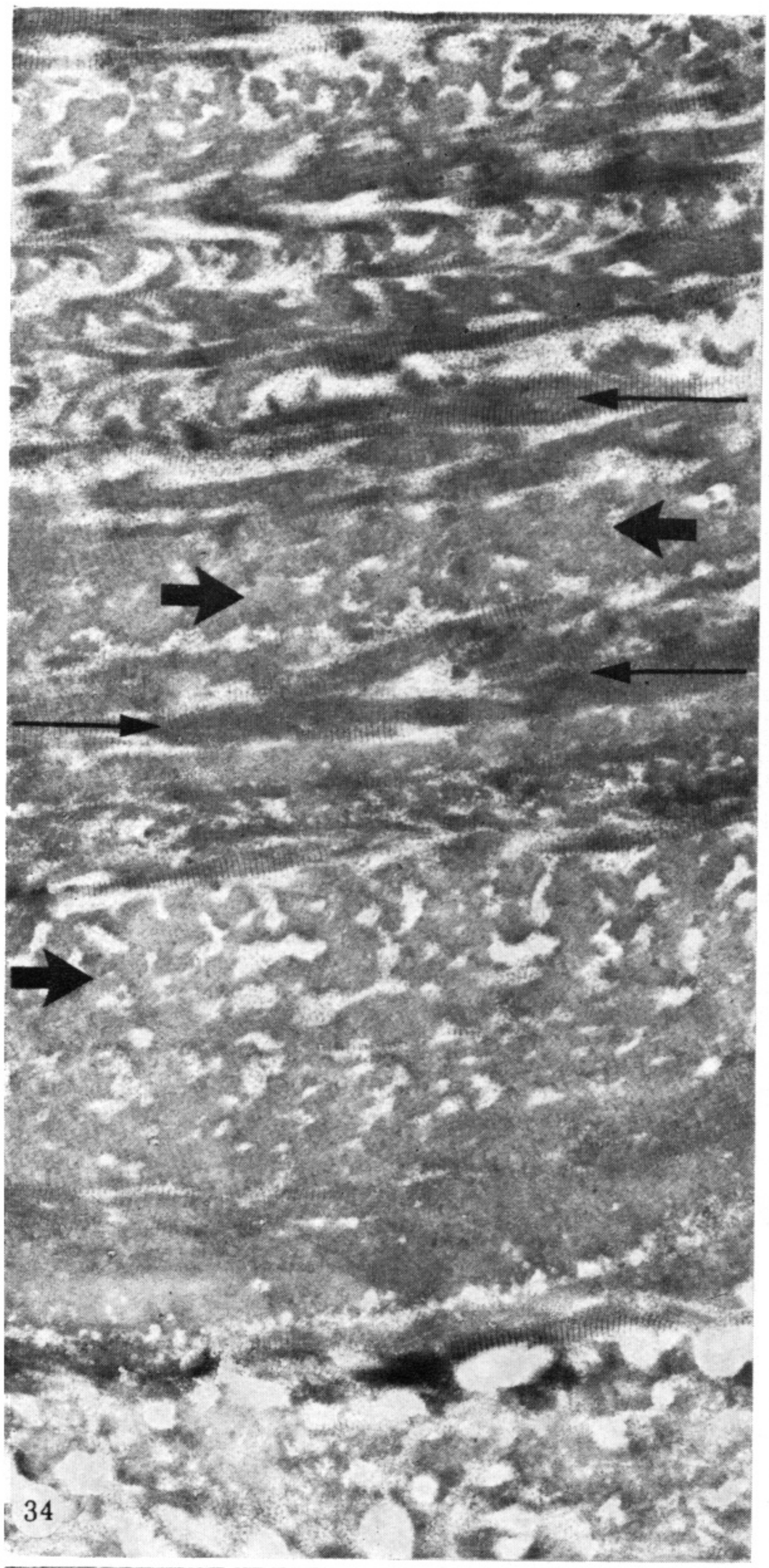

34

36

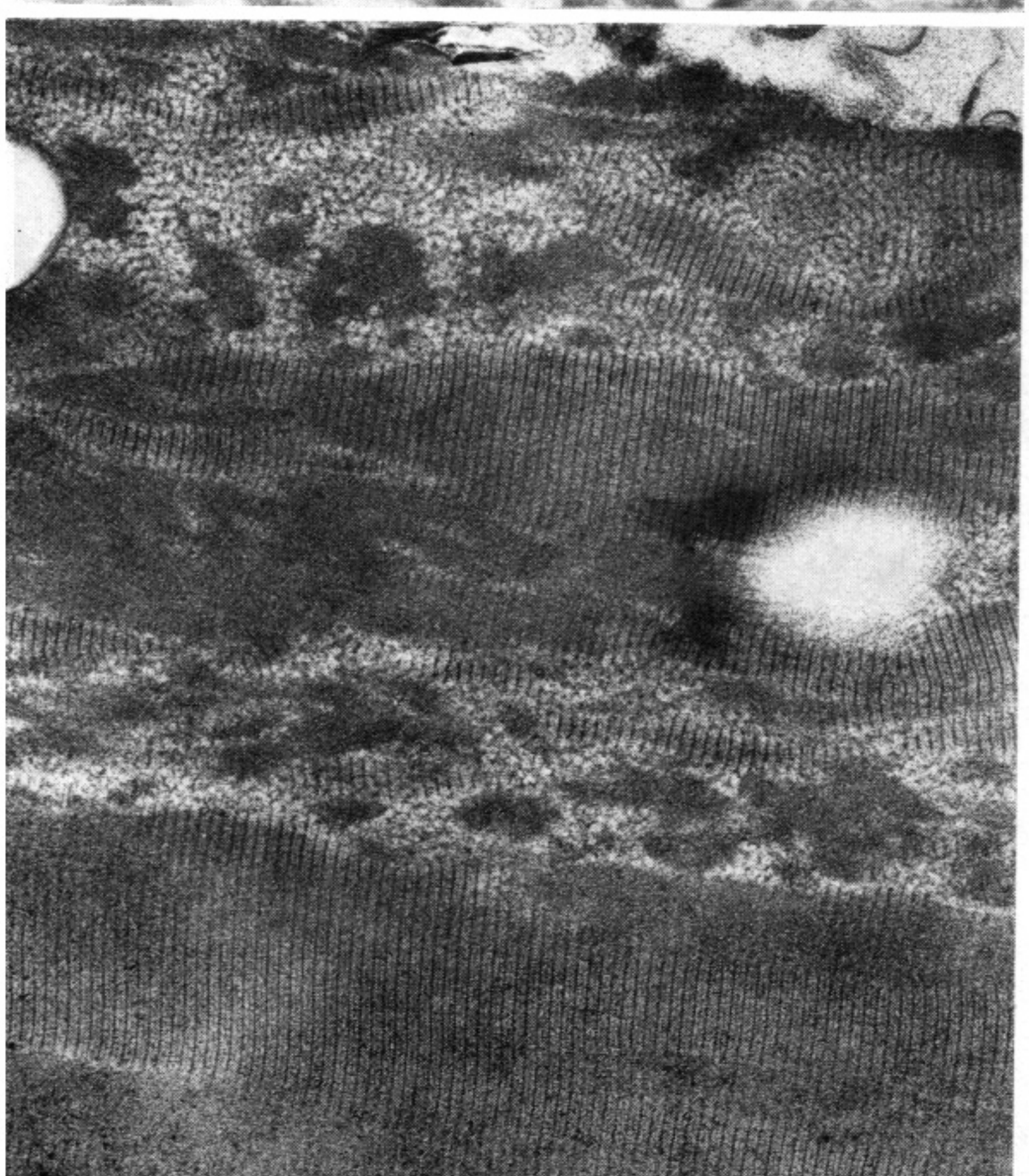

35

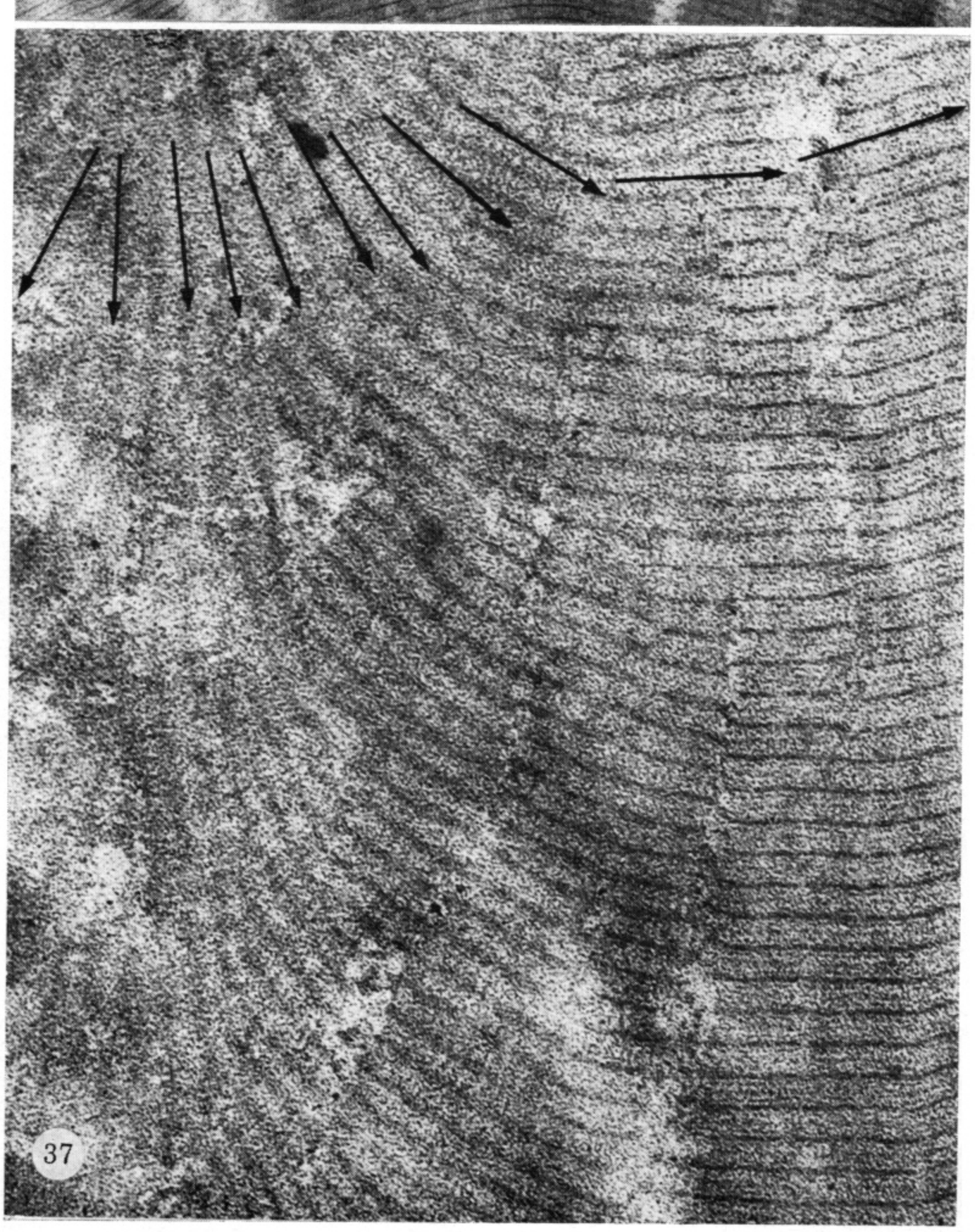

37

FIGURES 34–37. For description see opposite.

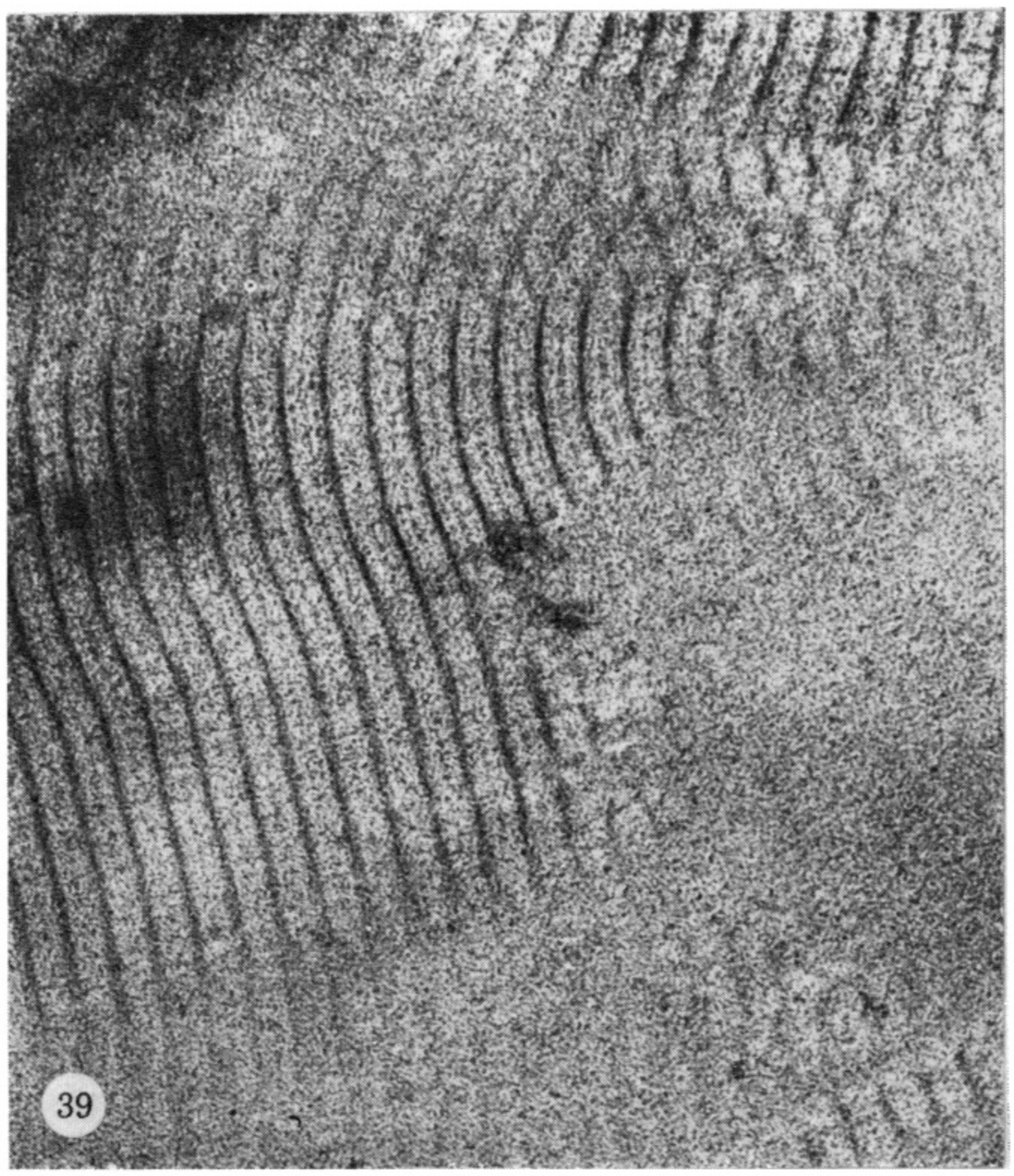

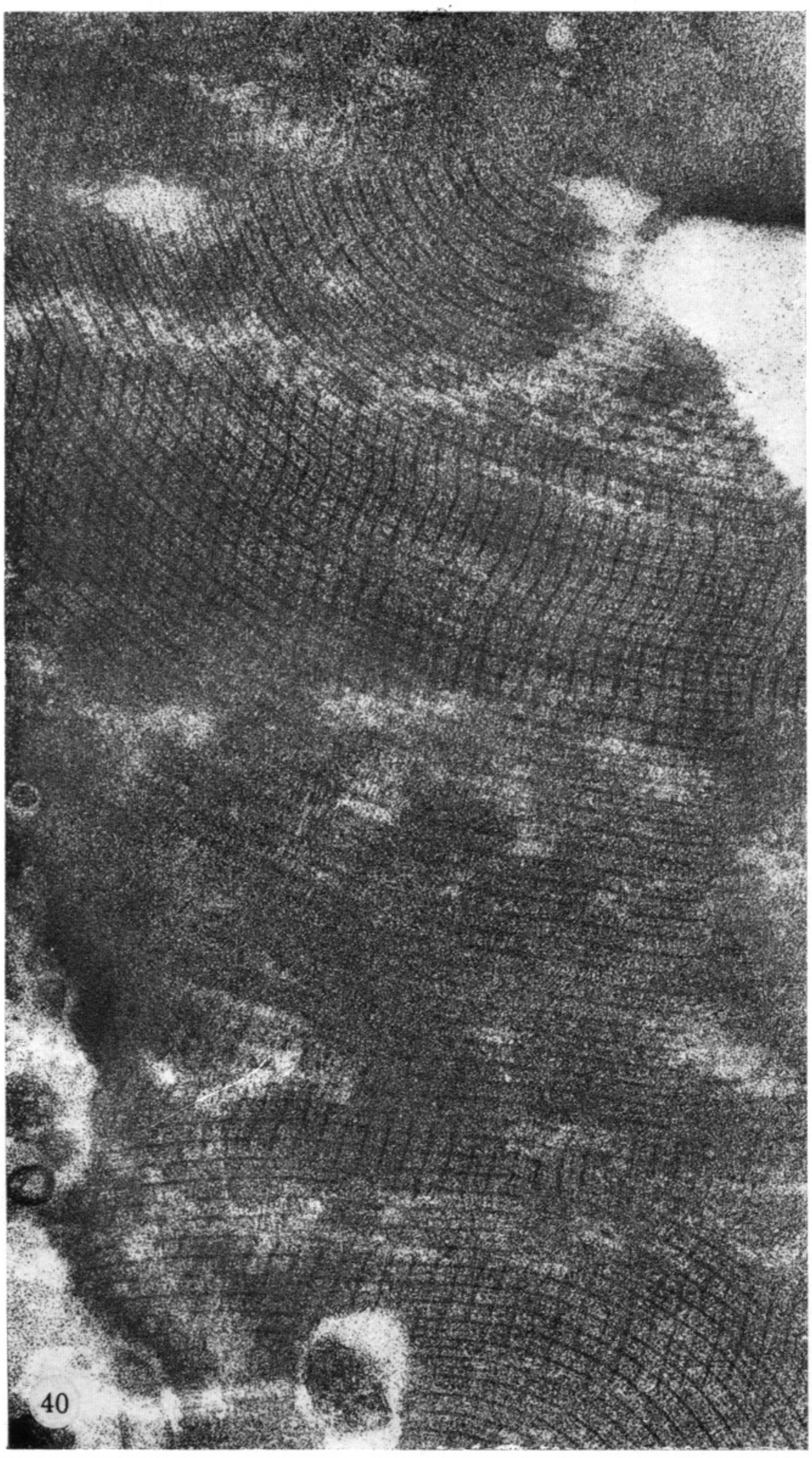

FIGURES 38–41. For description see opposite.

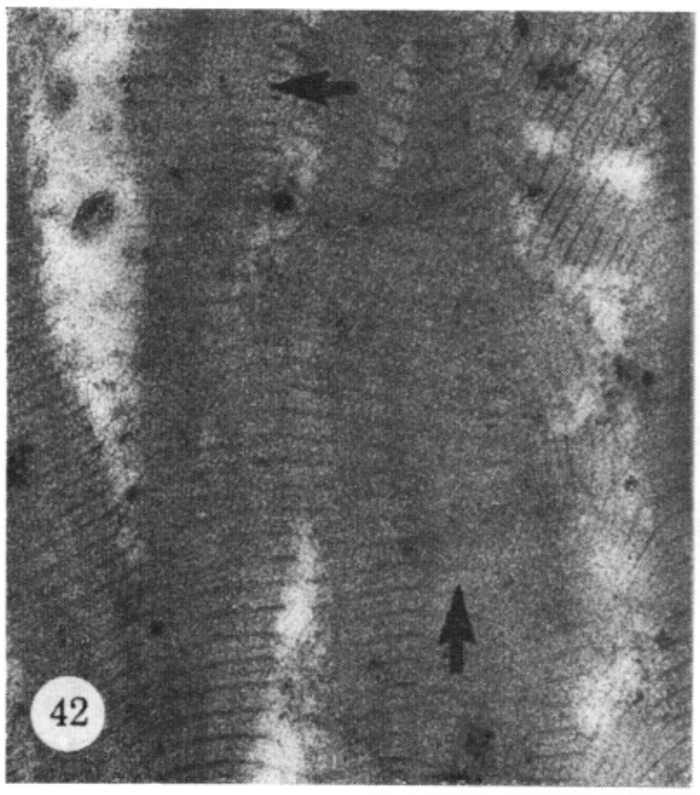

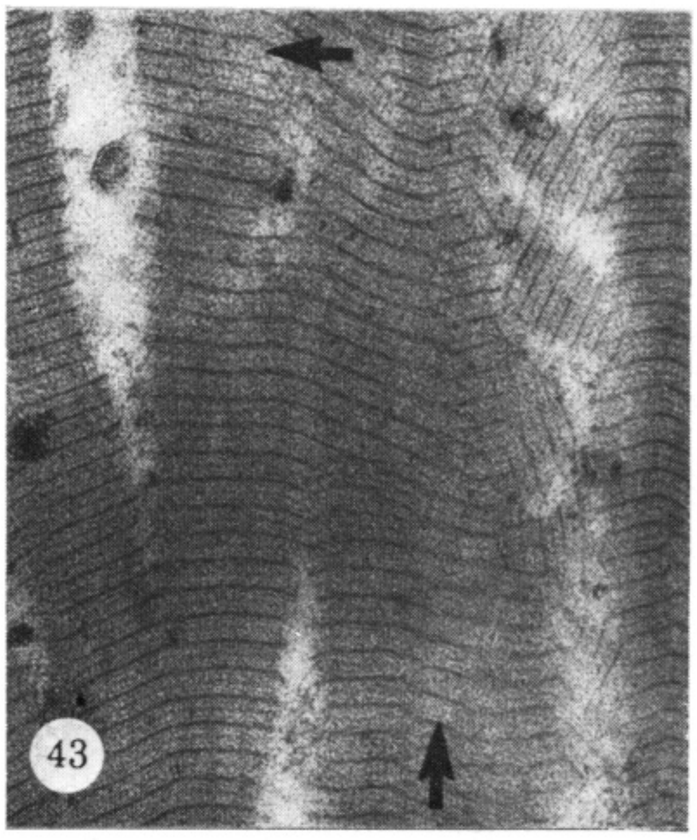

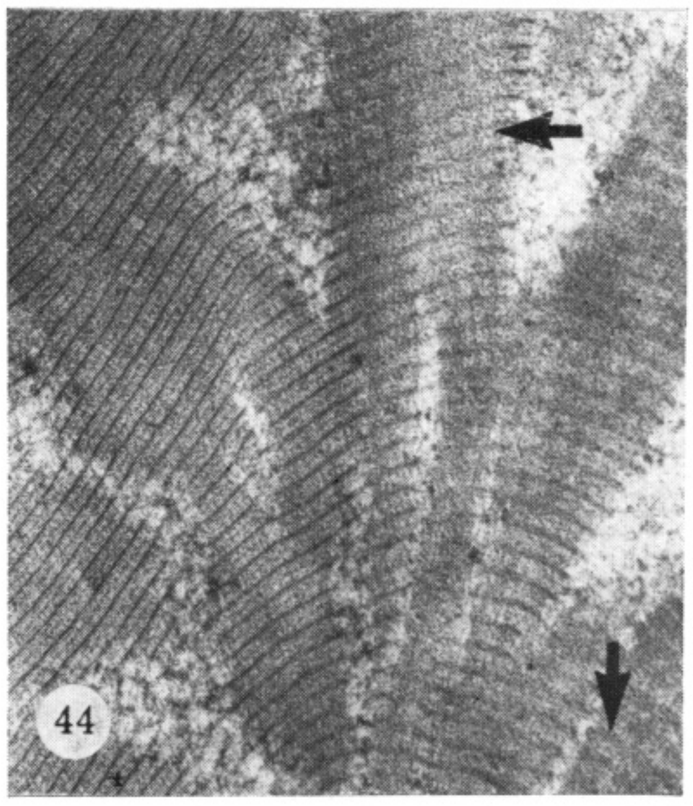

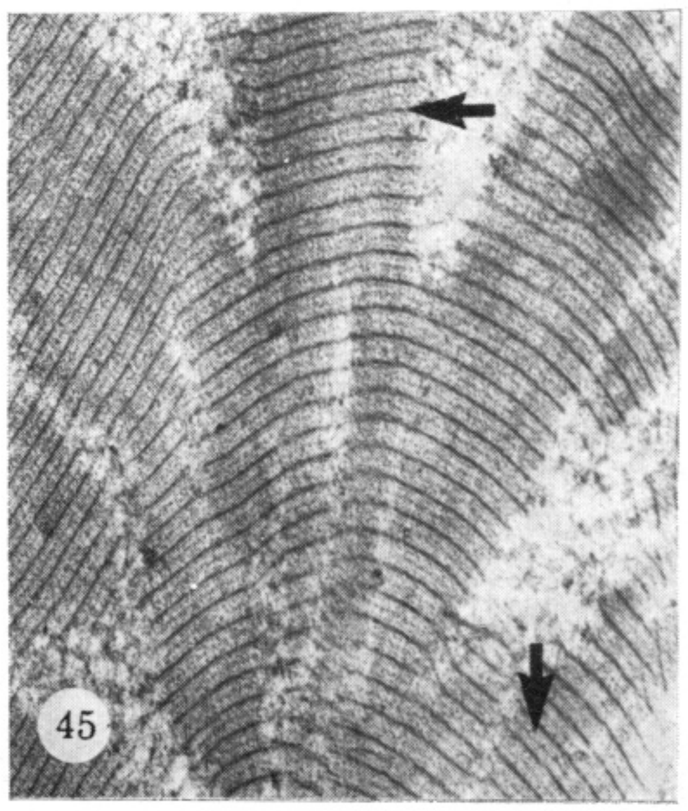

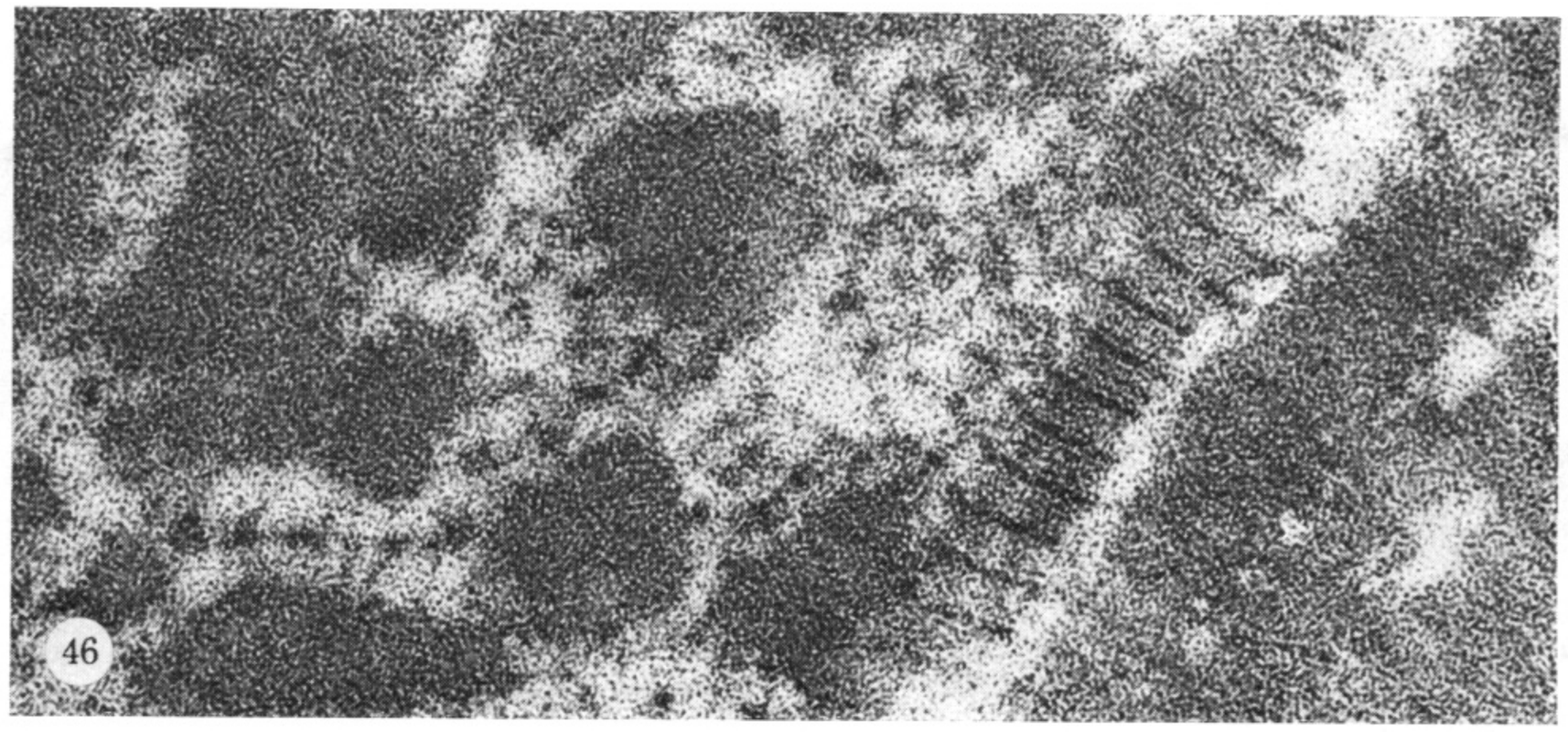

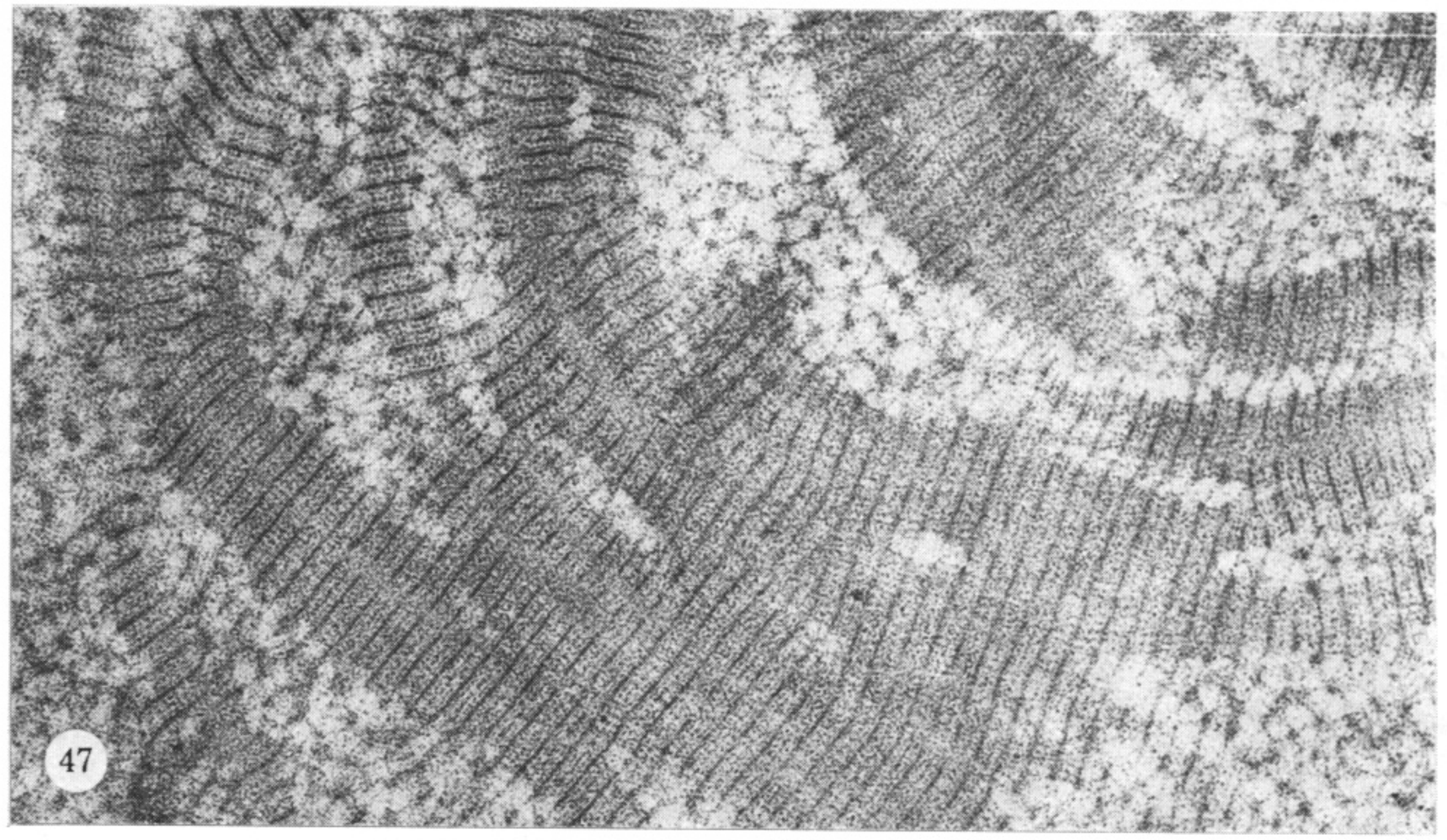

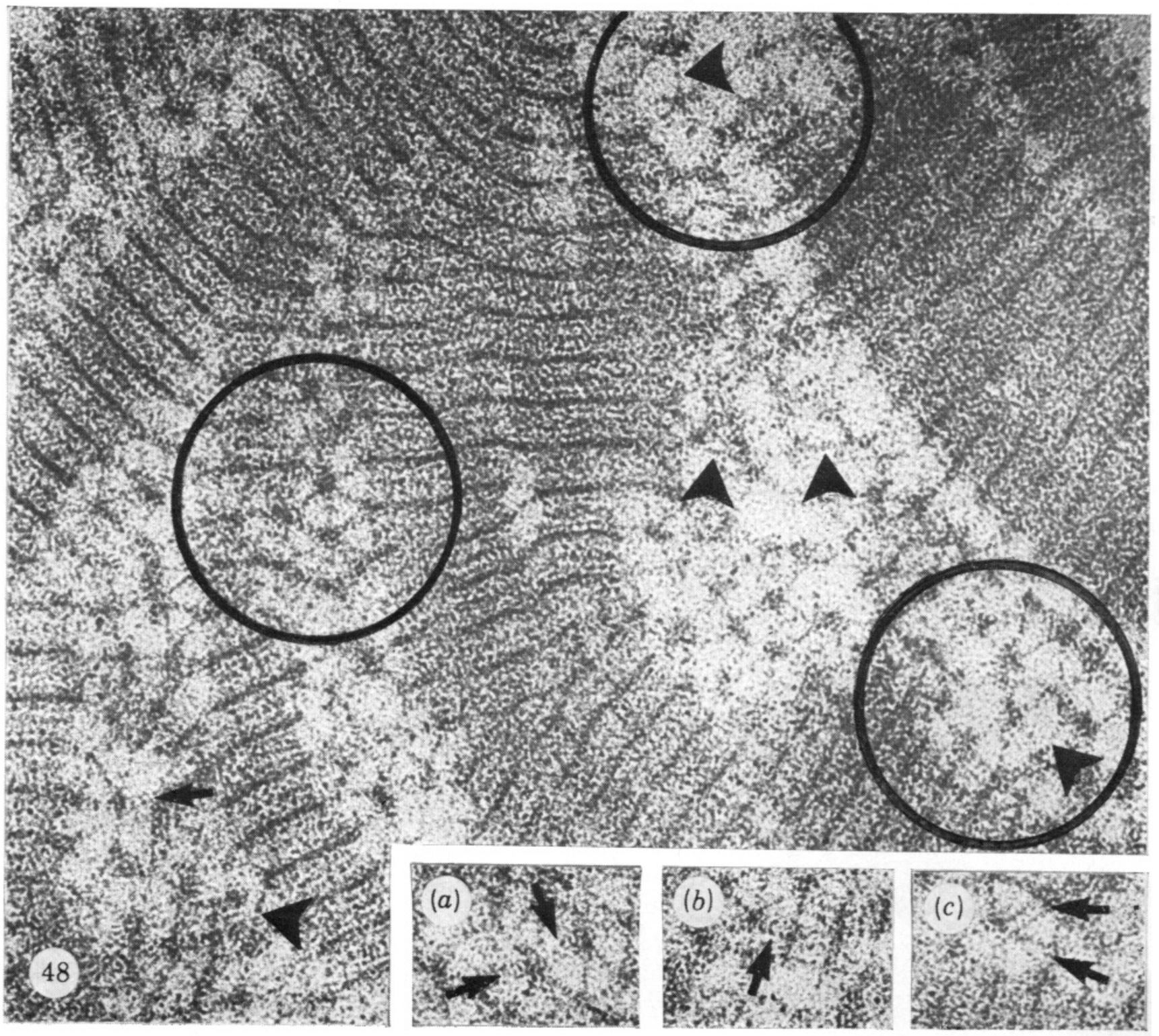

FIGURES 42–48. For description see p. 430.

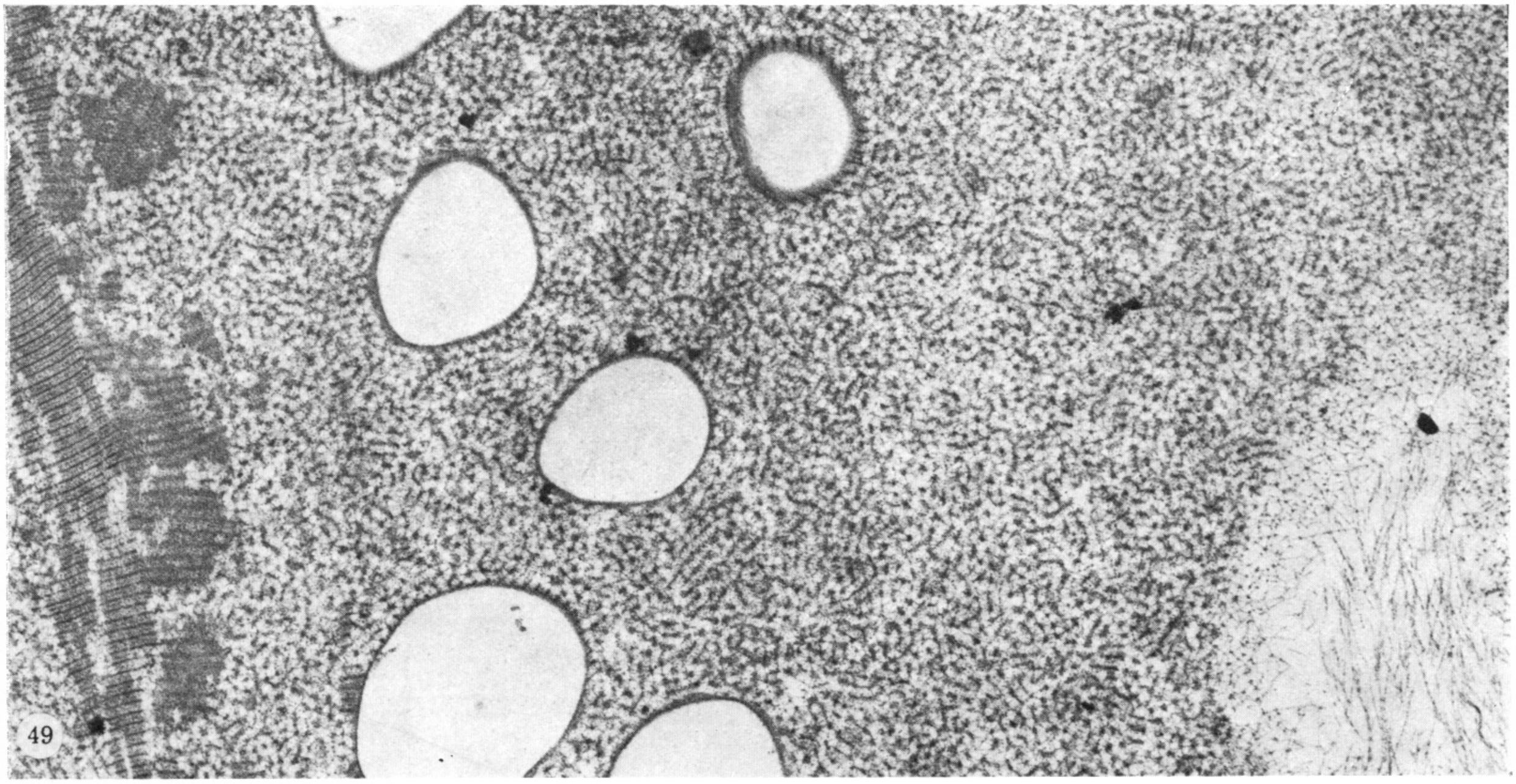

49

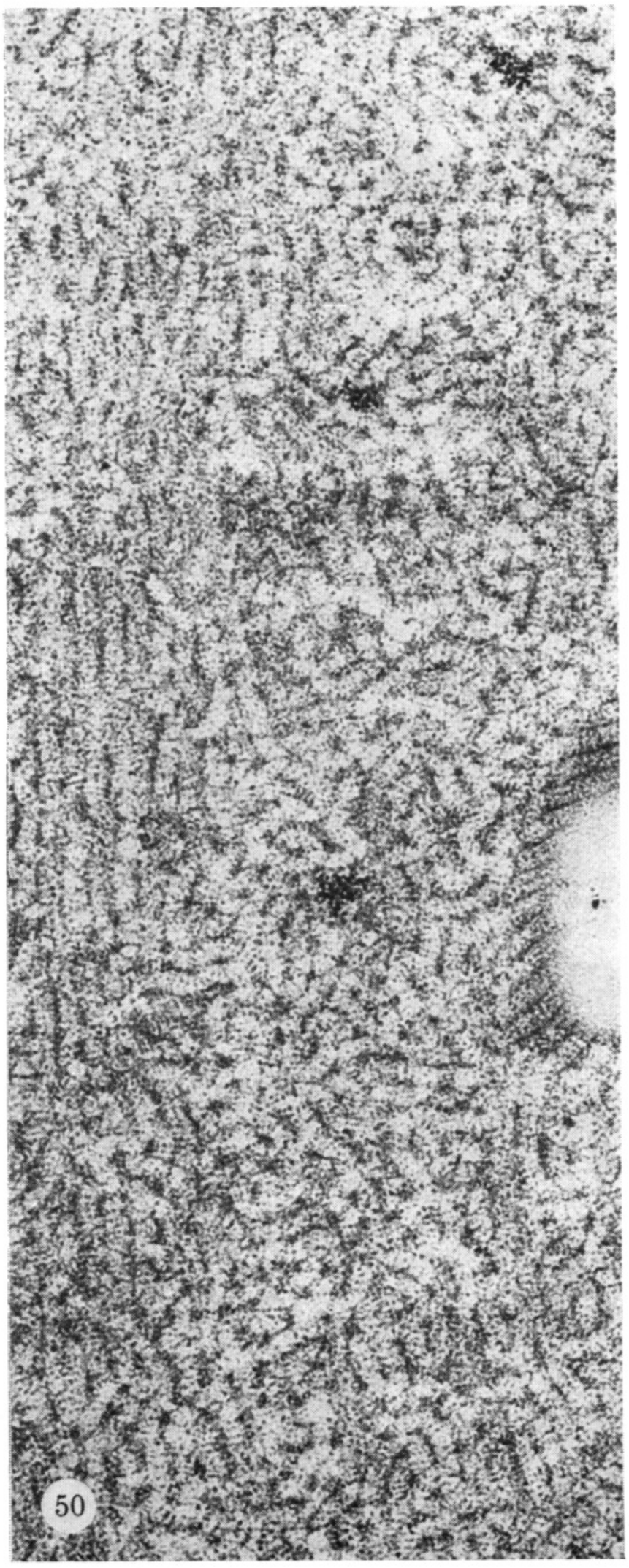

50

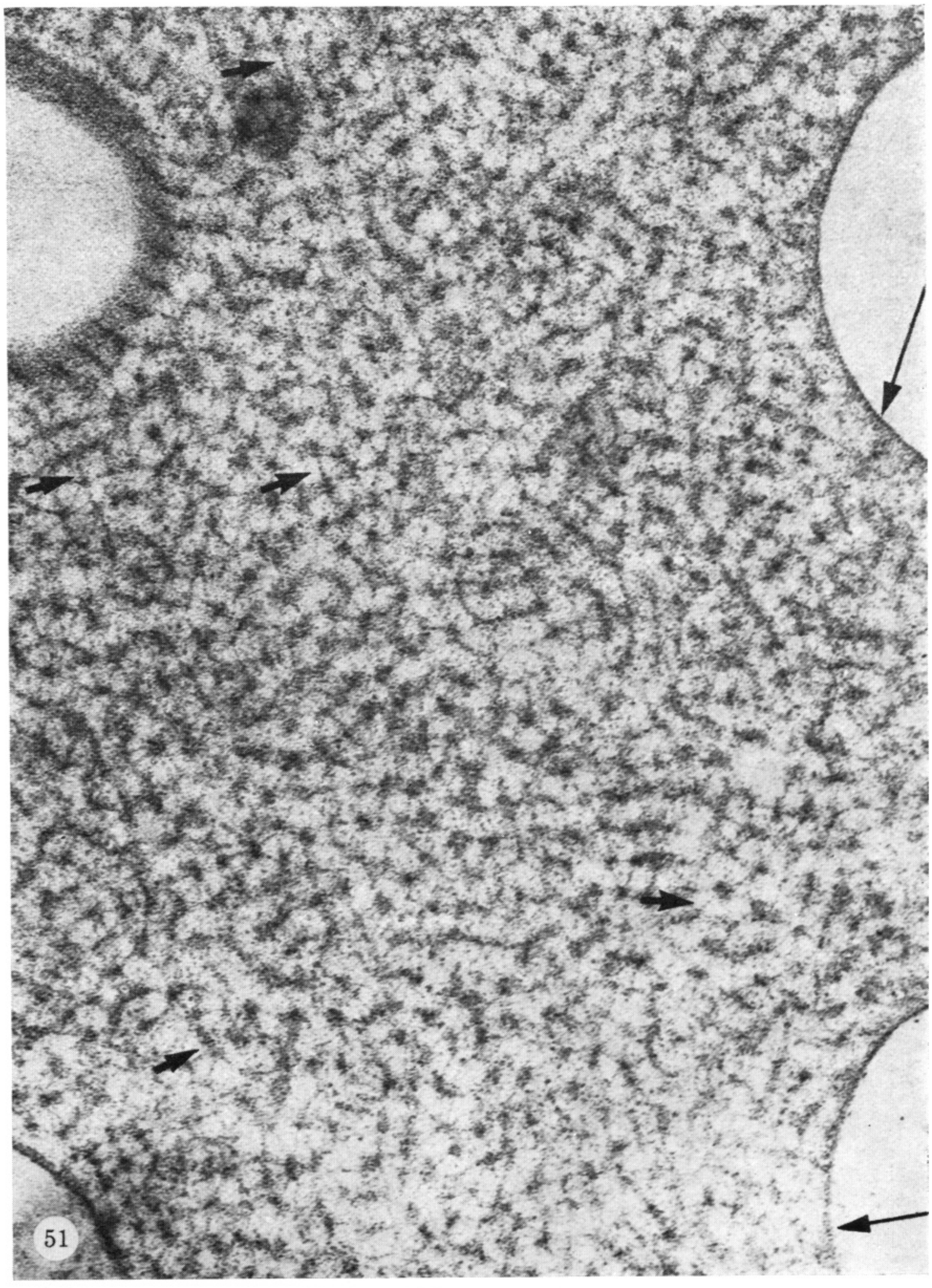

51

FIGURES 49–51. For description see p. 431.

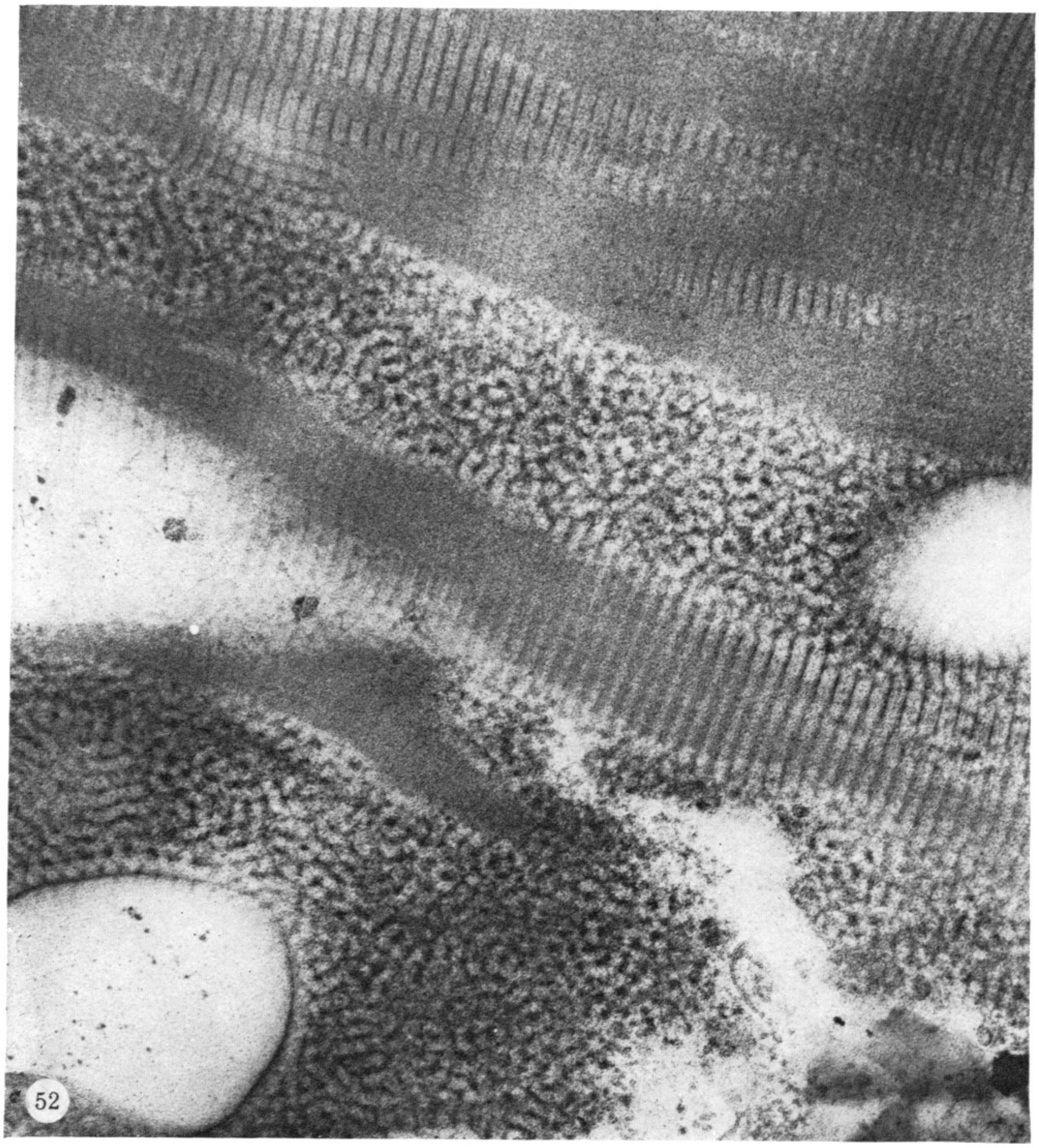

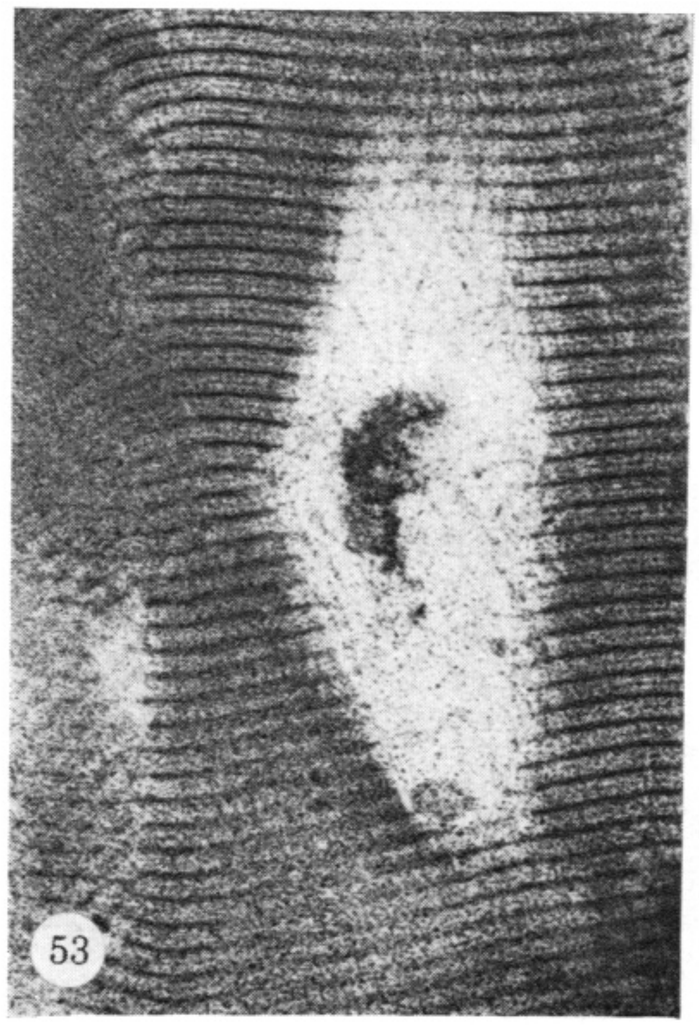

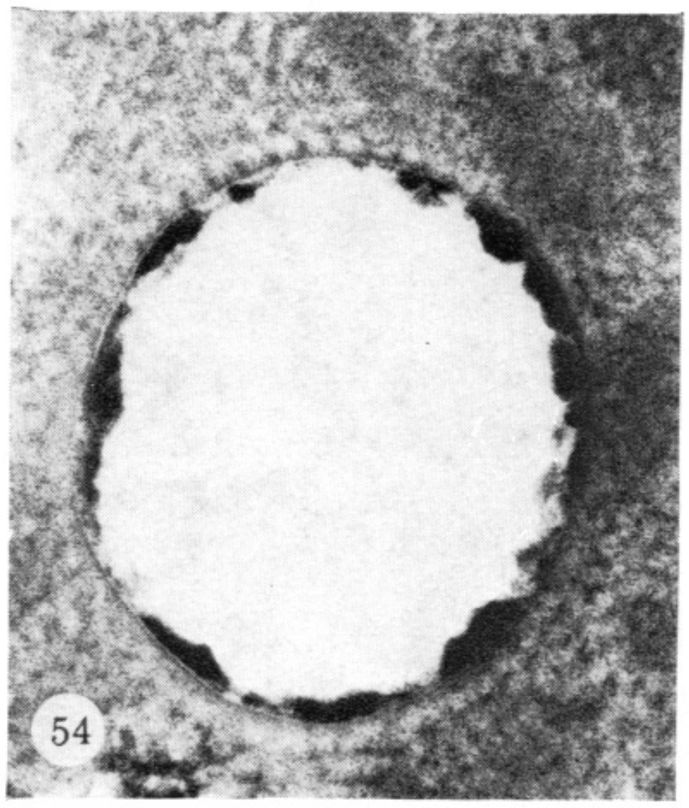

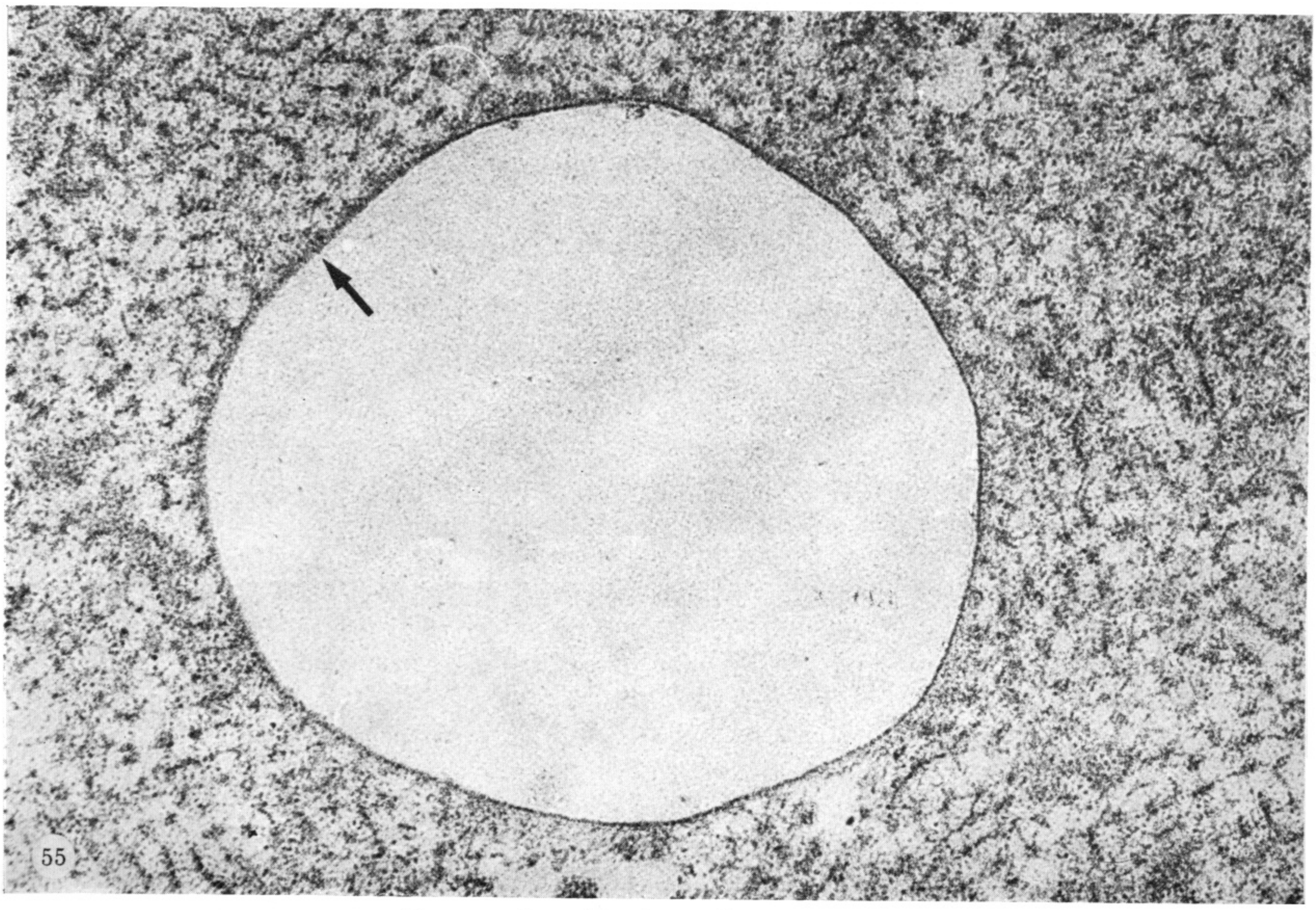

Figures 52–55. For description see opposite.

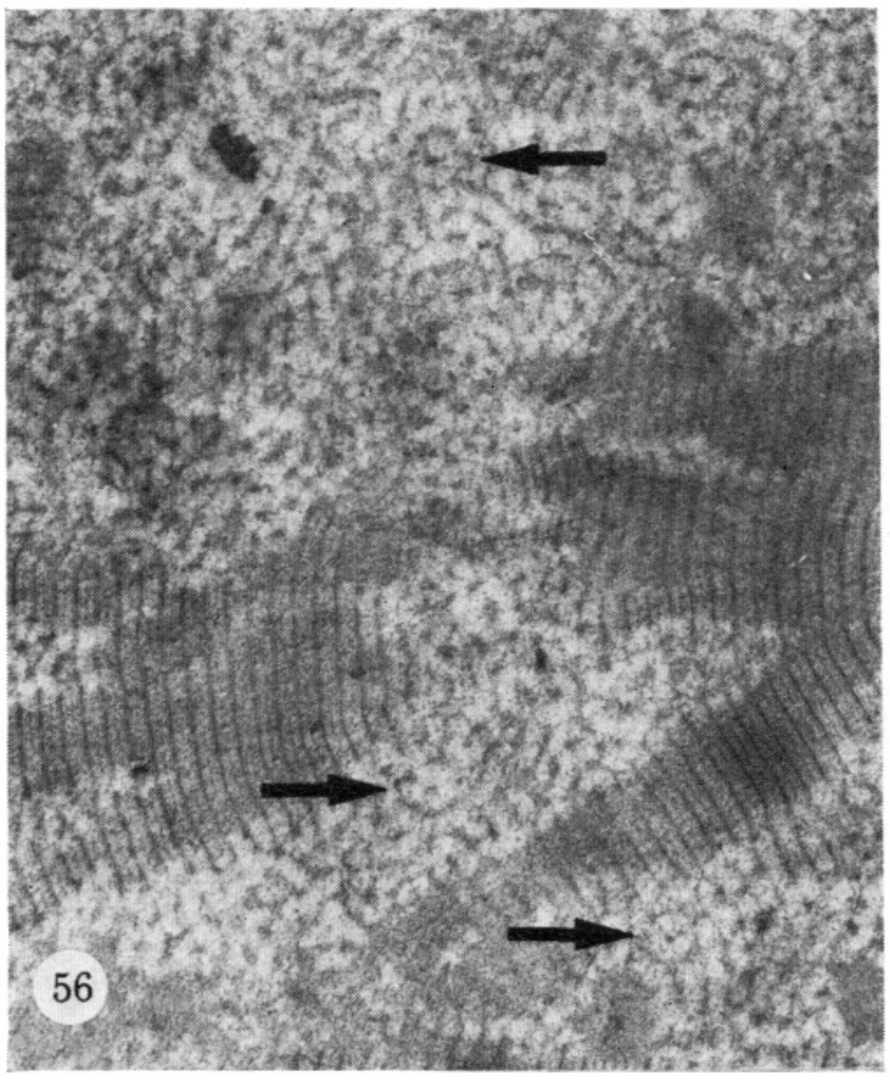

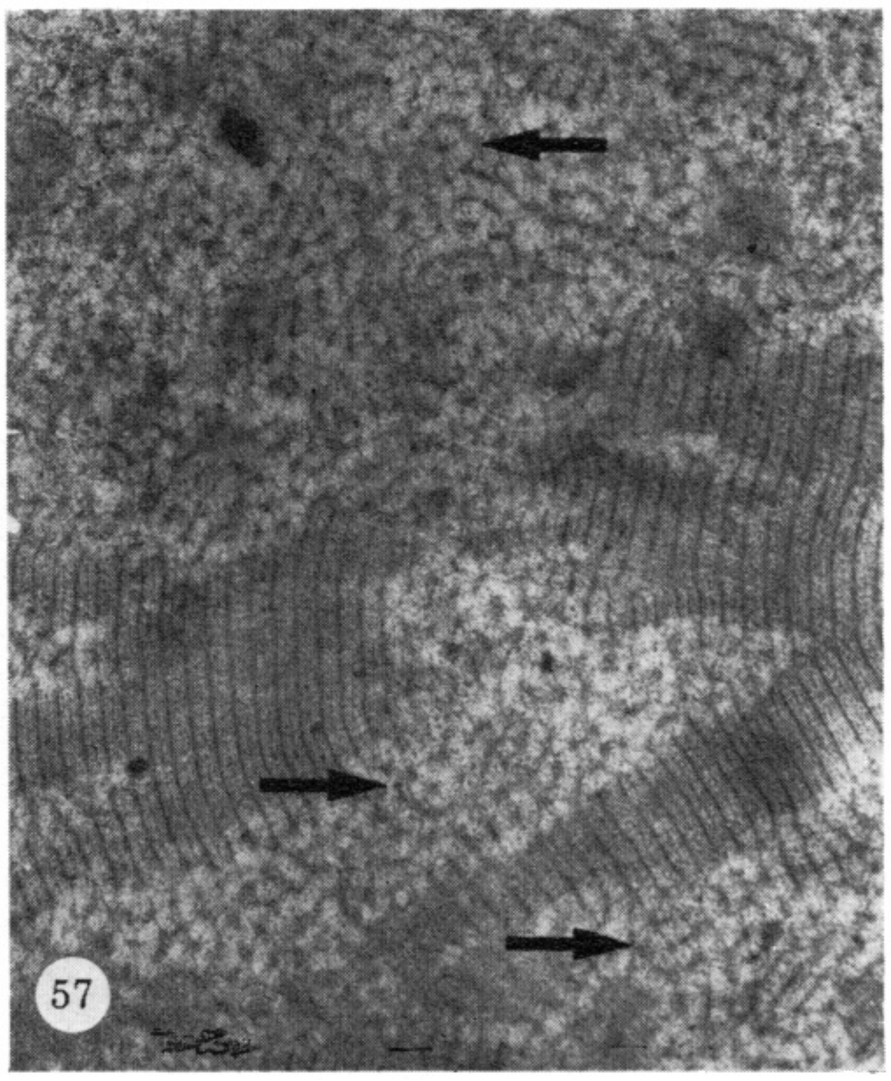

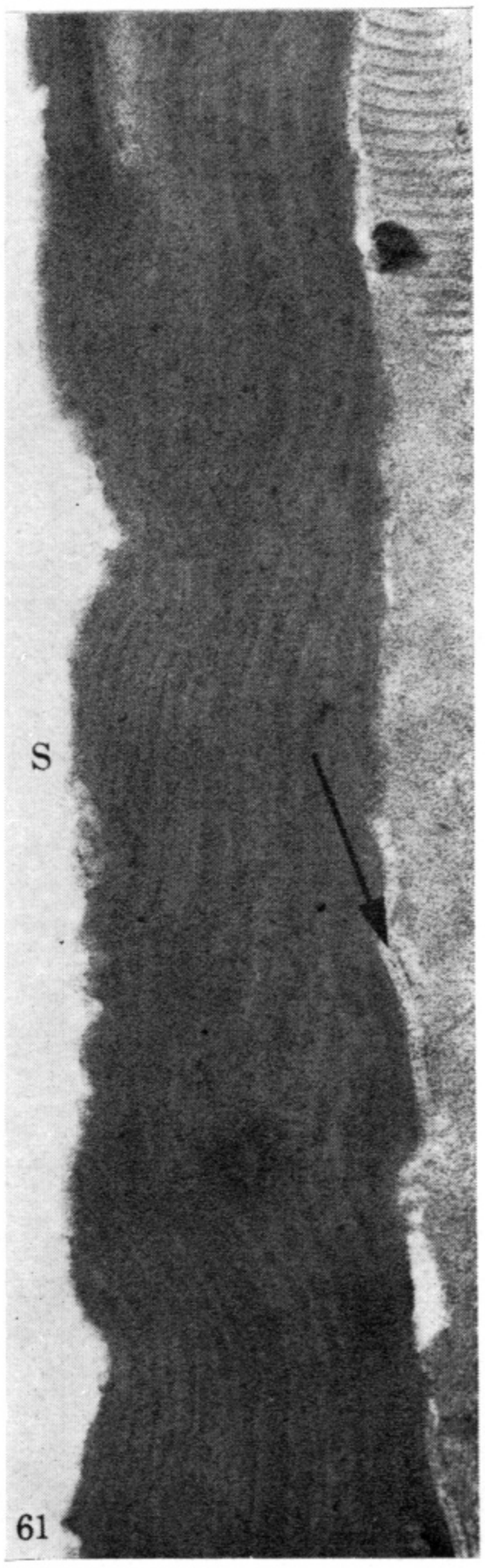

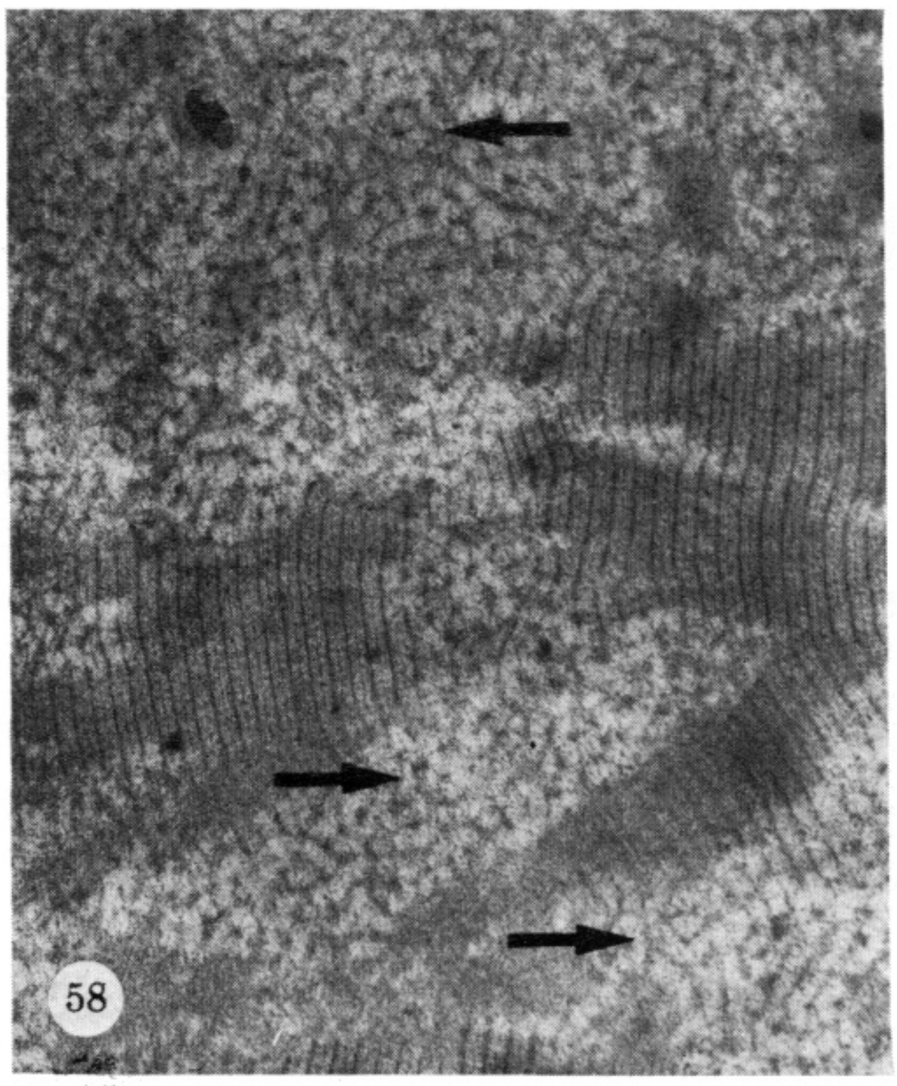

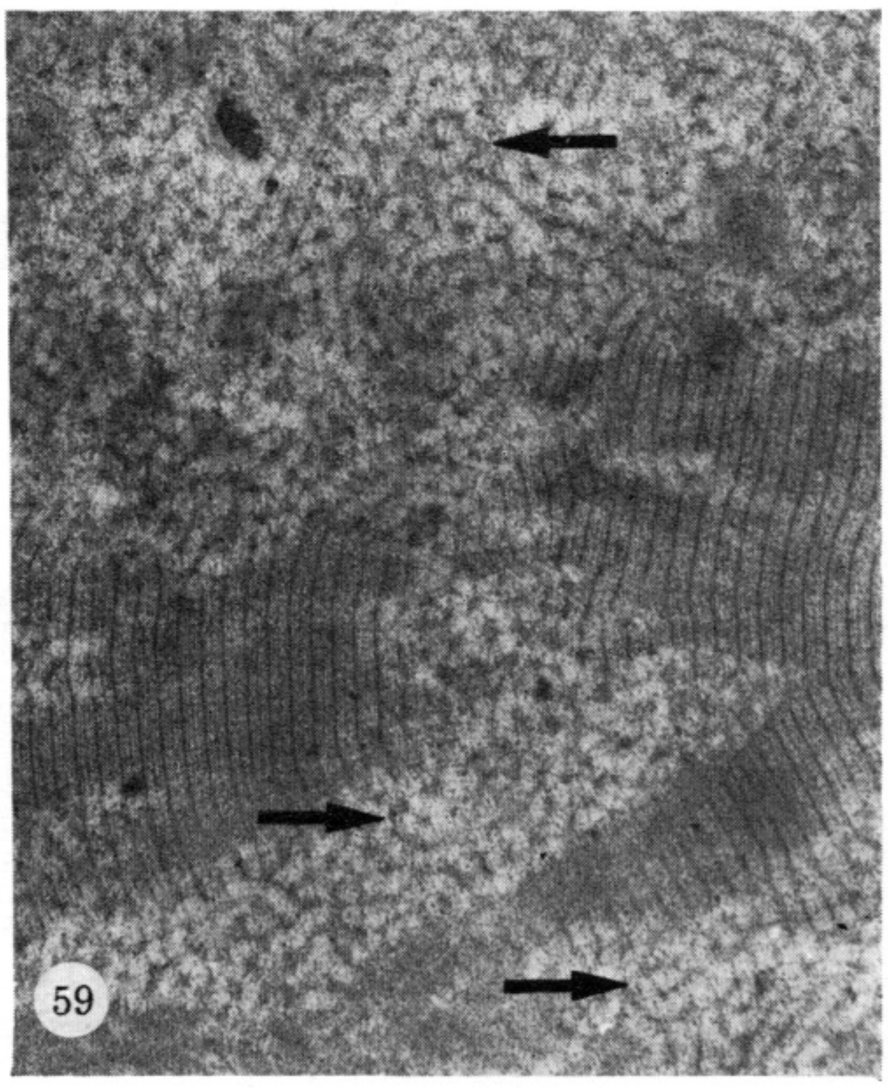

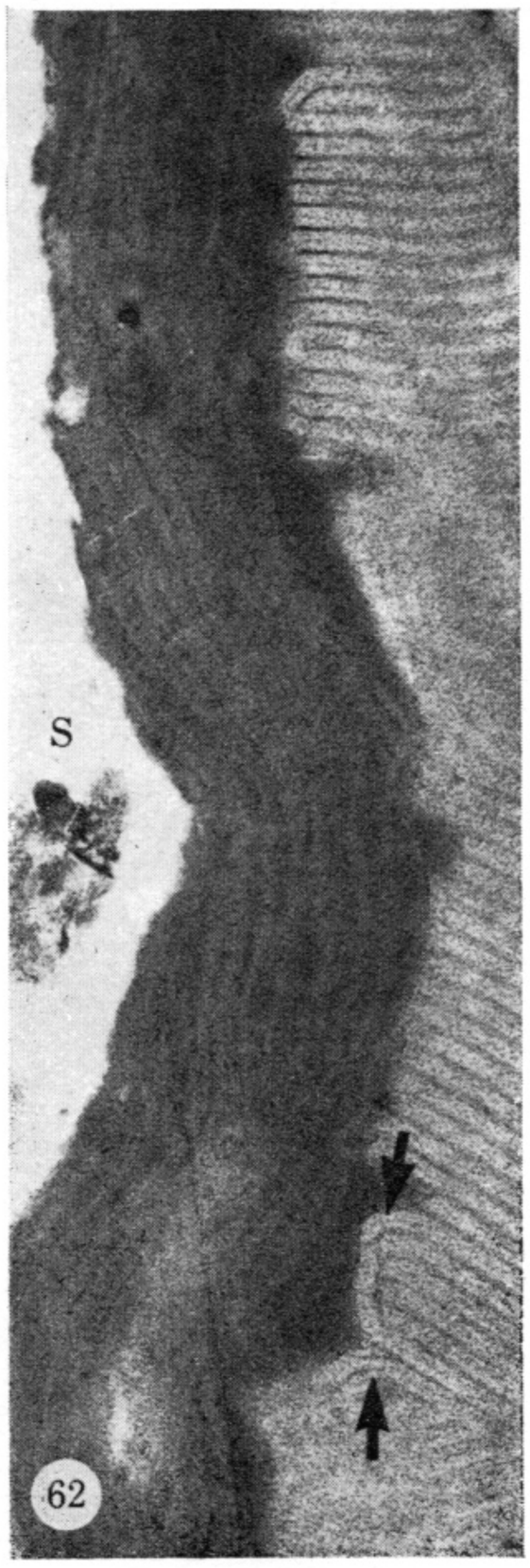

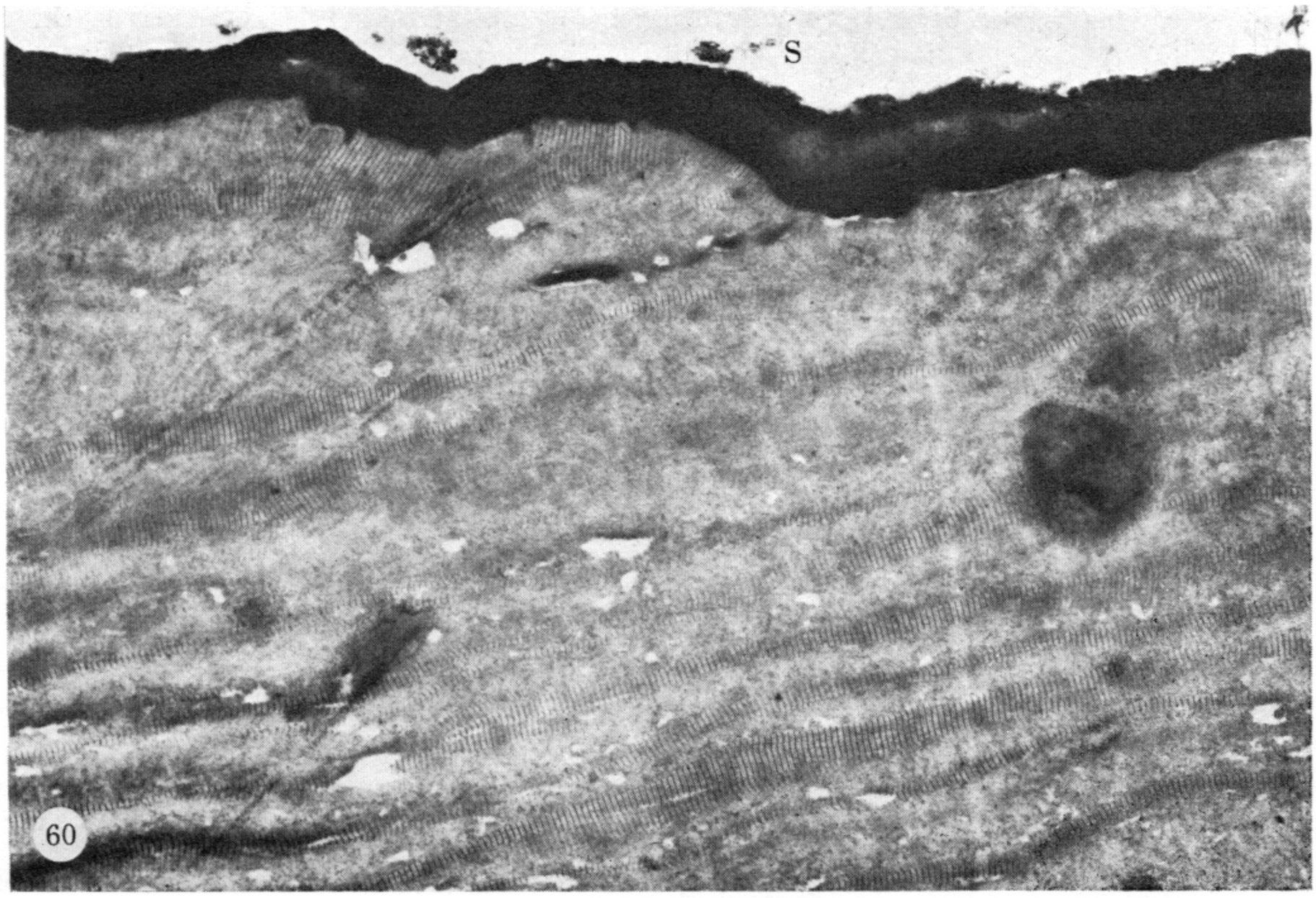

FIGURES 56–62. For description see opposite.

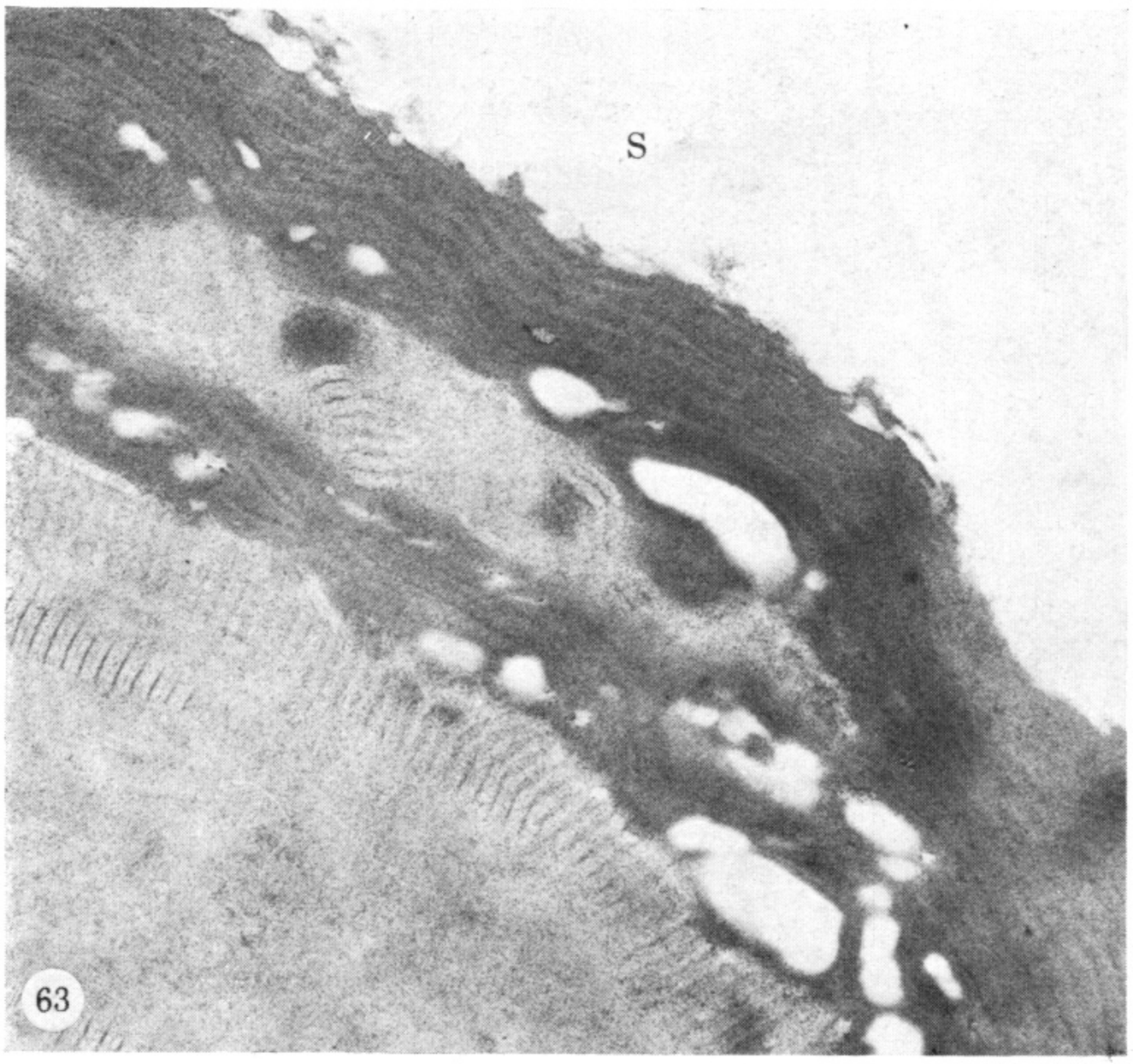

63

64

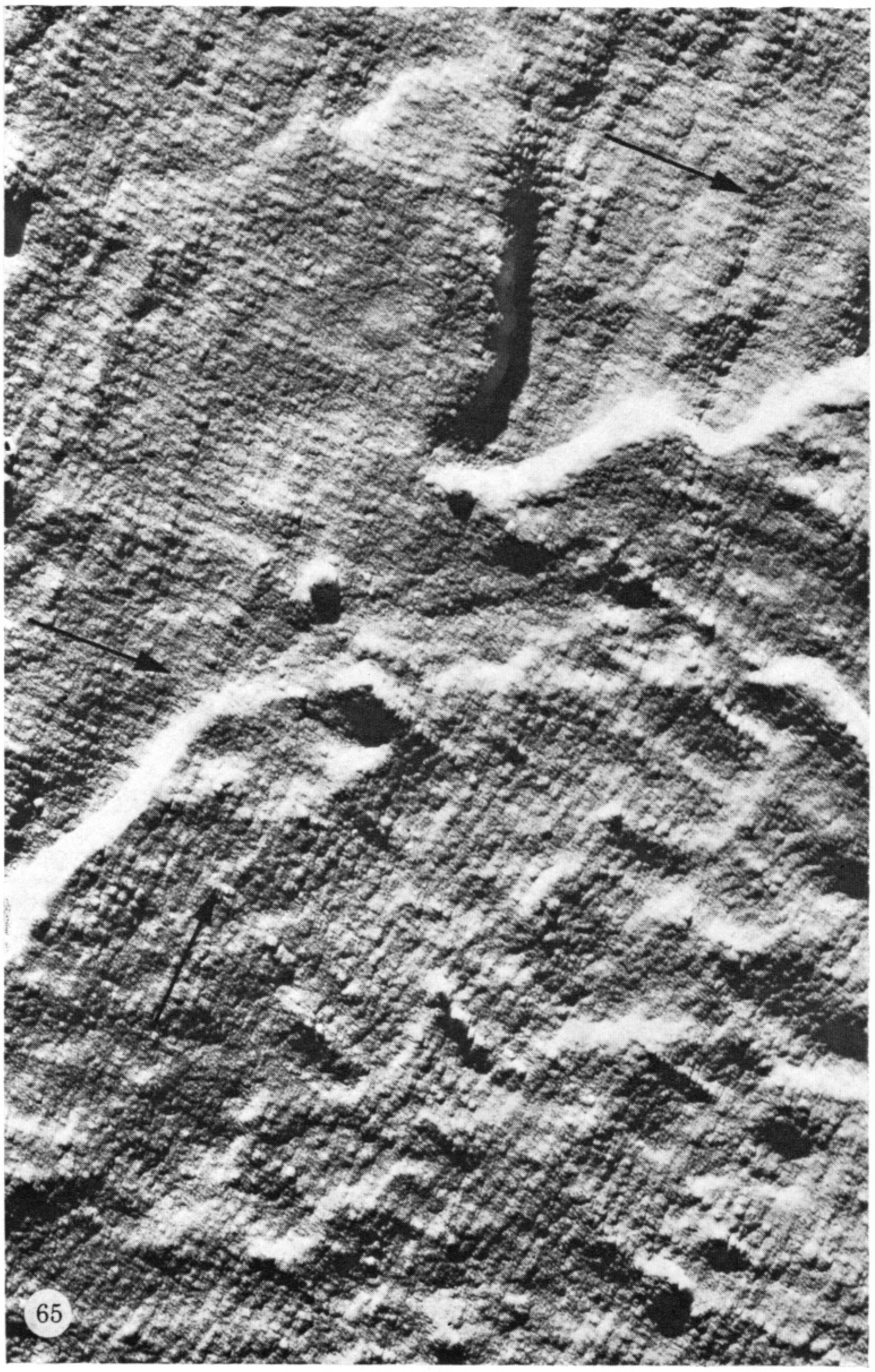

65

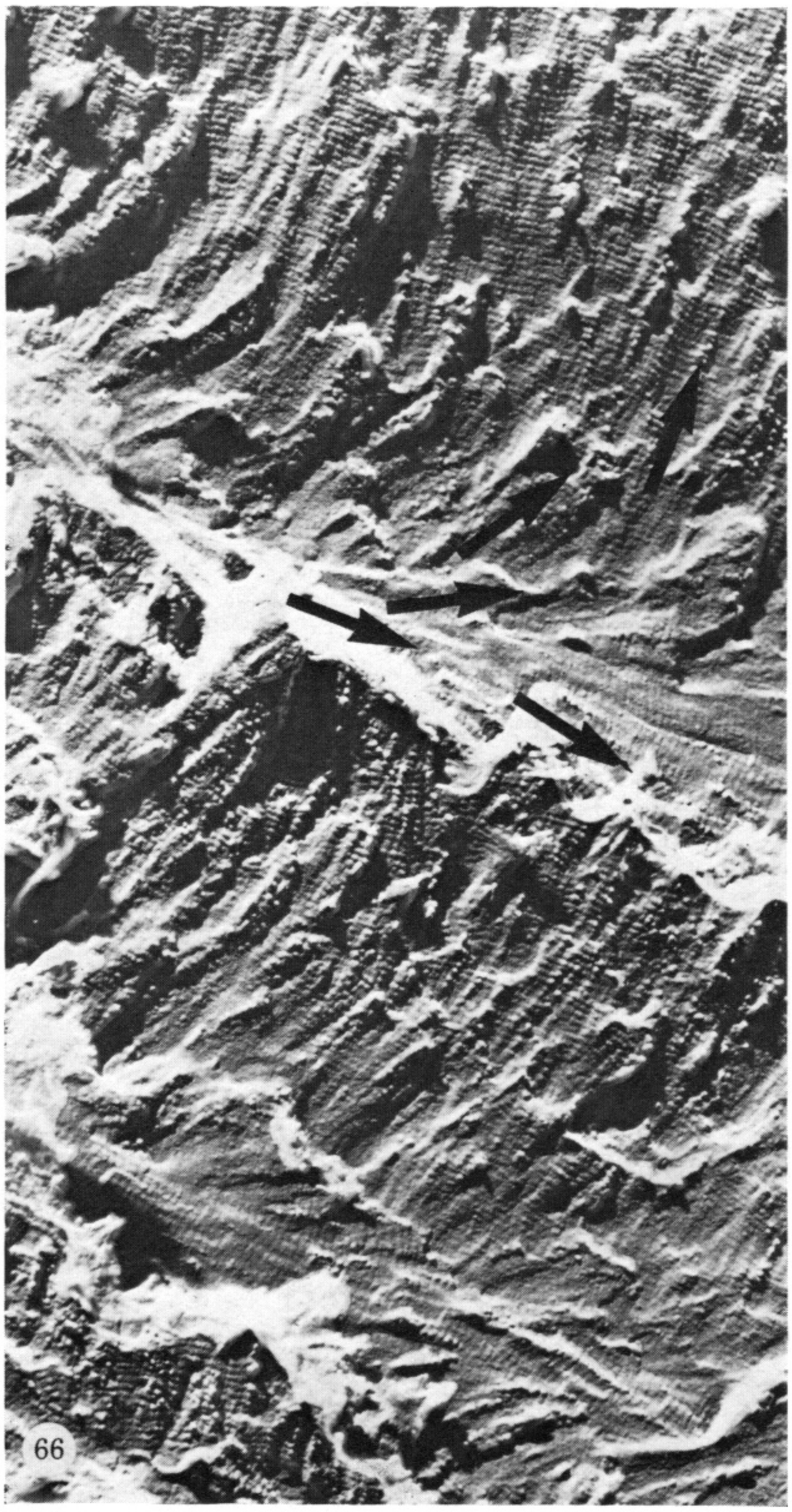

66

FIGURES 63–66. For description see p. 432.

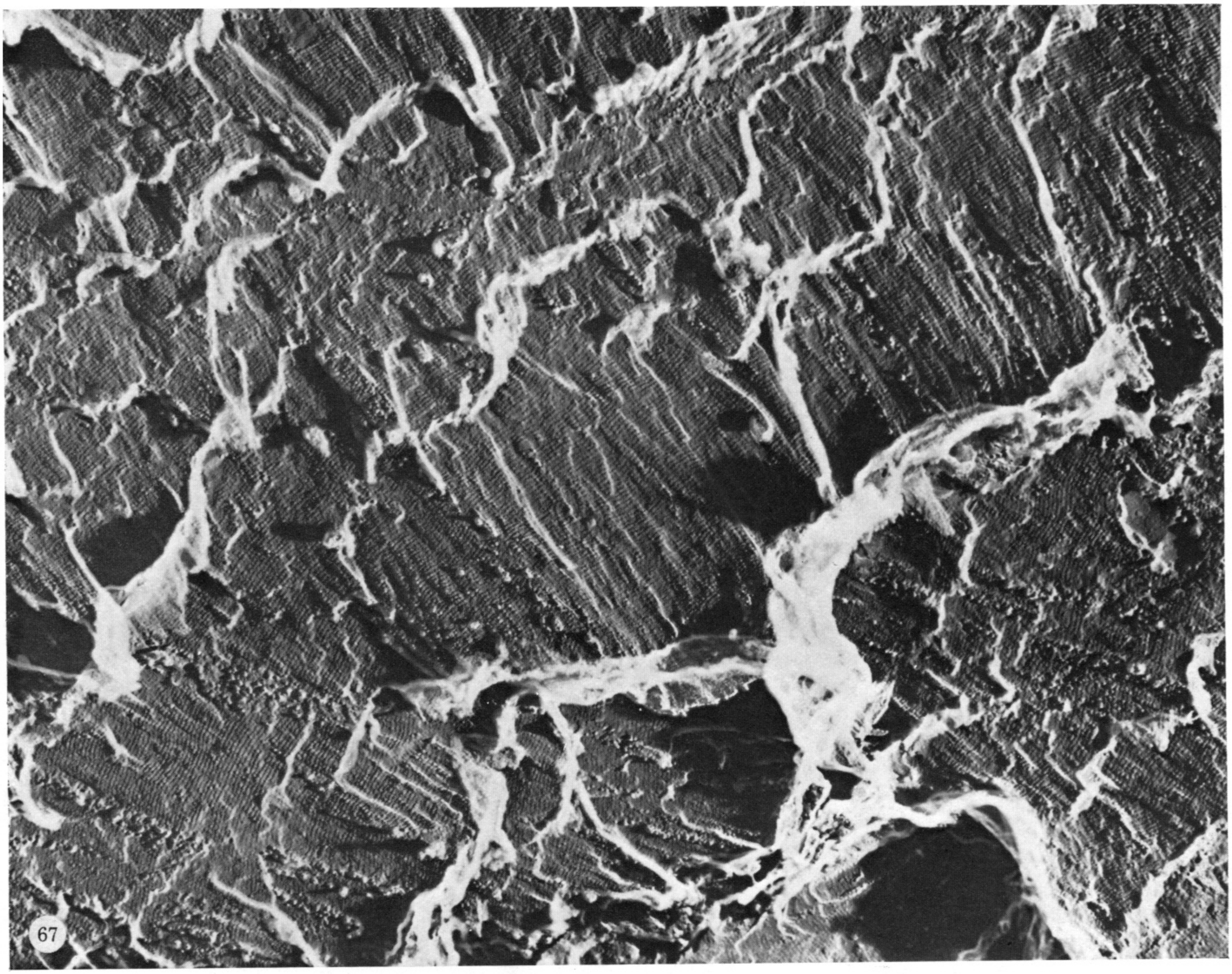

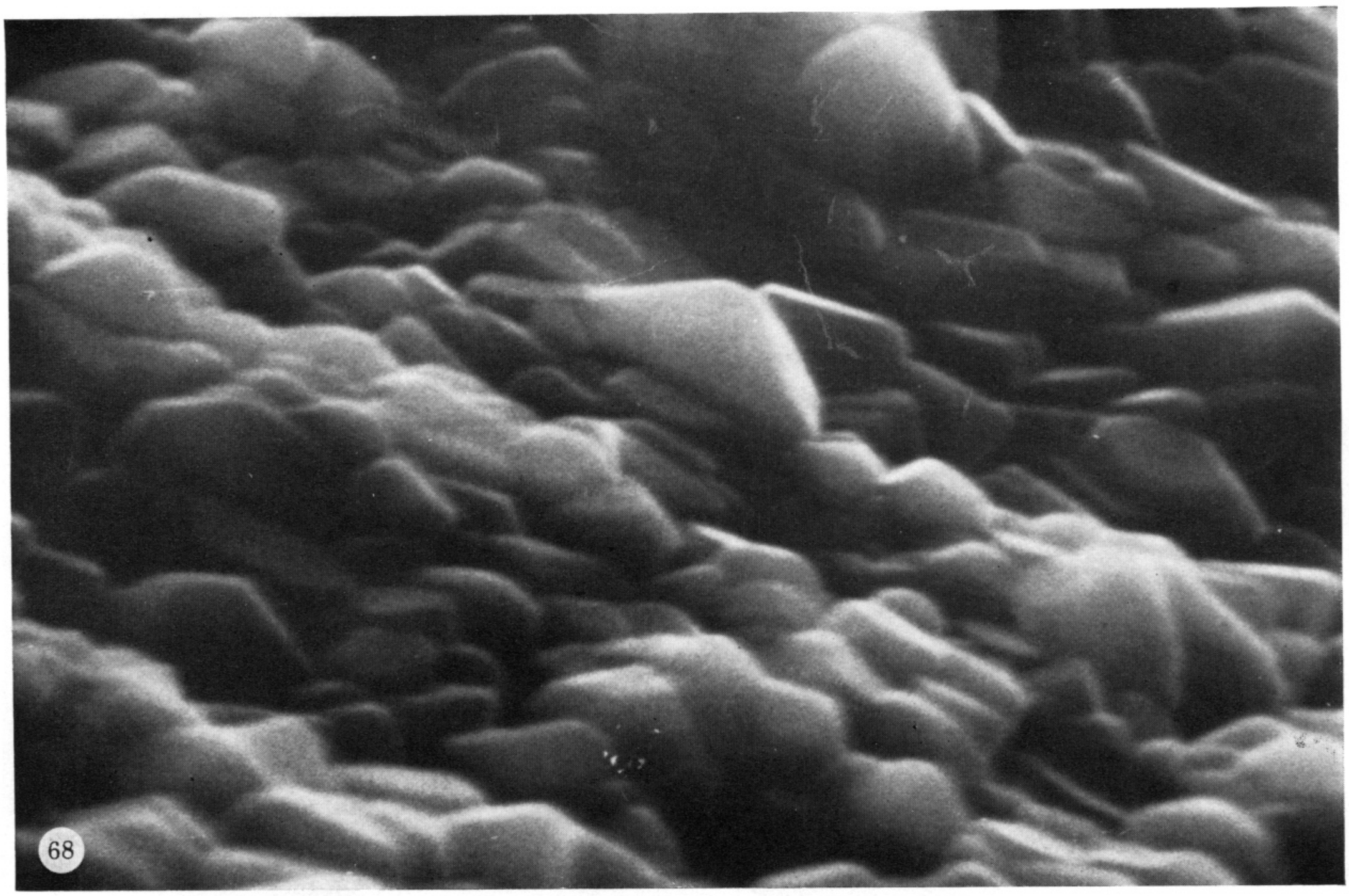

FIGURES 67 AND 68. For description see p. 433.

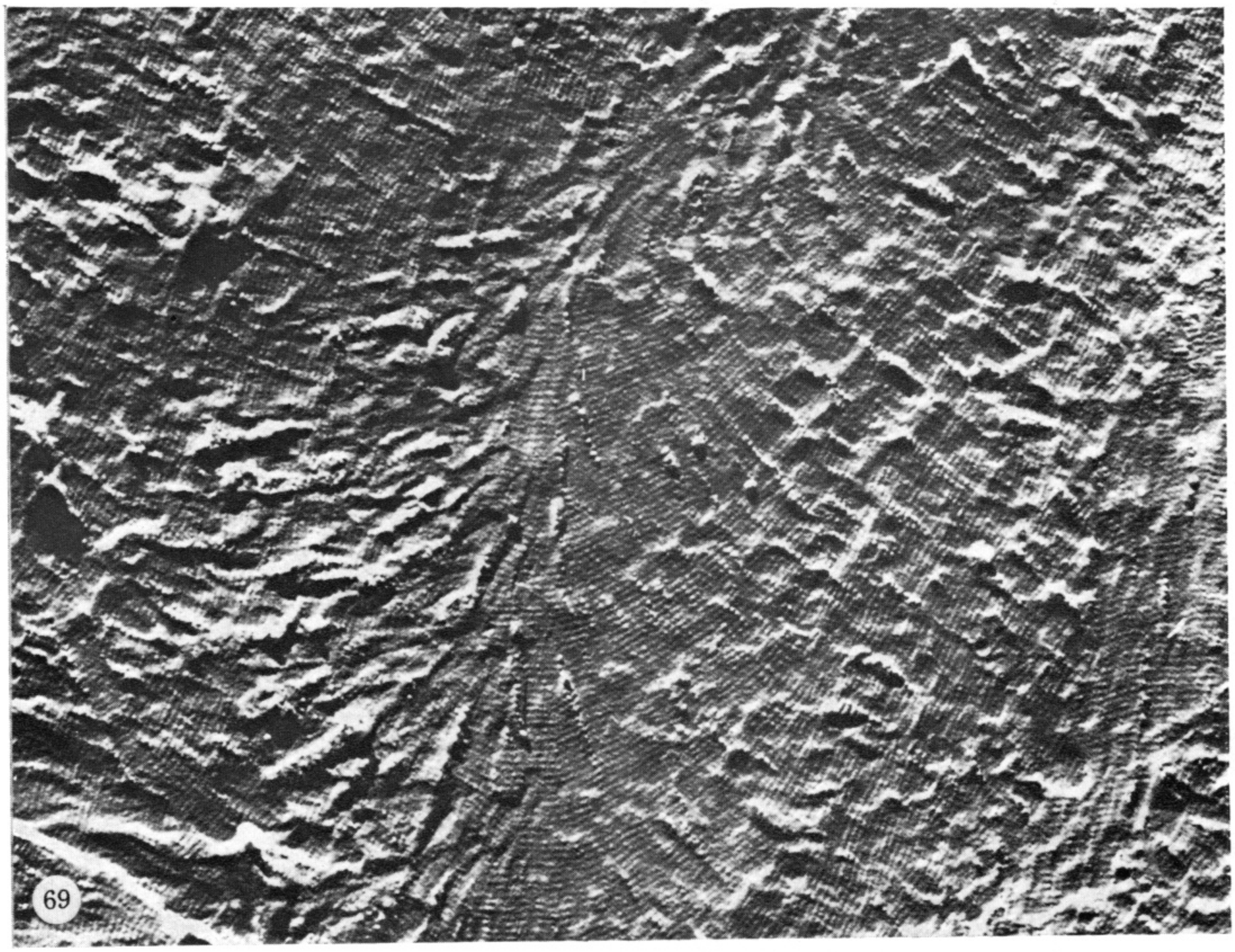

69

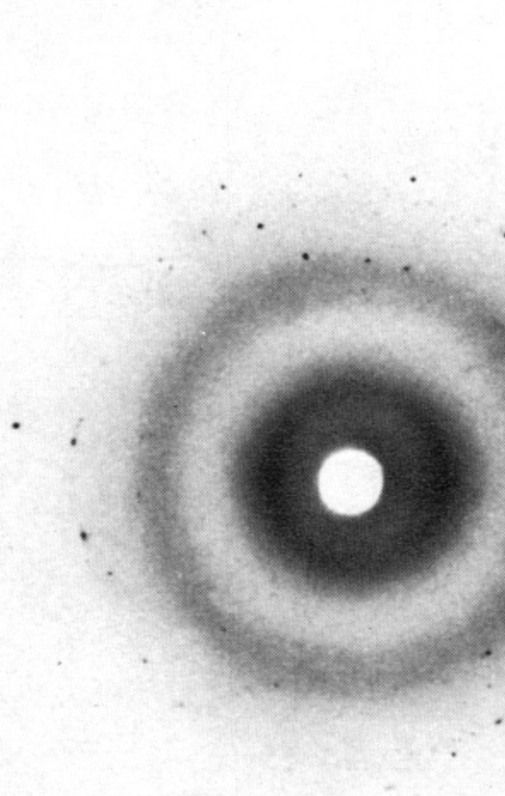

70

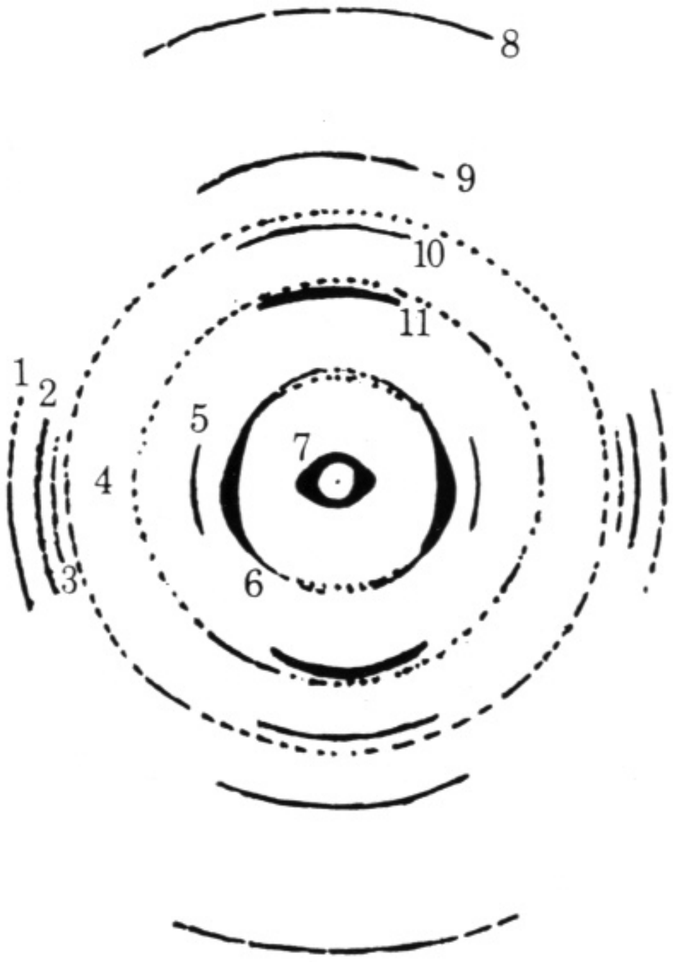

71

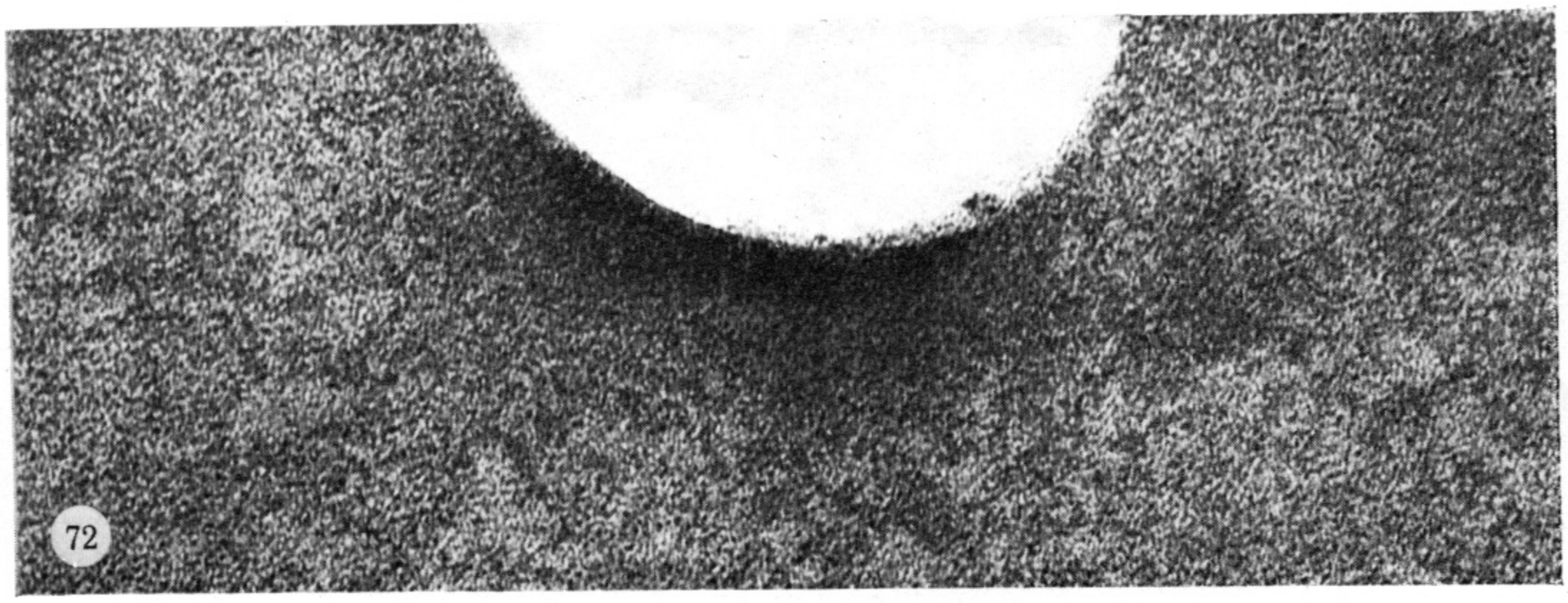

72

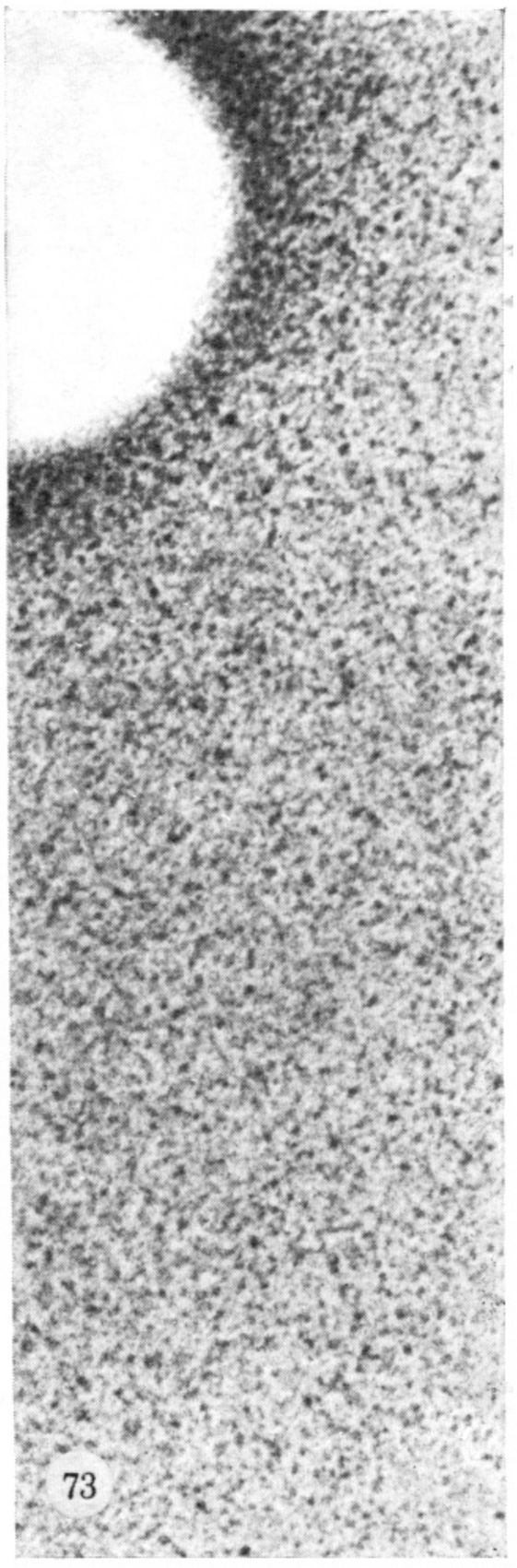

73

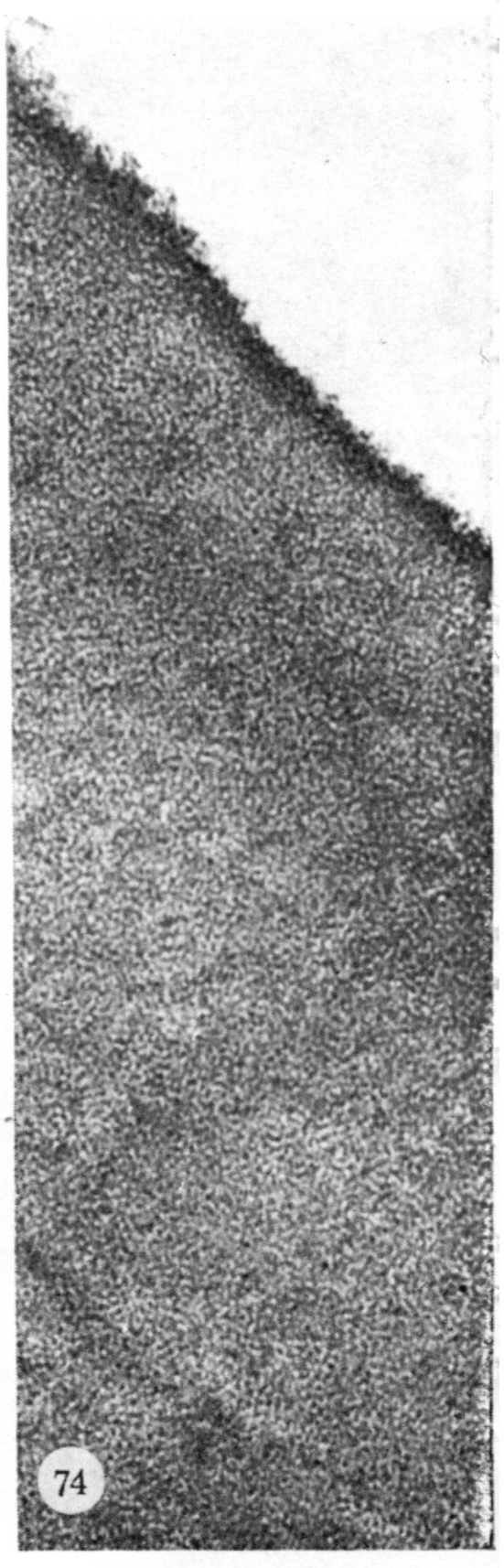

74

FIGURES 69–74. For description see opposite.